EXPERIMENTAL SIMULATION FOR THE ANALYSIS OF GEOMORPHOLOGICAL PROPERTIES OF COMETARY SURFACES WITH VOLATILE OUTGASSING

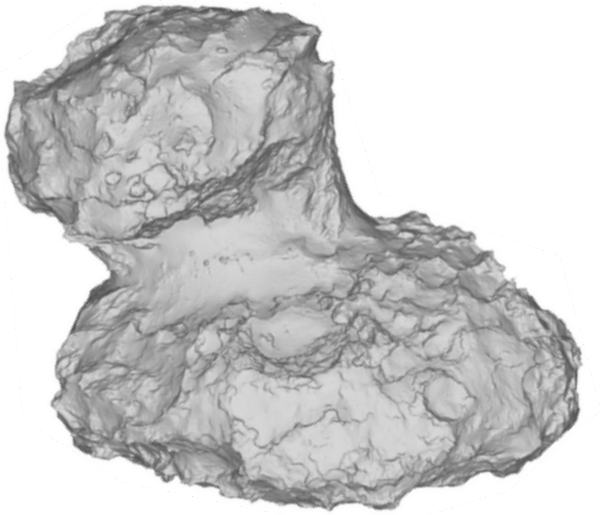

Dissertation
zur Erlangung des akademischen Grades
"doctor rerum naturalium"
(Dr. rer. nat.)

im Fachbereich Geowissenschaften
der Freien Universität Berlin

vorgelegt als kumulative Arbeit von

DAVID HAACK

Berlin, 2021

ERSTGUTACHTER: Prof. Dr. Ralf Jaumann
ZWEITGUTACHTER: Prof. Dr. Frank Postberg

Tag der Disputation: 14.01.2022

Titelbild aus Preusker et al. (2017)

This book contains a considerable volume of information.
I deeply regret this, but unfortunately it was inevitable.

Mark Twain
1835 – 1910

EIDESSTATTLICHE ERKLÄRUNG

Hiermit erkläre ich, dass ich die beigefügte Dissertation selbständig verfasst und keine anderen als die angegebenen Hilfsmittel genutzt habe.

Ich versichere weiterhin, dass ich die beigefügte Dissertation nur in diesem und keinem anderen Promotionsverfahren eingereicht habe und, dass diesem Promotionsverfahren keine endgültig gescheiterten Promotionsverfahren vorausgegangen sind.

Berlin, 01.10.2021

David Haack

ERKLÄRUNG

über den Eigenanteil an den drei veröffentlichten wissenschaftlichen Publikationen, deren Erstautor ich bin und die wesentliche Bestandteile meiner Dissertationsschrift gemäß §7 Abs. 2 der Promotionsordnung 2013 des Fachbereichs Geowissenschaften der Freien Universität Berlin darstellen:

1. **D. Haack**, B. Gundlach, C. Kreuzig, D. Bischoff, E. Kührt, J. Blum, K. Otto (2020), Tensile strength of dust-ice mixtures and their relevance as cometary analog material, Astronomy & Astrophysics, Vol. 642, Art. 218, DOI: 10.1051/0004-6361/202037763

2. **D. Haack**, A. Lethuillier, C. Kreuzig, C. Feller, B. Gundlach, J. Blum, K. Otto (2021), Sublimation of dust-ice mixtures in cooled vacuum environments to reproduce cometary morthologies, Astronomy & Astrophysics, Vol. 649, Art. 35, DOI: 10.1051/0004-6361/202140435

3. **D. Haack**, C. Kreuzig, B. Gundlach, J. Blum, K. Otto (2021), Sublimation of organic-rich comet analog materials and their relevance in fracture formation, Astronomy & Astrophysics, Vol. 653, Art. 153, DOI: 10.1051/0004-6361/202142069

Die Konzeption aller drei Studien erfolgte durch mich in Abstimmung mit Katharina Otto.

Die Laborarbeit der ersten Veröffentlichung wurden nach Einarbeitung durch Labormitglied Christopher Kreuzig von mir eigenständig durchgeführt. Analyse und Interpretation der Resultate erfolgte in Beratung mit Katharina Otto, Ekkehard Kührt und Bastian Gundlach.

Die Laborversuche der zweiten und dritten Veröffentlichung wurden von mir mit Unterstützung durch Christopher Kreuzig und Anthony Lethuillier durchgeführt. Analyse und Interpretation der Resultate erfolgten eigenständig.

Ich versichere, alle drei Manuskripte selbständig verfasst zu haben.

Berlin, 01.10.2021

David Haack

DANKSAGUNG

Diese Dissertation ist nicht das Resultat der Arbeit eines Einzelnen, sondern entstand unter tatkräftiger Mithilfe von Betreuern, Kollegen, Freunden und Familie. Ihnen allen möchte ich meine große Dankbarkeit aussprechen.

Meinen ersten und allergrößten Dank möchte ich an Dr. Katharina Otto richten, der es zu verdanken ist, dass diese Arbeit entstehen konnte. Die unzähligen spannenden Diskussionen und deine Bereitschaft jederzeit neue Ideen zu entwickeln, ließen ein Projekt entstehen, welches zu Beginn der Dissertation nicht zu erahnen war. Die Erfahrungen vieler anderer Doktoranden machen deutlich, dass eine solch intensive und ergiebige Betreuung nicht alltäglich ist und ich sehr dankbar bin, für dein großes Engagement.

Weiterhin gilt mein herzlicher Dank den Professoren Ralf Jaumann und Frank Postberg von der Freien Universität zu Berlin, die sich beide bereit erklärten die Gutachterrolle für meine Promotion zu übernehmen, sowie Prof. Gabriele Arnold und Dr. Katrin Stephan, welche mir überhaupt den Weg ins DLR bereiteten.

Mein weiterer Dank geht an alle Kollegen des CoPhyLab Projektes, welches der Erforschung von Kometen im Labor gewidmet ist. Insbesondere den Projekt- und Teamleitern an der Technischen Universität Braunschweig, Dr. Bastian Gundlach und Prof. Jürgen Blum, ist es zu verdanken, dass ich stets in ihren Laboratorien willkommen war und die mir immer mit guten Ideen zur Seite standen. Im Labor selbst wäre ohne die Unterstützung von Anthony Lethuillier und Christopher Kreuzig die praktische Arbeit gänzlich unmöglich gewesen, wofür ich auch ihnen sehr danke.

Ekkehard, Ernst und Solmaz möchte ich für ihre Hilfe und Freundschaft danken, und dass sie dank offener Türen immer für ein ergiebiges Gespräch zu haben waren. Dieser Dank gilt ganz generell allen Mitarbeitern und besonders der Mittagsrunde, die ein tolles Klima der Kollegialität pflegten und mir meine Zeit am DLR sehr angenehm machten. Danke Elke, Daniela, Stephan, Kai, Katrin, Andrea, Frank, Thomas, Volker und KDM. Insbesondere meinen beiden Bürokolleginnen Rutu und Tanja möchte ich für ihre Zusammenarbeit und den zuweilen sehr lustigen Momenten danken.

Besonderer Dank geht an Ines Büttner, die mir in wochenlanger Arbeit mein Probenmaterial für das Labor vorbereitet hat und an Prof. Uwe Altenberger der Universität Potsdam, der mir unkompliziert und mit persönlicher Hilfestellung Zugang zum Elektronenmikroskop ermöglichte.

Meine letzten, doch wichtigsten Worte des Dankes gehen an meine Familie und an Michaela, die die gesamte Zeit an meiner Seite stand und mir in jeder Situation mit den richtigen Worten Auftrieb gab. Egal ob sachlich, humorvoll oder absurd albern. Danke Michaela! Ohne dich hätte dies nicht wachsen können.

ABSTRACT

Despite a wealth of information from observations and experiments, the chemical and physical properties of cometary nuclei are not yet fully understood. The work presented here is intended to contribute to a better understanding of the processes on the surface of cometary nuclei by means of experiments in the laboratory. Special attention is given to the influence of sublimating volatiles in variable amounts. For this purpose, a number of consecutive laboratory experiments were performed with the aim to reproduce morphological features as observed on the surface of comets. The obtained results were used to draw conclusions about how representative the different material combinations in the laboratory are with respect to chemical and physical characteristics of a comet. This work combines three experimental studies, each published in peer-reviewed journals.

The first series of experiments tested which mixtures of mineralic and volatile components were suitable as analogs in the laboratory. SiO_2 dust, fly ash and water ice were tested. Of particular interest were the tensile strength and the cohesion of mixtures of these materials as functions of grain shape, mixing ratio, and at temperatures below 150 K. For this purpose, cylindrical samples of various mixtures of these components were prepared and their average tensile strength was determined by using the Brazilian disk test method. It was found that the tensile strength of two-component mixtures is dominated by that component with the higher tensile strength. The experiments also showed that it is possible to prepare cometary analogues of spherical fly ash and ice particles with an average tensile strength of a few hundred pascals.

For the second study, the previously characterized fly ash-ice mixtures were placed in a vacuum sublimation chamber and insolated with a light source for several hours. Different morphologies evolved and were depended on the insolation flux, insolation angle, and sample composition. Large amounts of ice caused rapid sublimation of the samples and the development of exotic morphologies. With decreasing ice content, the occurrence of episodic collapse events or outbursts increased, resulting in a rough surface texture of the samples. In addition, a dust layer formed on the surface that reduced or prevented further sublimation processes.

The third study extended the experiments of the second study by enriching the water ice particles with organic components. The amino acid glycine and the organic salt sodium acetate were used. Both are components that have been detected on comets and represented cometary organic components in the laboratory. The experiments showed that organic components have a distinct adhesive effect on the samples when the ice sublimates. Dominant morphological alterations of the samples surfaces are no longer due to collapse events or outbursts, but by a loss of volume of the ice-depleted remains and due to the formation of shrinkage fractures on the sample surface.

The morphologies produced in the experiment indicate that an ice content of >25 mass% (>40 vol%) is likely at the surface and near-surface layers of a comet. The amount of only a few percent of organic material is sufficient to adhesively solidify the ice-depleted comet surface and cause the formation of fracture patterns.

ZUSAMMENFASSUNG

Trotz einer Fülle an Informationen aus Beobachtungen und Experimenten ist noch nicht völlig verstanden, wie Kometenkerne in ihren chemischen und physikalischen Eigenschaften beschaffen sind. Die hier vorgelegte Arbeit trägt dazu bei mittels Experimenten im Labor die Prozesse auf der Oberfläche von Kometenkernen besser zu verstehen. Besonderes Augenmerk wird dabei auf den Einfluss sublimierender Volatile in variabler Anfangsmenge gelegt. Dazu wurden mehrere Reihen aufeinander aufbauender Laborexperimente durchgeführt, die zum Ziel hatten morphologische Charakteristika zu reproduzieren, wie sie auf Kometen beobachtet wurden. Aus den erzielten Resultaten wurden anschließend Rückschlüsse gezogen, wie repräsentativ die im Labor verwendeten Analogmaterialien für die tatsächlichen chemisch-physikalischen Charakteristika eines Kometen sind.

Diese Arbeit setzt sich aus drei experimentellen Studien zusammen, welche jeweils in Peer-Review-Verfahren als Veröffentlichungen erschienen. In den ersten Versuchen wurde getestet, welche mineralischen und volatilen Materialien im Labor als Kometenanalog geeignet sind. Getestet wurde SiO_2-Staub, Flugasche und Wassereis. Von zentralem Interesse waren die Zugfestigkeit und Kohäsion von Mischungen dieser Materialien in Abhängigkeit von Kornform, Mischungsverhältnis und von Temperaturen unter 150 K. Dazu wurden zylindrische Proben verschiedener Materialmischungen präpariert und mit der Brazilian Disk Test Methode ihre Zugfestigkeit bestimmt. Es zeigte sich, dass die Zugfestigkeit von Materialmischungen von jener Komponente mit der höheren Zugfestigkeit dominiert wird. Die Versuche ergaben weiterhin, dass es im Labor möglich ist aus sphärischen Flugasche- und Eispartikeln Kometenanalogmaterialien mit einer Zugfestigkeit von wenigen hundert Pascal herzustellen.

Für die zweite Studie wurden die zuvor charakterisierten Flugashe-Eis-Gemische in einer Vakuum-Sublimationskammer platziert und über mehrere Stunden mit einer Lichtquelle beleuchtet. Je nach Beleuchtungsstärke, -winkel und Mischungsverhältnis der Proben entwickelten sich unterschiedliche Morphologien. Hohe Konzentrationen von Eis verursachten eine schnelle Sublimation der Proben unter Entwicklung teils exotischer Morphologien. Mit sinkendem Eisgehalt kam es vermehrt zu episodischen Kollaps- oder Auswurfsereignissen, die eine sehr raue Oberflächenstruktur der Proben verursachten. Zusätzlich bildete sich eine Staubschicht, die fortlaufende Sublimationsprozesse reduzierte oder verhinderte.

Die dritte Studie erweiterte die Experimente der zweiten Studie indem die reinen Eispartikel um organische Bestandteilen erweitert wurden. Verwendet wurden die Aminosäure Glycin und das organische Salz Natriumacetat. Beides sind Materialien, die auf Kometen nachgewiesen wurden und repräsentierten die organischen Bestandteile eines Kometenkerns. Die organischen Komponenten haben einen deutlichen adhäsiven Effekt auf die Proben, sobald das Eis sublimiert ist. Die dominanten morphologischen Veränderungen der Proben sind keine Kollapsereignisse mehr, sondern ein Volumenverlust des eisreduzierten Materials unter der Bildung von Schrumpfungsrissen an der Probenoberfläche.

Die in den Experimenten produzierten Morphologien weisen darauf hin, dass ein Eisgehalt von <25 mass% (<40 vol%) nahe der Kometenoberfläche wahrscheinlich ist. Ein Anteil von wenigen Prozent organischen Materials reicht aus, eine eisreduzierte Kometenoberfläche adhäsiv zusammenzuhalten und die Bildung von Rissstrukturen zu verursachen.

CONTENTS

LIST OF FIGURES

LIST OF TABLES

1 INTRODUCTION

1.1 MISSIONS TO COMETS

Comets are small primordial objects with a characteristic size of a few kilometers and are remnants from the early days of the solar system. This makes them particularly interesting research objects, because they archive information about the early solar system. Their main location area is far in the outer solar system in the Kuiper belt and the Oort cloud. The Kuiper belt ranges between 30 and 50 AU in the plane of the ecliptic of the solar system. It is considered the origin of numerous short-period comets whose orbits are not significantly inclined to the plane of the ecliptic. (Duncan, Quinn, and Tremaine, 1988; Jewitt, 1999; Levison and Duncan, 1997). Oort's Cloud is a region that spherically envelops the solar system from a heliocentric distance of about 5000 AU and with its large number of small bodies is assumed the origin of many comets distinctly inclined against the ecliptic (Hills, 1981; Stern, 2003). This great distance from the Sun prevented comets from heating up and, in addition to dust and other non-volatile materials, they contain a high proportion of highly volatile substances, such as carbon monoxide, carbon dioxide, or methane (Biver et al., 2019; Bockelée-Morvan et al., 2016; Läuter et al., 2018). Of all the volatiles detected on comets, water is the most abundant (Bockelée-Morvan et al., 2016; Hässig et al., 2015). In this characteristic comets differ from the asteroids of the inner solar system, which are generally depleted in volatile content compared to comets and consist of predominantly refractory materials at their surface (Quirico et al., 2015; Schulz et al., 2015). Due to their origin in the outer solar system at large heliocentric distances, comets remain largely unaffected by alteration processes that take place in the inner solar system, such as sublimation, and retain their primordial character.

Occasionally it happens that comets are disturbed in their distant orbit and are deflected into an orbit that brings them closer to the Sun. This may happen if a massive belt member gravitationally disturbs the orbit of a less massive one and scatters it into the inner solar system (Fernández, 1980). Alternatively, Neptune's gravitational pull could pertubate the orbit of Kuiper belt objects and scatter them to an orbit that would bring them closer to the Sun (Duncan, Quinn, and Tremaine, 1988). Most comets are detected as they approach the Sun. The increased insolation warms the surface of the nucleus and surface-near volatiles start to sublimate (Brown, 2000). The gases and dust particles entrained by the gas drag form a highly visible cloud around the nucleus, called the coma. However, because of the comet's low gravity, this coma cannot be retained, expanding further and further into space. The solar wind and radiation pressure accelerate the constantly produced gas and dust away from the comet's nucleus, creating two typical comet tails. A narrow and straight plasma tail of molecular ions and a diffuse and curved dust tail. Particularly active comets with distinct comet tails can be observed with the naked eye in the night sky. Therefore,

comets are of great importance to science, as they bring archived information about the formation of the solar system within the reach of scientific observational methods.

After comets could only be studied with telescopes from Earth for a long time, space missions were launched from the mid-1980s to investigate comets in detail. Of these, the most notable are:

- 1986 Giotto passes comet 1P/Halley (Keller et al., 1986)
- 2001 Deep Space 1 passes comet 19P/Borrelly (Soderblom et al., 2002)
- 2004 Stardust sample return mission to comet 81P/Wild 2 (Brownlee et al., 2004)
- 2005 Deep Impact collision experiment on comet 9P/Tempel 1 (Harker, Woodward, and Wooden, 2005)
- 2010 Deep Impact passes comet 103P/Hartley 2 (Thomas et al., 2013a)
- 2014 Rosetta orbits comet 67P/Churyumov-Gerasimenko (Glassmeier et al., 2007) and landing of lander Philae (Ulamec et al., 2016)

The upcoming reappearance of comet 1P/Halley in 1986 was the trigger for ESA to start the Giotto mission. This was a rendezvous mission and, supported by the soviet VEGA missions, it showed for the first time details of the nucleus of a comet in a resolution of 45 meters per pixel (Keller et al., 1986). It was the first time that the concepts of comet evolution developed in previous decades could be tested by close-up observations. The comet nucleus was found to have a very low albedo of 0.04 and to develop temperatures above 360 K at its surface (Emerich et al., 1988), ruling out large amounts of exposed volatile components. In addition to volatile ices (e.g. H_2O, CO_2, CO), refractories, and organic materials were detected (Kissel et al., 1986), and the nucleus was found to have low density and tensile strength. The success of this first ESA interplanetary mission opened the door to its planetary exploration program.

NASA's DEEP SPACE 1 mission to Comet 19P/Borrelly confirmed Giotto's observation that comets are not composed predominantly of volatile ices and therefore cannot be described as dirty snowballs. It showed that the surface of the elongated nucleus was very rough and had a variety of morphological features, such as mesas, pits, ridges or troughs. Due to the lack of volatiles exposed at the surface, the sublimation activity and how it works became a special focus. For example, it was hypothesized that fresh volatile-rich material was exposed at collapsing cliffs of mesas and caused the formation of gas jets (Britt et al., 2004).

STARDUST was NASA's next mission to a comet and collected particles from the coma for the first time and brought them back to Earth (Brownlee et al., 2004). The analysis of these samples revealed that in addition to volatiles and a variety of mineral components, organic amino acids such as glycine were also components of a comet (Elsila, Glavin, and Dworkin, 2009). On its hardened surface many craters, cliffs and overhangs were observed, which indicate that the comet is an object with a long evolutionary history.

The third NASA mission to a comet was DEEP IMPACT, which was started to study the chemical and physical properties of comet 9P/Tempel 1 in more detail. For this purpose, a 372 kg impactor hit the comet's surface and produced a cloud of ejecta

material, which was subsequently analyzed. The material was found to be no different from the coma except for a slightly increased CO_2/H_2O ratio. In addition, it was observed that below a transition layer of less than 1 m thickness, components such as H_2O and others were uniformly distributed in the comet nucleus (Sunshine et al., 2007). However, the physical properties of the comet remained uncertain because the impact crater was covered by ejecta material and was no longer visible for analysis purposes.

After DEEP IMPACT visited 9P/Temple 1, the spacecraft's mission was extended and re-directed to Comet 103P/Hartley 2 for a flyby. The images taken show a bilobate nucleus with an elongated, almost axially symmetric shape. The two lobes, covered with scarps, boulders, and chunks, are connected by a smooth waist (Thomas et al., 2013a,b) formed of fallback material. The smaller of the two lobes showed numerous regions where gas jets emerge from the surface. They were mainly driven by the sublimation of H_2O and CO_2 and accelerated up to decimeter-sized solid fragments to above escape velocity (Kelley et al., 2013).

ESA's Rosetta Spacecraft with the Philae Lander was a mission to comet 67P/Churyumov-Gerasimenko (hereafter 67P). Its objectives included studying the formation of gas jets and the physical properties of the comet. Most prominent is the revealed shape of 67P with its two lobes connected by a narrow neck. As different as the general shape of the nuclei is, as diverse are the morphological features that have formed on their surfaces. Especially 67P shows on its surface flat and dusty regions (El-Maarry et al., 2015b; Thomas et al., 2015b) and also very rough areas with cliffs, pits, fractures, and boulders originated from mass wasting processes (El-Maarry et al., 2019; Pajola et al., 2015, 2016a; Thomas et al., 2015b). These landforms can provide valuable information about the characteristics and the ratios of volatile and refractory components.

Fig. 1.1 combines images taken during these missions and shows cometary nuclei whose size varies between a few kilometers. The satellite-based observations have shown that the surfaces of comets become very active as they approach the sun (Gulkis et al., 2015; Sierks et al., 2015). By this is meant that the volatile components near the comet's surface sublimate. This is caused by the direct irradiation of the surface with solar energy in an airless environment. Since comets also contain solid components such as dust or organic components (Capaccioni et al., 2015; Fulle, Blum, and Rotundi, 2019; Goesmann et al., 2015), these volatile-free materials accumulate over time (Kaufmann and Hagermann, 2018) and make comet nuclei the darkest objects in the solar system (Ciarniello et al., 2015; Hsieh, Jewitt, and Fernández, 2009). The sublimation of volatiles near the surface also creates a gas drag that may detach and transport away refractory mineralic and organic particles from the surface (Gundlach et al., 2015; Keller et al., 2017; Kührt and Keller, 1994). This process causes the comet surface to lose more material with each orbit around the Sun, and the observed morphologies are the result of progressive erosion and redeposition (Thomas et al., 2015a). The chemical composition, grain size, porosity, and gravitational and cohesive forces are important determinants of the resulting morphologies, which therefore can be used as indicators of the properties of the comet's interior. Thus, the tensile strength of the cometary material can be estimated from morphological features, such as cliffs or overhangs (Attree et al., 2018a; Groussin et al., 2015). Also different boulder size

frequencies (Pajola et al., 2015, 2016a,b), desiccation processes (El-Maarry et al., 2015a; Poulet et al., 2016) or the formation of fractures by thermal stresses (Auger et al., 2018; Spohn et al., 2015) can be used as indicators for the evolution of a cometary surface and its material properties (Fig. 1.2). In particular, this work will address in more detail the influence of tensile strength and variable chemical composition of dust, ice, and organic material on the evolution of morphological features in the laboratory and compare the results with observations on a comet.

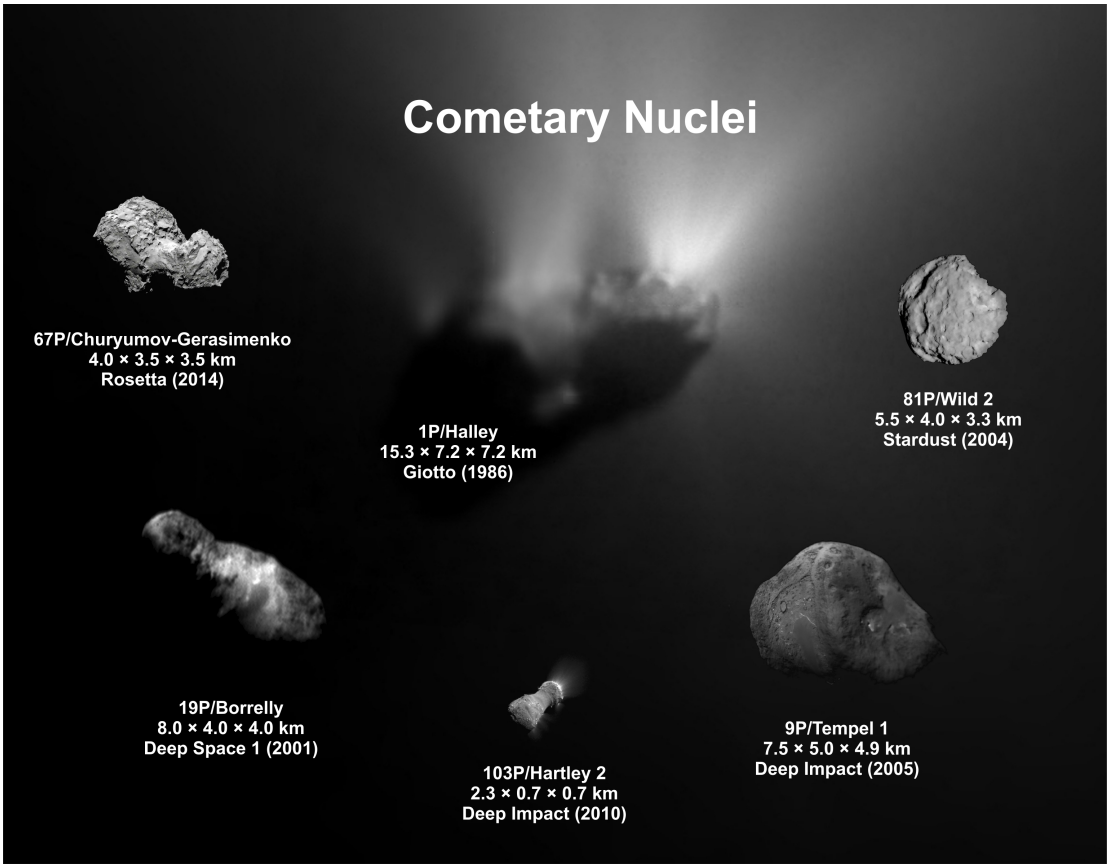

Figure 1.1: A to scale illustration of six comets approached by spacecrafts. The variety of irregular shapes of the nuclei can be seen. At 1P/Halley and 103P/Hartley 2 the emerging gas and dust particles scatter the sunlight and are visible as bright jets. Image credits: 1P/Halley: ESA/MPS (H. U. Keller); 9P/Tempel 1: NASA/JPL/UMF/Daniel Macháček; 19P/Borrelly: NASA/JPL/Daniel Macháček; 67P/Churyumov-Gerasimenko: ESA/Rosetta/NAVCAM; 81P/Wild 2: NASA/JPL; 103P/Hartley 2: NASA/JPL/UMD.

1.2 EXPERIMENTS IN THE LABORATORY

The space missions to comets revealed that they contain a wide variety of materials. In addition to mineralic dust and volatile ices, a large number of volatile and non-volatile organic substances have been detected that range from simple hydrocarbons to more complex amino acids (Capaccioni et al., 2015; Elsila, Glavin, and Dworkin, 2009; Goesmann et al., 2015; Raponi et al., 2020). As these volatile components start to sublimate with decreasing heliocentric distance of the comet, they alter the ap-

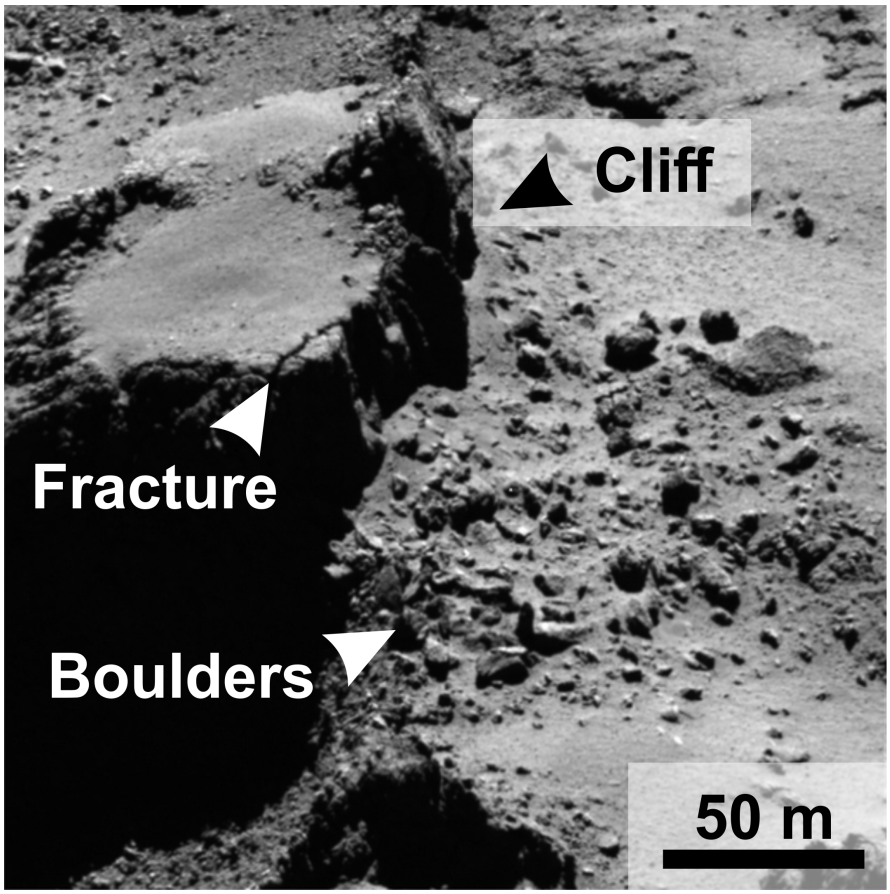

Figure 1.2: An example of various morphological features on the surface of 67P. In addition to flat areas, cliffs with developing cracks are observable, as well as boulders probably formed by mass movements. Image ID: N20141001T232953545ID30F22.

pearance and physical properties of the nucleus. To increase our understanding of these sublimation-driven processes including the morphological evolution of comets, a number of experiments were conducted in the past. Their purpose was to compare the morphologies on cometary surfaces with those in the laboratory and thus draw conclusions about chemical composition, grain size, or inter-particle forces between particles of a comet.

An important step in experimental cometary science were the KOmetenSImulation (KOSI) laboratory experiments in the early 1990s. In these experiments 11 mixtures in different ratios were prepared, containing volatile ices, such as water, carbon dioxide, methanol or ammonia, and the minerals olivine and montmorillionite (Grün et al., 1989, 1993; Lämmerzahl et al., 1995). These mixtures were filled into a cylindrical container with a diameter of about 30 cm and placed in a vacuum chamber with an angle of inclination of 40°–45°. Inside the chamber, the sample mixture was cooled to the temperature of liquid nitrogen and illuminated with approximately 1 solar constant (1 SC = 1370 W m^{-3}) (Grün et al., 1989). The surface of the samples was monitored with cameras. The resulting images were used to determine the velocity and trajectories of ejected particles. The advantage of this experimental setup was the large size of the sample surfaces, which allowed the potential emergence of macroscopic structures. In

addition, it was possible to simulate the diurnal cycle of a comet with a periodically changing insolation rate (Grün et al., 1989, 1993).

As a result of the sublimation process, a dust mantle formed on the surface within hours, which suppressed further sublimation activity (Grün et al., 1993; Kührt and Keller, 1994) and a solidified layer formed near the surface through recondensation of gaseous volatiles (Grün et al., 1993). In the early stages of the experiments, a significant amount of dust was detached from the surface and transported away and mass movements of the loose dust mantle were generated downwards the inclined sample surface (Grün et al., 1993).

A disadvantage in the experiments was that the sample mixtures differed in several components simultaneously. As a result, the influence of different volatiles, dusts and organics could not be determined systematically and independently of each other. In addition, the albedo and insolation rate differed from sample to sample, which made it difficult to compare the experiments with each other. Based on more recent knowledge, which suggests a water ice content of a comet on the order of about 25 mass% and less (Fulle et al., 2018, 2017; Herique et al., 2017; Pätzold et al., 2018), the samples water content between 75–90 mass% were also too high and not representative for comets. Nevertheless, the experiments were provided valuable insights into the evolution of comets and new protocols were developed for the production of large amounts of comet analog.

Our knowledge about comets significantly got boosted with the Rosetta mission and in the course of this mission more analog experiments were performed in the laboratories. The experiments with the Simulation Chamber for Imaging the Temporal Evolution of Analogue Samples (SCITEAS) are to be emphasized (Pommerol et al., 2015a). These experiments allowed the observation and analysis of volatile-rich samples during sublimation. The experiments focused especially on spectro-photometric analyses of volatile-rich samples and the development of their texture during sublimation. The samples with a 6×12 cm sized horizontal surface were exposed to a low pressure environment of 10^{-5}–10^{-6} mbar, cooled with liquid nitrogen, and insolated with about 1 solar constant (Pommerol et al., 2015a).

In initial experiments, samples mixed of carbon black, volcanic ash, and water ice were used, with ice particles having a diameter of 4.5 ± 2.5 µm. Major results were rapid smoothing of the originally rough surface topography and rapid darkening of the surface by carbon black and volcanic ash (Pommerol et al., 2015a). Occasional alterations of the dark layer revealed bright volatile-rich material beneath. This is consistent with observations on 67P, where bright material also became visible on the comet surface after mass movements (Barucci et al., 2016; Pommerol et al., 2015b). Further experiments with the SCITEAS experiment were carried out with mixtures of water ice organic tholins (Poch et al., 2016a). A distinction was made whether ice and tholins were combined within the individual particles (intra-mixing) or whether ice and tholins were present as separate particles (inter-mixing).

These experiments were extended by the addition of olivine and smectite, again distinguishing between intra- and inter-mixtures (Poch et al., 2016b). A significant result was that after sublimation of the water, a cohesive foam-like mantle formed on the surface of intra-mixtures, from which larger fragments detached and were ejected.

In contrast, a more compact and less cohesive mantle formed on inter-mixtures. Its subsurface was more solidified and ejected mantle fragments were much smaller (Poch et al., 2016b). However, these results are of limited validity for the development of cometary morphologies, since the proportions of tholins (<0.5 mass%) and mineral components (<1 mass%) are not representative of a comet. Also, the generally flat sample surface could not represent the complex 3-dimensional morphology of a comet. This is because these experiments were focused on studying spectral properties of the sample mixtures. Nevertheless, they provided important insights that it makes a difference whether the material in the experiment or on a comet is an intra-mixture or inter-mixture.

Kaufmann and Hagermann (2018) also performed sublimation experiments with water ice and carbon black. Their samples contained between 0.02 mass% and 0.5 mass% carbon and were exposed to a low pressure environment of 6×10^{-6} mbar. The samples were cooled to 173 K and were insolated with approximately 0.5 SC. As in previous KOSI experiments (Kochan et al., 1989; Kossacki et al., 1997), they verified the subsurface hardening of the sample material. A layer of solidified material forms during sublimation by recondensation under a volatile-free mantle with extremely low porosity. The authors assume that for different components with variable volatility, such as CO_2, CO, or methane, these layers form at different depths.

All these experiments have in common that the samples were cooled with liquid nitrogen before and during the measurements. This is necessary to prevent sintering of the ice particles, which means the coalescence of touching particles due to the heat-induced motion of the molecules (Kuroiwa, 1961). In this process, the molecules migrate from one particle to the neighboring one and form a sintering neck. Over time and with increasing temperature, this sinter neck becomes thicker and forms a stiff connection between the particles. This dramatically reduces the ability of the particles to be accelerated and transported away by the gas drag of sublimating volatiles. For water ice, the temperature at which this process no longer occurs is below 150 K (Gundlach et al., 2018a). For more volatile materials this temperature may be even lower, but is usually neglected, since most sublimation experiments are limited to water as volatile material.

In the experiments described, the temperature dependent material properties and different mixing ratios have been predominantly neglected. Though, the porosity of mixtures varies depending on the shape of the particles (Omura and Nakamura, 2017; Rogers and Head, 1961) and when the components are mixed in different ratios. Also, the surface energy of a material changes significantly when its temperature is lowered to below 150 K (Gundlach et al., 2018b; Kimura et al., 2015). As a result, the tensile strength of a sample under experimental conditions is different from that under atmospheric conditions. In order to obtain valid results in the laboratory that are comparable to the material properties of a comet, the physical properties of the sample mixtures has to be determined before the actual sublimation experiments. In addition to tensile strength and porosity of the sample mixture, this includes the shape and size of the particles as well as their density and chemical composition. Most of the latter properties can be determined with electron microscopic examinations.

To bring the investigation of comets in the laboratory to a new level, the international research project Comet Physics Laboratory (CoPhyLab) was founded. It was launched as a joint project of the Institute of Geophysics and extraterrestrial Physics of the Technical University of Braunschweig, the Physics Institute of the University of Bern and the Space Research Institute in Graz. Other participating institutes are the Max Planck Institute for Solar System Research in Göttingen, the DLR Institute for Planetary Research in Berlin and the University of Luleå.

The objective of the project is to investigate the physics and processes that generate cometary activity (e.g. Bischoff et al., 2019, 2020; Gundlach, Fulle, and Blum, 2020; Gundlach et al., 2018b). To achieve this, the properties of the most important cometary constituents, such as water, CO_2, dust and organic components, are studied initially. These materials will be combined step-wise and the new properties of the mixtures will be measured. To investigate the properties of the comet analogs under space conditions, several sublimation chambers are available in Braunschweig. In these chambers, samples of a few centimeters in size can be kept stable at $\sim 10^{-7}$ mbar and ~ 110 K and activity can be generated by insolation with an artificial sun. The duration of a single measurement would theoretically be unlimited, but for practical reasons it is limited to one day. In addition, the partner institutions provide numerous smaller facilities for experimental studies. Further phases of the project envision a combination of up to 14 instruments in a large chamber, capable of simultaneously analyzing a single sample.

This thesis was undertaken in the framework of the CoPhyLab project, conducting several sublimation experiments to further our current understanding of the relation between cometary activity and morphology. The main objectives are to analyze the evolving morphologies of samples with different compositions in the laboratory and to compare them with the morphology of 67P. To obtain results comparable to observations on 67P, particle and energy scalings must be used that address the different gravitational and cohesive forces in the laboratory and on the comet. If it is possible to reproduce morphological features in the laboratory as observed on 67P (El-Maarry et al., 2019; Pajola et al., 2016a; Thomas et al., 2015b), this may provide important implications as to the actual chemical and physical properties of the comet. These experiments are divided into three successive complexes and their results were published in three papers, which constitute Chapters 3–5 of this thesis.

- SELECTING SUITABLE COMET ANALOG MATERIALS

In these experiments, various mineralic dusts and water ice are mixed together and their suitability as analog materials are tested. The focus is on the cohesion of the analogs in dependency of particle shape and temperature.

Particle shape and size determine the porosity of a granular material and thus the number of inter-particle contacts in a given volume. The cohesion of the particles between each other depends on the surface energy of the material and translates into the macroscopic property of tensile strength. In these fundamental experiments, the tensile strength of pure materials with different surface energies and their mixtures is to be determined as a function of the particle shape and at temperatures below 150 K. The objective is to produce samples with as high porosity and low tensile strength as possible, which would be comparable to those of a comet (Hornung et al., 2016; Pätzold

et al., 2018). Data obtained from these experiments have also be used to improve and calibrate numerical models that simulate granular materials of comets (Kappel et al., 2020). The most suitable mixtures will be used as comet analogs in further sublimation experiments.

- ANALYSIS OF THE SUBLIMATION ACTIVITY OF MIXTURES OF DUST AND ICE

An understanding of the composition of the comet's nucleus is essential to interpret the morphology displayed in images from the Rosetta mission. For this purpose, sublimation chambers that can simulate space conditions as realistically as possible can be used in the laboratory. Temperature, near vacuum, and insolation flux of a comet can be reproduced comparatively easily in such a chamber. It is more complex to adapt the experiments in such a way that Earth's gravity plays only a minor role. To achieve this, the cohesive forces determined in the first step are scaled with gravity and the ratios of both forces are adjusted to cometary values.

The first sublimation experiments are performed with sample mixtures consisting of only two components. This allows to keep the degree of complexity low and to analyze the influence of a separately changed parameter to the development of the sample morphology, such as dust-ice ratio, insolation angle, or insolation flux. The results will be analyzed to determine which conditions in the laboratory most realistically reflect the observed morphology of 67P.

- EXTENSION OF SUBLIMATION EXPERIMENTS WITH ORGANIC COMPONENTS

In the third step, the degree of complexity is increased and an organic component is added to the dust-ice mixtures. Since a large number of different organic compounds have been detected on 67P (Capaccioni et al., 2015; Goesmann et al., 2015; Raponi et al., 2020), their influence on the evolution of the comet's surface cannot be neglected. Because the actual amount of organic material in the comet's nucleus is not known, these experiments are performed to investigate the effect of different amounts of organic material on the sublimation process. Since there are many different compounds, it is not practical to use only one organic analog in the experiment. Such a material could not simulate the multitude of different effects to a cometary surface. Therefore, the two different organic substances glycine and sodium acetate are combined and used simultaneously, each representing the larger classes of amino acids and organic salts, respectively. They were chosen in such a way that their occurrence on 67P has been proven, yet their properties are interchangeable with other substances. Again, to keep the complexity of the experiments as low as possible, all organic substances are checked before the sublimation experiments to ensure that they are not volatiles and remain as refractory material on the sample surface. Finally, the resulting morphologies in the laboratory are compared with observations on 67P and the responsible laboratory conditions are assessed for their plausibility as representative cometary properties.

1.3 THESIS ORGANIZATION

This cumulative dissertation results from the collaboration of the Institute for Planetary Research as part of German Aerospace Center (DLR) with the international CoPhyLab

project. The central parts of the work were the determination of the properties of cometary analog materials and the sublimation experiments, carried out at the Technical University of Braunschweig. Particle shape, particle size distribution, density, and chemical composition of the mineralic dusts and the porosity of the sample mixtures were determined at DLR. A scaling model of force ratios and insolation flux was developed, allowing laboratory data to provide implications about the evolution of a cometary surface. The focus of the experiments was at the morphological evolution of the samples as a function of composition and insolation. The results were compared to morphological features on 67P to draw conclusions about the material properties of the comet. The thesis is divided into six chapters including this introduction.

Chapter 2 describes the methods that were used in order to meet the objectives. It describes properties and preparation of the samples and the operating principle of the Brazilian disk test. In addition, the design and characteristics of the vacuum sublimation chamber are described. The following three Chapters 3, 4, and 5 correspond to articles whose first author is the author of this dissertation and which have been submitted to and published in peer-reviewed journals. They are independent articles and therefore contain their own introductions and conclusions. The size and positions of the figures have been adapted to the format of this thesis. The references of all three articles have been combined with those of other chapters at the end of the thesis and were not listed separately.

Chapter 3 includes the article "The tensile strength of dust-ice mixtures and their relevance as cometary analog material" published in "Astronomy & Astrophysics" in 2020. In this study, the tensile strength and surface energy of various particle types and their mixtures are determined as a function of particle size, shape, and temperature and are assessed for their suitability as comet analogs.

Chapter 4 was published in 2021 as "Sublimation of ice-dust mixtures in cooled vacuum environments to reproduce cometary morphologies" in "Astronomy & Astrophysics". In this article, two series of sublimation experiments with either vertical or horizontal insolation are described. Samples of refractory mineralic dust and volatile water ice in different mixing ratios were placed in a vacuum sublimation chamber and the evolution of the samples was monitored over time and analyzed with respect to composition and illumination angle. The results show which ratios of dust and ice realistically reproduce observed processes and morphologies of a comet.

Chapter 5 is an article published as "Sublimation of organic-rich comet analog materials and their relevance in fracture formation" in "Astronomy & Astrophysics" in 2021. In this work, the sublimation experiments from Chapter 4 were extended by a refractory organic component, added to mineralic dust and volatile water ice. The analyses focus on the evolution of sample morphology as a function of the mixing ratios of the three components and the implications on cometary surfaces.

Chapter 6 discusses the results of the three articles and summarizes the conclusions that can be drawn from these studies.

2 METHODS

2.1 SAMPLE PREPARATION

Since the composition of comets is very complex (e.g. Choukroun et al., 2020), a compromise had to be found between chemical and physical accuracy and a complexity as low as possible. For this work a number of experiments were performed with sample compositions consisting of two or three components. These components were polydisperse particles of either silica, fly ash, water ice, or a compound of glycine and sodium acetate, each in variable ratios.

The silica or fly ash particles represented the refractory dust fraction and were analyzed for their chemical composition and grain shape by electron microscopy before the experiments. Silica particles consist of pure SiO_2 and had a very angular grain shape. Fly ash particles were spherical and their chemical composition correspond approximately to that of plagioclase (Table 3.1). The amount of dust in the sample mixtures was determined with a scale.

Water ice represented the volatile fraction detected on comets (Fulle et al., 2018, 2017; Sierks et al., 2015; Sunshine et al., 2006). The ice particles were generated by spraying mist from a water droplet dispenser into a Dewar vessel that was filled with liquid nitrogen (Gundlach et al., 2018b). The water droplets immediately froze, retaining their spherical shape, and sank to the bottom of the vessel. Thus, a suspension of liquid nitrogen and water ice was produced. To determine the amount of water ice in the Dewar vessel, Archimedes' principle was used since the volume of the vessel and the densities of liquid nitrogen and water ice were known (Table 5.1).

To obtain the sample mixtures for the experiments, predefined amounts of dust were added to the suspension of liquid nitrogen and ice in the Dewar vessel. This liquid mixture was manually stirred with a ladle, until all components were evenly distributed. This mixture was immediately taken from the Dewar vessel and filled into a cylindrical pre-cooled metal mold. Still in a well-mixed suspension and cooled by the cylindrical mold, the liquid nitrogen slowly evaporated and a very porous sample of dust and ice remained in the cylinder. Finally, the cylinder was removed and the freestanding sample could be used for experiments.

With this method, the particles in the samples consisted of pure dust and pure ice, forming a "salt-and-pepper" inter-mixture (Poch et al., 2016b). The combination of dust and ice in a suspension of liquid nitrogen had the advantage that all particles were uniformly cooled. On the one hand, the particles had the temperature necessary to simulate the temperature conditions of a comet (Blum et al., 2014; Kührt, 1984), and on the other hand, sintering of the ice particles was prevented (Gundlach et al., 2018a; Kuroiwa, 1961), which would create stiff connections between the particles and lead to high tensile strength values that are unrealistic for comets.

The compounds glycine and sodium acetate used in the experiments, were supposed to represent the large variety of organic material that has been detected on comets (Capaccioni et al., 2015; Fulle et al., 2017; Goesmann et al., 2015). Under normal laboratory conditions these compounds exist in crystalline form and were tested for their refractory character in the chamber before the actual experiments.

To bring the organic-rich particles into a shape comparable to that of the dust and ice particles, the method of spraying mist into liquid nitrogen was modified. Predefined amounts of organics were dissolved completely in a given volume of liquid water and filled into the water droplet dispenser. Analogous to pure water, the produced organic-rich mist was sprayed in liquid nitrogen, froze, and sank to the bottom of the Dewar vessel as spherical particles. The amount of the resulting organic-rich ice particles was again determined by using Archimedes' principle. In contrast to the two-component dust-ice mixtures, these particles were intra-mixtures (Poch et al., 2016b) of organic molecules in a matrix of water ice, since different components are present in a single particle. To complete the sample mixtures, predefined amounts of dust were added to the suspension of liquid nitrogen and organic-rich ice particles. Hadraoui et al. (2019) have shown that using intra-mixtures of ice and organics is also the most promising method to reproduce the presence of refractory organic material observed in the coma of a comet.

To obtain the porosity for each of the different sample mixtures, 15 samples of each mixture were prepared with the cylindrical mold as described above before the actual sublimation experiments. After the liquid nitrogen had evaporated from the sample mixtures, their weight and volume were measured and with the known densities and ratios of the used components, the average porosity of the mixtures was determined. This porosity was used as reference value for the samples in the experiment and was also used to determine the tensile strength of the different sample mixtures after the following Brazilian disk test.

2.2 BRAZILIAN DISK TEST

The Brazilian disk test is an established method to measure the tensile strength of a material (Gundlach et al., 2018b; Li and Wong, 2013; Meisner, Wurm, and Teiser, 2012). In this test, the cylindrical shaped samples are split by a slowly descending piston into approximately two equal halves along their longitudinal axis. The pressure at which the samples break is determined and can be interpreted as the tensile strength σ of the sample. In combination with the porosity Φ, the particle radius r, and the average number of inter-particle contacts N, the surface energy γ of the material can be calculated with $\gamma = 8r\sigma/3N\Phi$ (Blum et al., 2006) (for detailed description see Sects. 3.2.2 and 3.3.3). The surface energy is a material property and independent of the shape of the particles. Therefore, if the particle shape is spherical, the known average surface energy and porosity of a sample can be used reversely to determine its unknown tensile strength. So far, the Brazilian disk test has been used to determine the tensile strength of pure substances, such as water, silica (Gundlach et al., 2018b), or granular organic substances (Bischoff et al., 2020). In this work, the first step was to determine the tensile strength of each component and their combinations. This was a prerequisite to interpret the results of the actual sublimation experiments with

complex sample compositions in a meaningful way.

Although the Brazilian disk test is a simple method to determine the tensile strength of a material, it is also restricted by some limitations. Most importantly, the tensile strength of a sample cannot be arbitrarily low. The piston must descend to a sample that initially resists the applied pressure until it abruptly breaks under. Otherwise, if the porosity of the sample material or the mobility of the particles are very high, the piston will continuously push or cut into the sample without breaking it. To avoid this, the cylindrical samples were compacted with pressure during the preparation for the Brazilian disk test. A pre-cooled stamp with the exact size of the inner diameter of the cylindrical mold was placed on top of the nitrogen-free sample material inside the mold and pressed down. During this process decreased the porosity of the sample and increased the average cohesion and tensile strength of the sample material. Then the volume and mass of each individual sample were measured and the new sample porosity was determined. Subsequently, the tensile strength of the compacted samples was measured with the Brazilian disk test method. Using the porosity and the average number of inter-particle contacts of the compacted samples (Gundlach et al., 2018a; Murphy, 1982; Yang, Zou, and Yu, 2000), the constant surface energy of the sample material was calculated. This surface energy was used to reversely calculate the tensile strength of samples that were not compacted and whose properties were not suitable for the Brazilian disk test.

During the Brazilian disc test, it was necessary to ensure that the temperature of the samples was constantly below 150 K and that they were protected from atmospheric moisture from their preparation until the end of the measurement. The entire sample preparation and the measurement were carried out in a Styrofoam box, which was initially cooled with liquid nitrogen and filled with a moisture-free protective atmosphere of evaporated nitrogen (see Sect. 3.2.2). The gaseous nitrogen inside the box had a sufficiently low temperature and high density to form a stable barrier against the surrounding atmosphere at room temperature. In addition, immediately after the sample was prepared in the Styrofoam box, a pre-cooled metal housing was placed around the sample. This housing had only two openings. A narrow slit through which the piston descended onto the sample and a lateral opening through which the camera was focused at the sample. The pre-cooled housing, the volume inside the housing, and the sample holder were equipped with thermal sensors and their temperature was monitored in real time throughout the whole experiment. This ensured that only measurements with temperatures below 150 K were analyzed and that sintering of the ice particles could be excluded.

2.3 PARTICLE AND ENERGY SCALING

One of the biggest challenges to simulate cometary conditions in the laboratory is the Earth's gravity, which is about five orders of magnitude higher than on 67P (Agarwal et al., 2016). Assuming that comets are composed of granular material with millimeter-to-centimeter-sized particles (e.g., Blum et al., 2014, 2017; Fulle et al., 2016; Kretke and Levison, 2015; Lorek, Lacerda, and Blum, 2018; Zsom et al., 2010), the cohesive forces

between these particles are more important than the gravity affecting them (Scheeres et al., 2010; Sánchez and Scheeres, 2014). If these conditions are not addressed in the laboratory, experiments cannot provide meaningful results. Since gravity is invariant, a method must be found to change the cohesive force between particles in the laboratory to a threshold at which the ratio of gravity and cohesion is equivalent to that on a comet. This can be achieved by selecting granular matter with very small grain sizes.

The cohesive force F_C between two spherical particles is linearly dependent on the particle radius r and the surface energy γ and follows

$$F_C = 3\pi r\gamma\,. \tag{2.1}$$

Small particle radii thus lead to reduced cohesion between two particles. However, in a given volume, the number of small particles and their mutual contacts increases with the third power and thus the total cohesion of a granular material. Bischoff et al. (2019) presented a model suggesting that on Earth particles with radii of $\sim$35 µm are subject to approximately equal cohesive and gravitational forces. For sufficiently small particle sizes below this threshold, a cohesion-to-gravity ratio equivalent to that on 67P can be achieved in the laboratory, even though the absolute values of the forces on Earth and on 67P differ significantly.

With this approach, spherical particles used in the laboratory offers several advantages:

- The cohesive force between particles is easy to calculate.
- The spherical shape prevents mutual interlocking of the particles, which would lead to reduced particle mobility.
- The porosity of materials composed of polydisperse spherical particles is higher than those of angular particles (Rogers and Head, 1961). This allows the preparation of samples with porosities closer to that of a comet.

For the particle size scaling the assumption was used that the ratio of gravity and cohesion affecting material on 67P is comparable to that of weak rock on Earth (Groussin et al., 2015). This assumption seems plausible as observed morphological features on 67P (e.g., cliffs, fractures, or mass movements) are very similar to those on Earth (Fig. 1.2; El-Maarry et al., 2019; Pajola et al., 2016a; Thomas et al., 2015b). If cohesion would be much more dominant on 67P, exotic morphologies could be expected on ist surface, such as extreme overhangs or filigree structures, which would collapse on Earth because of their own weight. On the other hand, if gravity were more dominant compared to conditions on Earth, the surface of 67P would be expected to be much smoother, as cliffs and rocks are unstable and would collapse under their own weight (Kappel et al., 2020). Following this suggestion, the force ratios on 67P and on Earth are

$$\frac{F_{G_{67P}}}{F_{C_{67P}}} \approx \frac{F_{G_{\text{Earth}}}}{F_{C_{\text{Earth}}}}\,. \tag{2.2}$$

With the gravitational forces F_G given and the cohesion F_C of the samples determined with the Brazilian disk test, it was possible to estimate the size-depended cohesion

(Equ. 2.1) between particles on 67P, which were simulated with particles in the laboratory. The particle scaling also allowed to select the size of spherical particles in the experiment so that they were suitable to simulate presumably irregular particles on 67P (Blum et al., 2017; Fulle et al., 2016; Kretke and Levison, 2015; Lorek, Lacerda, and Blum, 2018). A detailed description of the particle size scaling can be found in Sect. 4.2.2.

The scaling of the particle size increased the inter-particle forces of the sample material with respect to the Earth's gravity. To detach particles from the surface and to transport them away these increased inter-particle forces must be exceeded by another force. In the experiments, the force responsible for this is the near-surface pressure drag, caused by the vapor pressure of sublimating water ice. To generate sufficient pressure drag, the energy insolated to the sample surface must be scaled with the increased cohesion of the samples. This second scaling in the laboratory allowed the reproduction of the ratios between cohesion and pressure drag on 67P.

In a first step the surface temperature of 67P was estimated as a function of ist heliocentric distance. The energy balance of insolation and sublimation is given by the Stefan-Boltzmann law plus a term for the sublimation heat flux, derived from Hertz-Knudsen (Kührt and Keller, 1994) (for details see Sect. 4.2.3).

In a second step it was assumed that the ratios of pressure drag and cohesion on 67P and in the laboratory are comparable, since in both environments the pressure drag has to exceed the cohesion slightly to detach particles from the surface. This relationship follows

$$\frac{F_{D_{67P}}}{F_{C_{67P}}} \approx \frac{F_{D_{\text{Earth}}}}{F_{C_{\text{Earth}}}} \tag{2.3}$$

in analogy to the particle size scaling. The pressure drag, F_D, results from the vapor pressure, acting on the particle cross section (Fanale and Salvail, 1984) as

$$F_D = \pi r^2 \, 3.56 \times 10^{12} \, \text{Pa} \, \exp\left\{\frac{-6142 \, \text{K}}{T}\right\}. \tag{2.4}$$

Using the calculated temperature T from step one, the particle radius r in the laboratory, and from the particle scaling the cohesions F_C in the laboratory and on 67P, the temperature-dependent gas drag in the laboratory can be estimated with Eq. (2.3).

It should be noted that the addition of blackening materials such as carbon to the sample material was intentionally omitted. The particles of these materials would have a non-spherical shape and their size would be more than an order of magnitude larger than that of ice and fly ash particles. This would change the calculated tensile strength of the samples and would increase the complexity of the experiments. Therefore, the only darkening material used was fly ash, whose albedo was determined to be 0.35. To take into account the very low albedo of 0.06 of 67P (Ciarniello et al., 2015), the higher albedo of fly ash was considered in the energy scaling and compensated for by a higher energy input (see Sect. 4.2.3). The albedo of the fly ash was also used as an approximation for the ice-dust mixtures, since the albedo of ice-bearing materials is mainly determined by the albedo of the dust component (Chýlek, Ramaswamy, and

Srivastava, 1983; Clark and Lucey, 1984; Oehler and Neukum, 1991). With the energy scaling, it was possible to estimate the simulated heliocentric distance in the laboratory at a predefined insolation flux (see Eq. (4.4)).

2.4 SUBLIMATION EXPERIMENTS

For the sublimation experiments described in Chapters 4 and 5, a cylindrical vacuum chamber was used. The chamber was 80 cm high, had an inner diameter of 25 cm and two windows for simultaneous vertical or horizontal insolation and observation. To minimize the influence of thermal background radiation on the sample, a cooling shield was installed inside the chamber. It was a 10×10 cm cuboid metal housing and actively cooled with liquid nitrogen for the duration of the experiments. The cooling shield had one opening at a side wall and one at its top to allow insolation and observation of the sample, which was placed on a sample holder inside the cooling shield. To prevent light from reflecting back from the inner walls onto the sample, the cooling shield was coated black on the inside (for detailed information see Fig. 4.4 and Sect. 4.2.6).

Before the start of the measurement, the chamber was filled with an argon atmosphere and cooled down to 110 K. The argon prevented atmospheric moisture from entering the chamber once it was opened for sample insertion. The prepared samples were immediately placed inside the cooling shield. In the chamber, constant low temperatures and the absence of moisture prevented the samples from altering before the start of the experiment. After the samples were mounted, the chamber was closed again and the pressure was lowered to $\sim 10^{-7}$ mbar. Pressure and temperature inside the chamber were permanently monitored and ensured to be constantly comparable to those on a comet (Kührt, 1984).

When the pressure in the vacuum chamber reached its operating value of $\sim 10^{-7}$ mbar, the samples were insolated from one direction through the windows in the vacuum chamber and the cooling shield. In the experiments described in Chapter 4, a halogen lamp with variable intensity was used to insolate sample mixtures of dust and ice. Two series of measurements were performed with an insolation flux of either ~ 1 or ~ 3 solar constants. This setup allowed the insolation angle to be changed between horizontal and vertical to the sample surface. Insolation angle and flux were varied from sample to sample, but remained constant during a measurement.

For the experiments with samples mixed of dust, ice, and organics (Chapter 5), a solar simulator was used with a fix insolation flux of 1.9 solar constants. With this setup, the samples could only be insolated in the vertical direction. For visual monitoring, a camera with a 3000×2000 pixel sensor was focused at the sample through the side window in the cooling shield and captured images at a frame rate of one image per second. Theoretically, the duration of a measurement would be unlimited, but was reduced to a maximum of 20 h when the nitrogen supply had to be replenished.

At the end of the experiment, the remnants of the samples were removed from the chamber and qualitatively analyzed for strength and the amount of remaining ice. The images taken of the sample surface were analyzed and used to compare with images of 67P.

3

TENSILE STRENGTH OF DUST-ICE MIXTURES AND THEIR RELEVANCE AS COMETARY ANALOG MATERIAL

David Haack[1] (corresponding author), Bastian Gundlach[2], Christopher Kreuzig[2], Dorothea Bischoff[2], Ekkehard Kührt[1], Jürgen Blum[2], Katharina Otto[1]

[1]*Institut für Planetenforschung, Deutsches Zentrum für Luft- und Raumfahrt (DLR), Berlin, Germany*

[2]*Institut für Geophysik und Extraterrestrische Physik, Technische Universität Braunschweig, Braunschweig, Germany*

Published in Astronomy&Astrophysics, Volume 642, October 2020, Article Nr. 218
https://doi.org/10.1051/0004-6361/202037763, reproduced with permission © ESO

ABSTRACT

The tensile strength of granular matter is of great importance to our understanding of the evolution of comets and to our attempts to reproduce processes on cometary surfaces in laboratory experiments. In this work, we investigate the tensile strength of three different materials and their mixtures, which can be used as cometary analog materials in the laboratory.
We used two types of siliceous dusts and granular water ice whose polydisperse particles were either angular or spherical. Our samples were cooled to below 150 K to better simulate the conditions of a cometary surface and to avoid thermal alteration of the material. We used the Brazilian disk test method to exert stress on the cooled samples and determine the tensile strength at the moment the samples broke.
We find that the tensile strength of two component mixtures is strongly dominated by the component with the higher tensile strength. The materials made of mostly angular dust particles have a lower filling fraction, but a higher tensile strength compared to materials made of spherical particles. Furthermore, the tensile strength of the cooled components is substantially lower than the tensile strength of the same components at room temperature. This implies that the surface energy of the investigated materials at low temperatures is significantly lower than previously assumed.

3.1 INTRODUCTION

Despite visits of recent space missions to comets (e.g., ESA's Rosetta mission and NASA's Deep Impact mission), the activity of comets is not yet well understood. Direct observations and laboratory experiments on Earth have shown that cometary surfaces are very active when approaching the Sun. Near-surface volatiles enter the gas phase through sublimation and drag nonvolatile particles with them (Gundlach et al., 2015; Keller et al., 2017; Kührt and Keller, 1994). Through this process a comet loses material

during each orbit until it finally extinguishes. In the 1990s sublimation experiments with dust-ice mixtures were performed as part of the KOSI (KOmetenSImulation) project to simulate and understand these cometary surface processes (e.g., Grün et al., 1989, 1993; Lämmerzahl et al., 1995). However, these experiments are not suitable and were not designed to understand complex morphologies such as cliffs, cracks, or mass movements that have only later been observed on 67P/Churyumov-Gerasimenko (El-Maarry et al., 2019; Pajola et al., 2016a; Thomas et al., 2015b). The composition and grain size of the material, interparticle forces, and porosity are of fundamental importance in processes that form these morphologies. These parameters find their macroscopic expression in the tensile strength of the comet-forming materials and determine whether cliffs, cracks, or boulders can form on the surface of a comet (El-Maarry et al., 2015a; Groussin et al., 2015; Vincent et al., 2016a).

In this work we examined the suitability of different components and their mixtures as cometary analogs with respect to their tensile strength. According to the Johnson-Kendall-Roberts (JKR) theory from Johnson et al. (1971) the tensile strength is linearly dependent on the surface energy of a material. This approach is suitable to calculate the surface energy of granular materials made of spheres and to compare liquid nitrogen cooled samples and uncooled samples of previous works (Kimura et al., 2015). The tensile strength of granular matter is also dependent on the number of mutual contacts of individual particles. This number transfers into the macroscopic value of the filling fraction and describes how much free space is in a volume filled with particles.

To realize the analyses, the Brazilian disk test is an established method to measure the tensile strength of a material (Li and Wong, 2013; Meisner, Wurm, and Teiser, 2012). In this test, pressure is applied to cylindrical samples until they break. The pressure exerted in the moment of the breakup refers to the tensile strength and can be analyzed. So far, using the Brazilian disk test method, the tensile strength has only been measured for the pure components from which a comet could be formed, for example, water ice, or dust with a tensile strength of a few kilopascals (Gundlach et al., 2018a; Steinpilz, Teiser, and Wurm, 2019) or granular organic materials (Bischoff et al., 2020). In this study, we present Brazilian disk test measurements of mixtures of different components that could be considered as cometary analog materials and show their dependence on particle shape, tensile strength, filling fraction, and surface energy. With the data obtained from these measurements, numerical models simulating granular matter on comets (Kappel et al., 2020) can be improved or calibrated.

A major challenge to design Earth-based experiments and to find suitable analog materials is to overcome Earth's gravity that usually is orders of magnitude larger than comets. On a comet gravity plays a minor role in solidity, which is dominated by the cohesion of its components (Scheeres et al., 2010; Skorov and Blum, 2012; Sánchez and Scheeres, 2014). In order to achieve a regime dominated by cohesion in the laboratory, the used particles have to be very small. When the particle radius is less than 50 µm, the amount of mutual particle contacts in a given volume produces cohesive forces that exceed gravity (Bischoff et al., 2019). Thus, to produce cometary analog materials whose mechanical properties are dominated by cohesion, particle sizes in the laboratory must be on the order of a few microns. We selected the three materials water ice, silica, and fly ash with particle sizes in this range, but different particle

shapes, and we analyzed their influence on filling fraction, tensile strength, and surface energy of a sample.

In recent years, experiments with vacuum sublimation chambers were used to simulate space conditions to investigate the evolving surfaces of dust-volatile mixtures (Kaufmann and Hagermann, 2018; Poch et al., 2016a,b). As part of the Cometary Physics Laboratory (CoPhyLab) project, we aim to support these and similar experiments by studying various siliceous dust and water ice mixtures not only for their tensile strength but also their suitability as cometary analog materials. In addition to the influence of different materials and low temperatures, we investigate how spherical and angular grain shapes affects the tensile strength. The results contribute to a better understanding of the formation of the observed morphologies on a surface of the comet.

3.2 METHODS

3.2.1 *Sample preparation*

We conducted three series of experiments with samples that were composed of two of three materials in varying mixing ratios. The first mixture comprised water ice spherules and angular silica (icy spherical-angular mixture), the second comprised water ice spherules and fly ash (icy spherical-spherical mixture), and the third mixture included fly ash and silica (dry spherical-angular mixture). We used these mixtures to test the dependence of the tensile strength on the ice content of the mixture and the shape of the involved particles. We picked these three materials to simulate the different components of a comet. Silica or fly ash represent the siliceous dust content of a comet and the water ice represents its volatile component. Furthermore, with angular silica and spherical fly ash we were able to study the influence of different particle shapes on the tensile strength. All three components (silica, fly ash, and water ice) had a comparable average grain size (Fig. 3.1, Table 3.1). Notably, the grain size distribution of fly ash is wider than that of silica (Fig. 3.2).

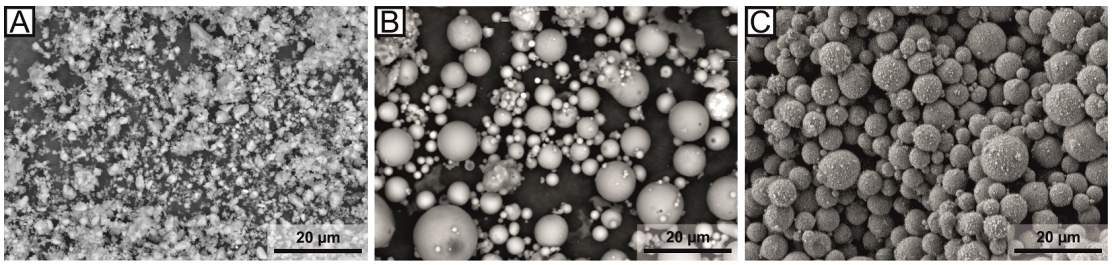

Figure 3.1: Images of particles used in this work taken with an electron microscope. In panel A) angular silica particles, panel B) spherical fly ash particles, and panel C) spherical water ice particles at the same scale are shown.

In order to investigate the tensile strength of ice-dust mixtures, we used silica and fly ash as the dusty component of a cometary regolith and combined these in two-component mixtures with water ice. The first dusty component was silica with polydisperse particles of highly angular shape and with the physical and chemical properties shown in Table 3.1. The second dusty component was fly ash with polydis-

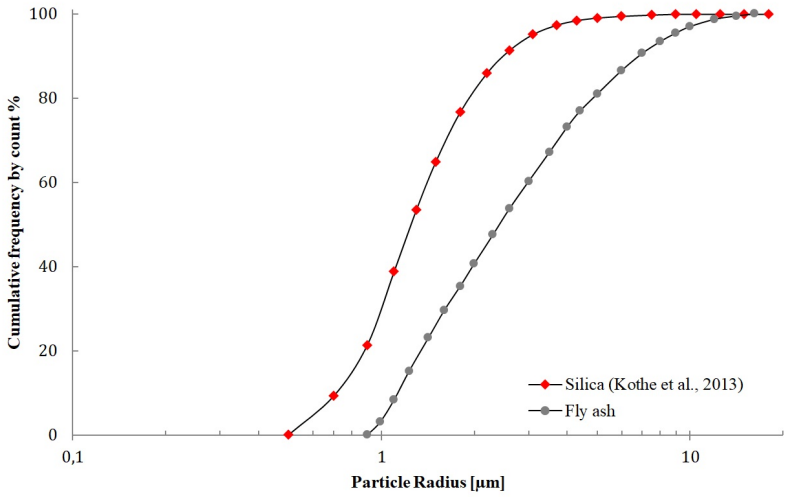

Figure 3.2: Cumulative size distributions of dust particles. Irregularly shaped silica particles are indicated as red diamonds and spherical fly ash particles as gray dots. The grain size distribution of fly ash is wider than that of silica.

perse particles of approximately spherical shape. This material is a mixture of mostly SiO_2 and Al_2O_3 (Table 3.1). To constrain the particle size distribution, the fly ash was sieved to a maximum particle diameter of 25 µm. Another advantage of fly ash is that it is inexpensive and available in large quantities. It must be noted that fly ash may contain minor amounts of magnetic components. These magnetic particles are not spherical and, at more than 25 µm, much larger than the majority of the fly ash particles. Before our experiments started, these components were largely removed by sieving and remained in negligible quantities in the samples. Electron microscopic comparisons of non-sieved and sieved fly ash confirmed the removal of these particles. Furthermore, the samples were not exposed to strong electromagnetic fields during the experiment, which could have an influence on the fracture behavior of the samples. Therefore, we neglected potential magnetic behavior of these particles in our analysis. The volatile component was water ice with particles of spherical shape. To produce the water ice particles, mist from a water droplet dispenser was sprayed into a Dewar vessel filled with liquid nitrogen (Gundlach et al., 2018a). The water droplets instantaneously froze and sank to the bottom of the liquid. The result was a suspension of polydisperse spherical ice particles in liquid nitrogen.

To determine the amount of water ice in the Dewar vessel we used Archimedes' principle. We measured the weight of a certain volume of pure liquid nitrogen and the weight of the same volume of liquid nitrogen with suspended water ice. The weight difference between both measurements and the known density of liquid nitrogen and water ice allowed us to calculate the mass of water ice in the Dewar vessel. The amount of the used dust was directly measured with a scale.

The usage of liquid nitrogen as a coolant also simulated the required temperature conditions of a comet (Kührt, 1984) and prevented sintering of the ice particles (Gundlach et al., 2018b; Kuroiwa, 1961; Thomas, Ratke, and Kochan, 1994) in the samples and the experimental setup. Otherwise, sintered ice particles would result in unrealistically high values for the tensile strength.

Table 3.1: Characteristics and chemical composition of individual components mixed to simulate cometary materials. *Specifications for silica given by the manufacturer: 99 % of particles have radii between 0.5 µm and 10 µm and 80 % of particles between 1 µm and 5 µm. This size distribution was analyzed and fitted by a log-normal distribution by Kothe et al. (2013).

	Silica	Fly ash	Water ice
Particle shape	angular	spherical	spherical
Particle radius [µm]	1.3*	2.43±1.41	2.38±1.11
Density [g cm^{-3}]	2.65	1.91	0.93
Compd %			
SiO_2	100.00	59.20	
Al_2O_3		27.90	
FeO		3.86	
CaO		3.62	
K_2O		2.67	
MgO		1.51	
TiO_2		1.40	
Na_2O		0.68	
H_2O			100.00

To produce the icy spherical-angular and the icy spherical-spherical mixtures predefined amounts of either silica or fly ash were added into the Dewar vessel filled with liquid nitrogen and the known amount of water ice spherules. To get the exact mixing ratios, the amounts of used silica and fly ash were measured with a scale. The two types of particles and the liquid nitrogen were mixed manually with a ladle until all particles were in suspension. We then immediately removed material with the ladle from the Dewar vessel and filled it into the cylindrical steel mold while the particles were still in suspension. Given the difficulties in preparation and the fragility of the material involved this is the currently best method to mix the particles sufficiently well. The dry spherical-angular mixture was also prepared in liquid nitrogen to maintain consistency during sample preparation and the experiment.

The mixtures of particles and liquid nitrogen were then filled into a precooled steel mold with an inner diameter of 26 mm. After the evaporation of the liquid nitrogen, cylindrical samples were pressed by manually pushing a stamp down onto the material. To maintain consistency, a lid was placed over the stamp and the experimenter pressed onto the lid with his full body weight for 5 seconds. Given that the weight of the experimenter was constant over the experiment series time frame, this method allowed for a reliable and reproducible implementation of 1.2 MPa to the cylindric sample. However, to reflect variations in weight due to clothing and other natural fluctuations, we assumed an error of 0.05 MPa. At the end of the preparation process, and while

still inside the mold, the length and mass of each sample were determined to calculate the filling fraction. The cylindrical samples were subsequently used to measure the tensile strength of the mixtures with the Brazilian disk test (details next section).

3.2.2 *Brazilian disc test*

Initially, the atmosphere in a precooled polystyrene box was replaced by the evaporation of liquid nitrogen to provide minimal air humidity during the measurement. The samples produced in Sect. 3.2.1 were horizontally placed in this polystyrene box while still in the cylindrical pressing mold. Then the detachable pressing mold was removed so that the now free sample rested on a sample holder inside the polystyrene box (Fig. 3.3A). A metal box (cooling shield) was placed around the sample on its holder to keep it at constantly low temperatures. To ensure this, the sample holder and cooling shield were stored in liquid nitrogen and placed inside the polystyrene box directly before the measurement. Thermocouple sensors monitored the temperatures of the sample holder, cooling shield, and atmosphere inside the cooling shield and ensured constant low temperatures of less than 150 K. This temperature is necessary to prevent sintering of the water ice particles before and during the measurement (Gundlach et al., 2018a,b; Kuroiwa, 1961). The cooling shield also reduced the formation of frost on the sample surface from atmospheric moisture that could penetrate the box during the measurement. A camera was installed in front of the sample to record the experimental process.

Through a narrow slit in the cooling shield ,an actively cooled piston (1 × 30 mm) was used to apply pressure on the full length of the cylindrical surface of the horizontal sample (Fig. 3.3A). The pressure was continuously increased by lowering the piston with a motor that descends at a constant speed of 0.05 mm s^{-1}. The polystyrene box with the entire precooled experimental setup inside was placed on a scale to record the weight and thus the exerted force. The increasing force transforms into a stress on the sample. The stress at which the sample broke longitudinally in two similar sized half-cylinders was determined (Figs. 3.3B and 3.4) and reflects the tensile strength σ of the sample material by

$$\sigma = \frac{2F}{\pi DL}. \tag{3.1}$$

In this equation, F is the force applied to the cylindrical sample in the moment of breakup, D is the sample diameter of 26 mm, and L the length of the sample, which slightly varied for each sample with an average of 25 mm. Simultaneously, images of the samples and evolving cracks were taken with the camera (Fig. 3.3B) for visual reference of the quality of each individual experiment. As a consequence of the low strength of the involved materials and the challenges arising when handling equipment cooled with liquid nitrogen, this method is very delicate and requires practice; therefore not every experiment resulted in a satisfying measurement. Only samples that showed a clear and central break along their longitudinal axis were used for the analyses

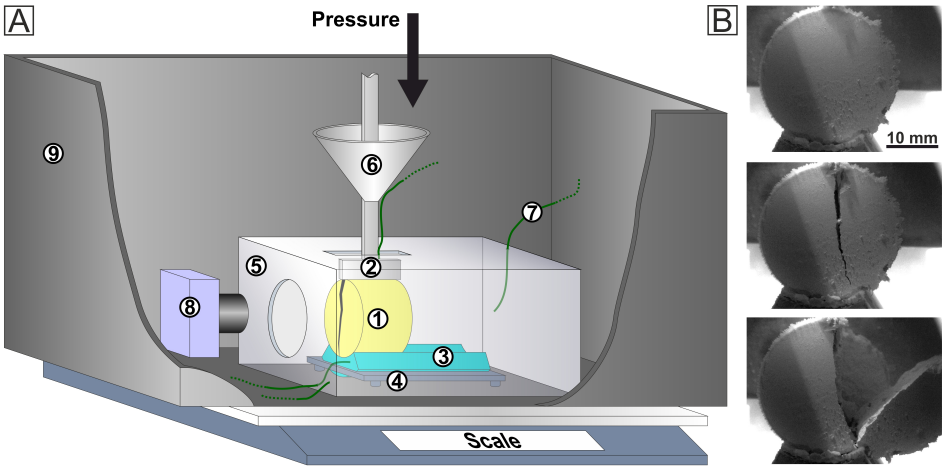

Figure 3.3: A) Schematic and not to scale diagram of the Brazilian disk test. The sample (yellow) rests on a section of the mold in a sample holder and is surrounded by a metal cooling shield. These parts were kept in liquid nitrogen until the moment of measurement. A narrow piston descends onto the sample and generates a crack when the force is sufficient. The corresponding mass to the force is measured by a scale. B) An image series to illustrate the sample size and the crack evolution in a sample.

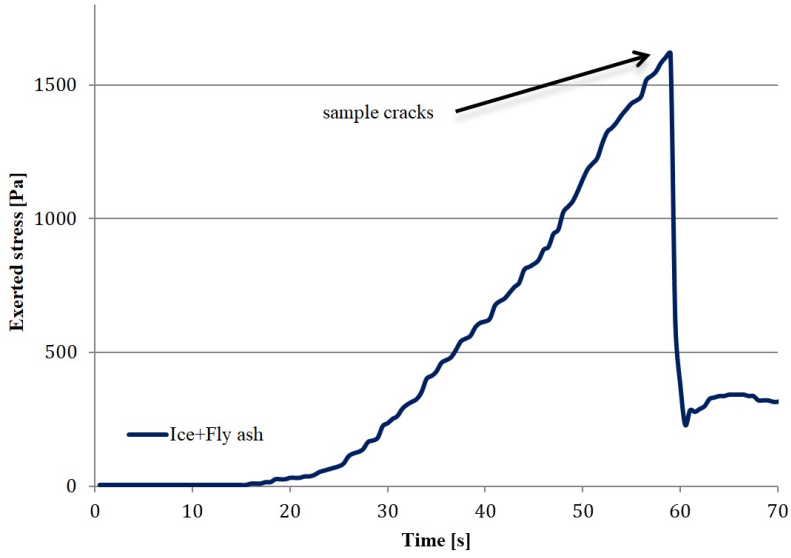

Figure 3.4: Example of a typical pressure curve for a water ice-fly ash mixture in the volume ratio 1:1. The descent of the piston increases the stress on the sample and weight on the scale. The tensile strength is the maximum stress reached at the moment when the sample breaks.

3.3 RESULTS

3.3.1 *Filling fraction*

The mass and volume of the samples were measured to determine the samples' bulk density before applying the above described Brazilian Disc Test on the samples. With the known densities of the dust and ice particles, the filling fraction Φ of the samples was calculated by dividing bulk density by particle densities. We determined the average filling fraction of the individual components (water ice, silica, fly ash) and of their two-component mixtures in various ratios.

Samples made of pure spherical water ice particles had an average filling fraction of Φ=0.74, which means that 74 % of the space is filled with ice particles (Fig. 3.5). For different icy spherical-spherical mixtures (water ice and fly ash) the average filling fraction varied as the proportion of fly ash was increased, but a clear trend could not be observed. The average filling fraction for pure fly ash was Φ=0.84. For different icy spherical-angular mixtures (water ice and silica) the filling fraction decreased significantly when the proportion of silica exceeded 25 vol%. With higher silica content the pore space between the particles increased up to a filling fraction of Φ=0.43 for pure silica dust.

To investigate the influence of particle shape on the filling fraction, we prepared dry spherical-angular mixtures including silica and fly ash without any ice. In this case the filling fraction dropped monotonously from the value of pure fly ash to the value of pure silica (Fig. 3.6).

3.3.2 *Tensile strength*

For each cylindrical sample used in the Brazilian disk test, we recorded the load exerted by the slowly sinking piston onto the disk. The measured weight rose as the piston contacted the sample and dropped abruptly at the moment the samples cracked (Fig. 3.4). Equation (3.1) was used to calculate the tensile strength from the measured maximum force at the moment of breakup (Figs. 3.3 and 3.4). For each mixing ratio of ice and dust approximately nine individual measurements were analyzed and averaged. First, the tensile strength of pure ice samples was determined to be σ=1800 Pa (Fig. 3.7). The addition of only 10 vol% angular silica to the ice resulted in an increase of the tensile strength to σ=5400 Pa. With a further increase of the angular silica content the tensile strength increased slowly to σ=7300 Pa, which is the value of pure angular silica.

The same procedure was repeated for ice-fly ash mixtures. With increasing proportions of spherical fly ash the tensile strength of the samples decreased slightly. At a fly ash content of more than 80 vol% the tensile strength started to decrease significantly and reached its minimum at σ=140 Pa for pure spherical fly ash.

A comparison of pure components with their mixtures shows that the tensile strength of mixtures is dominated by the component with the higher tensile strength. The tensile strength of the whole mixture starts to decrease when the proportion of the component with the lower tensile strength exceeds 80–85 vol%. Then, the tensile strength of the mixture decreases to the value of the component with the lower tensile strength.

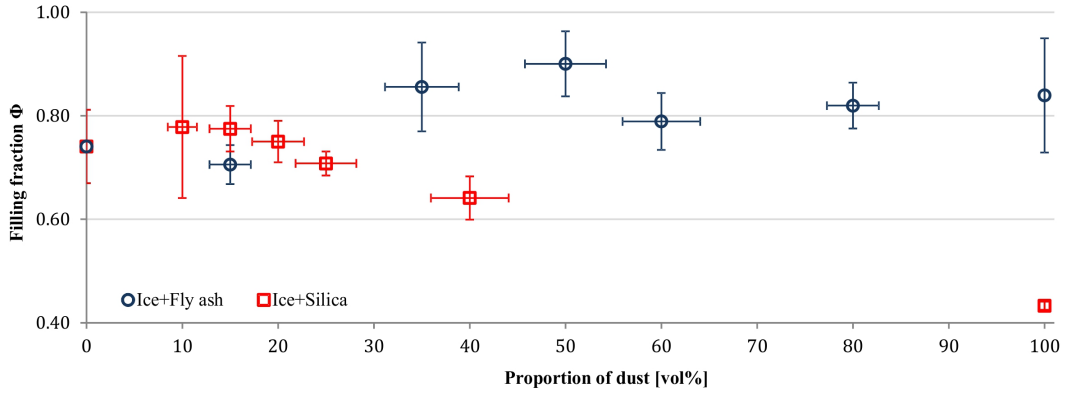

Figure 3.5: Filling fractions of different ice-dust mixtures with varying amounts of ice. The value for pure ice is shown at 0 vol% on the left and for pure dust at 100 vol% on the right. The error of the ice-dust mixing ratio stems from the uncertainty of the ice mass determination. Spherical water ice particles mixed with spherical fly ash particles are shown as blue circles and mixtures containing angular silica particles as red squares. The number of investigated proportions is different for the two types of mixtures.

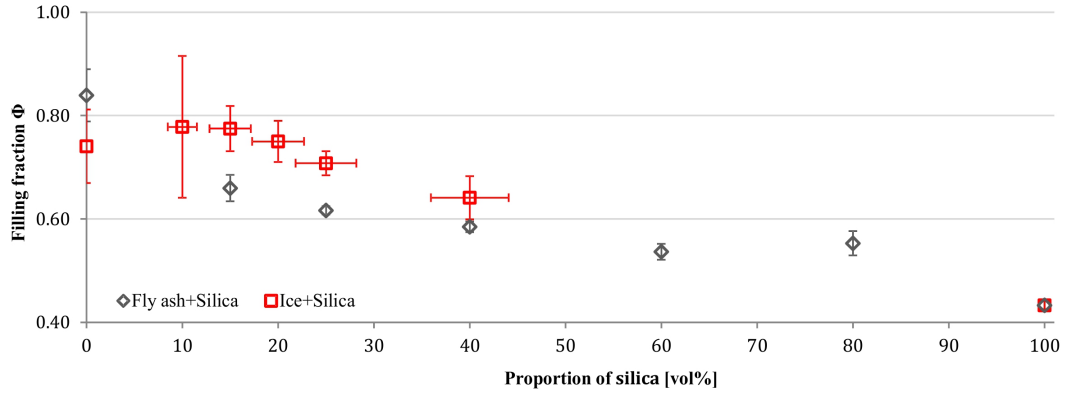

Figure 3.6: Filling fractions of angular silica particles mixed with varying amounts of spherical ice particles (red squares) and spherical fly ash particles (gray diamonds). The values for pure spherical particles are shown at 0 vol% on the left and for pure angular silica particles at 100 vol% on the right. The number of investigated proportions is different for the two types of mixtures.

To analyze the influence of the particle shape on the tensile strength, we conducted Brazilian disk tests with dry mixtures of angular silica and spherical fly ash. In contrast to samples with water ice, the tensile strength of dry samples increases steadily toward the value of pure silica with increasing amounts of angular particles (Fig. 3.8). The angular silica component in the dry spherical-angular mixture has a less dominant effect on the tensile strength compared to the icy spherical-angular mixture. The tensile strength of the dry mixture increases consistently above 25 vol% silica in the mixture. This increase spans over wider range of mixing ratios compared to the icy silica mixture for which the tensile strength increases abruptly at 10 % silica content.

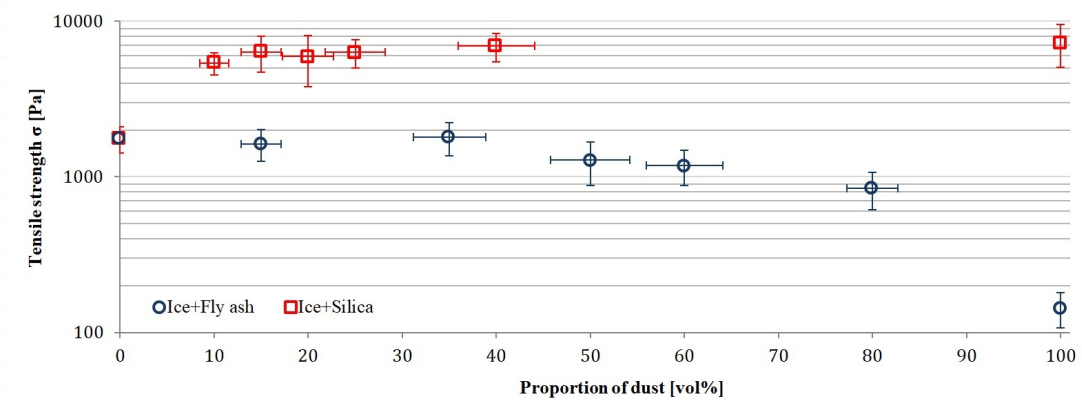

Figure 3.7: Tensile strength σ of different ice-dust mixtures. The value for pure ice is shown at 0 vol% on the left and for pure dust at 100 vol% on the right. Mixtures of spherical water ice particles and spherical fly ash particles are represented as blue circles and mixtures containing angular silica particles as red squares. The number of investigated proportions is different for the two types of mixtures.

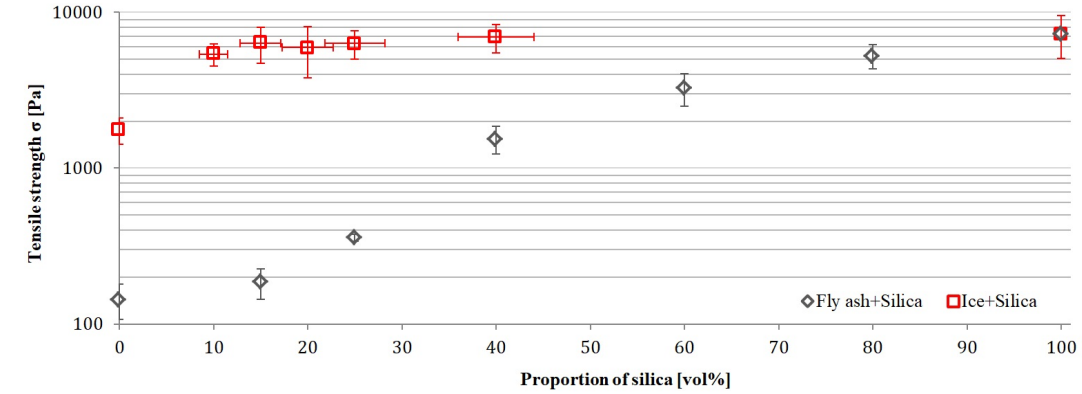

Figure 3.8: Tensile strength σ of spherical particles mixed with angular particles. The tensile strength values for pure spherical particles are shown at 0 vol% on the left and for pure angular silica particles at 100 vol% on the right. The number of investigated proportions is different for the two types of mixtures.

3.3.3 *Surface energy*

Assuming that during the Brazilian disk test in the moment of crack formation all cohesive bonds between the particles break simultaneously, the upper limit of the tensile strength σ can be calculated with the formula of Blum et al. (2006) as follows:

$$\sigma = \frac{3N_C\Phi\gamma}{8r}. \tag{3.2}$$

This equation is derived from the JKR theory (Johnson et al., 1971) and used to calculate the specific surface energy γ of the sample material. The quantity Φ is the filling fraction and r is the particle radius. We used the average particle radius as our mixtures were polydisperse. The coordination number N_C is the average number of contacts per particle. Following Murphy (1982), Yang, Zou, and Yu (2000), and Gundlach et al. (2018a), a value between 5 and 7 is reasonable and thus we adopted

the value of 6 in this equation. Accordingly, the endmembers of 1 and 12 contacts per particle would result in a sixth and twice the tensile strength value, respectively. The exact coordination number is of minor importance in this equation, since a variation between 5 and 7 has little influence on the calculated trend of the surface energy.

For samples composed of pure water ice and temperatures below 150 K the surface energy was calculated to be γ=0.0026 Jm^{-2}. In the icy spherical-spherical mixture including fly ash and water ice, the surface energy does not change considerably with increasing proportions of fly ash at low fly ash proportions. When the proportion of fly ash exceeds 80 vol%, γ decreases and reached very low values of γ=0.00019 Jm^{-2} for pure fly ash (Fig. 3.9).

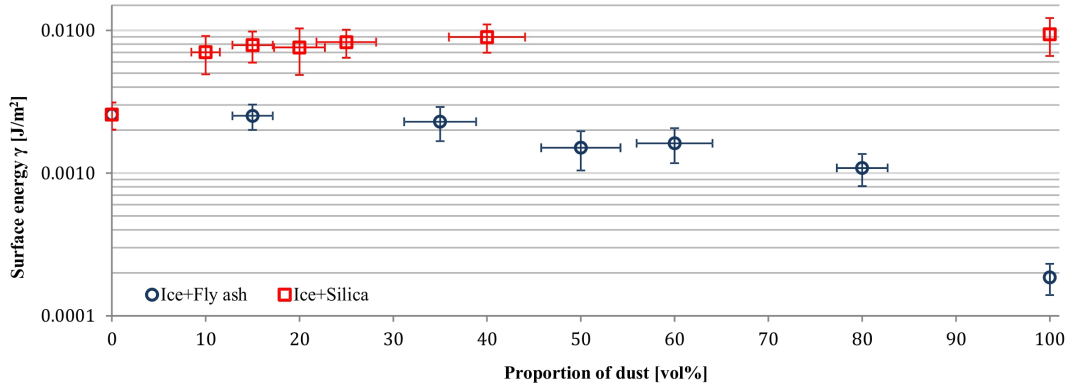

Figure 3.9: Surface energy γ of different ice-dust mixtures. The value for pure ice is shown at 0 vol% on the left and for pure dust at 100 vol% on the right. Mixtures of water ice particles and spherical fly ash particles are indicated as blue circles and mixtures containing angular silica particles as red squares. The number of investigated proportions is different for the two types of mixtures.

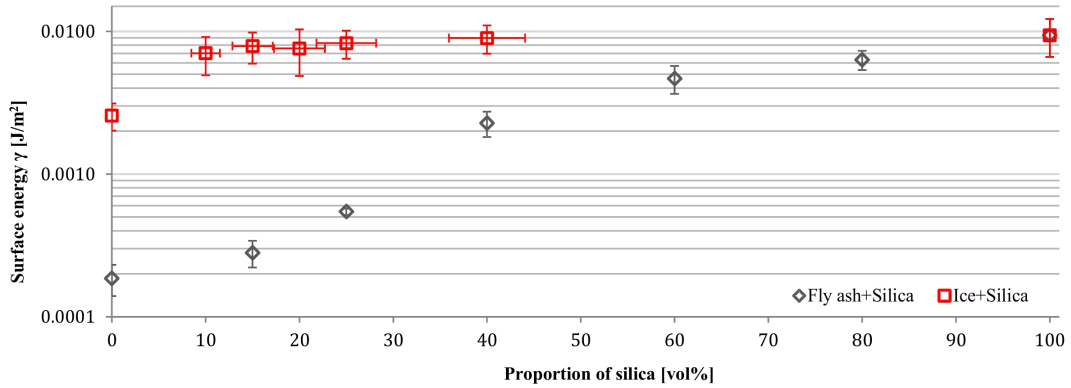

Figure 3.10: Surface energy γ of different spherical particles mixed with angular particles. The values for pure spherical particles (fly ash indicated as gray diamonds and water ice indicated red squares) are shown at 0 vol% on the left and for pure angular silica particles at 100 vol% on the right. The number of investigated proportions is different for the two types of mixtures.

When angular silica is added to the water ice the surface energy increases rapidly to the value of pure angular silica. The calculated surface energy of pure angular silica

is γ=0.0094 Jm^{-2} and thus higher compared to water ice and fly ash in particular (Figs. 3.9 and 3.10). Because of the direct dependence on the tensile strength, the trend of the surface energy at varying mixing ratios is very similar.

3.4 DISCUSSION

3.4.1 *Filling fraction*

As observed in experiments by Omura and Nakamura (2017), our samples of primary angular particles trend toward having a lower filling fraction compared to those of spherical particles (Figs. 3.5 and 3.6). Rogers and Head (1961) found that the more irregular polydisperse particles are, the lower the filling fraction of a sample. Since the silica used consists of the most irregular grains of the three compounds (Table 3.1), the lower filling fraction of silica-rich samples can be explained. This may be caused by increased interparticle friction between angular particles. The angular shape of silica particles may cause restricted rotation and translation against each other. In contrast, the spherical fly ash particles are more mobile than silica particles and can roll into voids upon exerted pressure (Heim et al., 1999; Schellart, 2000). As the proportion of angular silica particles in the mixtures exceeds 20 vol%, more of these particles contact each other and interlock without rearranging. Consequently, the space between particles is less effectively filled and the filling fraction decreases. In contrast to angular-spherical mixtures the filling fraction of spherical-spherical mixtures remained rather stable for all mixing ratios. The filing fraction varied around 0.8 with a deviation of 0.07 in all analyzed spherical-spherical mixing ratios (Fig. 3.5). In these samples, the size and shape of the two particle types were very similar and so were the filling fractions of their mixtures. Therefore, the arrangement of the particles was similar in all samples. The variations of the filling fraction of the spherical-spherical samples may be the result of the sample preparation procedure. Despite all the care taken, it cannot be ruled out for all series of measurements that minor variations occurred in the pressure applied to press the disk. This uncertainty was reduced by standardizing the sample preparation and by repeating the measurement many times. However, since the pressing of the disk was done manually, some variations are unavoidable.

3.4.2 *Tensile strength*

The tensile strength of samples mixed of two different components does not change linearly with the proportions of the components. The component with the higher tensile strength dominated the tensile strength of the whole sample until its proportion was significantly lower than that of the material with lower tensile strength. In our icy spherical-angular experimental series the silica (σ=7300 Pa) had a higher tensile strength compared to water ice (σ=1800 Pa). In this series the angular silica particles determined the tensile strength of the sample when its content exceeded 15 vol% mixed with spherical water ice particles (Fig. 3.7). On the other hand, in the icy spherical-spherical series, the tensile strength of water ice was higher than that of fly ash. In this case, water ice dominated the tensile strength of the sample until its proportion decreased below 20 vol%. We explain this threshold of about 15–20 vol%

that too few particles with high surface energy are present and do not connect to each other directly. Starting from a pure ice sample, a critical number of dust particles is required to cause a significant change in tensile strength. This number depends on the coordination number and the particle shape. Powell (1979) has shown that this value is 18 vol% for monodisperse spheres in random packing, which is in good agreement with our measurements. This observation is described by the percolation theory and the minimum of particles that must be added to achieve an effect is called critical volume fraction. When the concentration of high surface energy particles is above this critical volume fraction, these particles dominate the cohesion of the whole mixture and the surface energy on the microscopic scale translates into a high tensile strength on the macroscopic scale. If the concentration of particles with high surface energy is lower, the cohesion quickly decreases to the value of the component with the lower surface energy.

The tensile strength of samples containing angular silica particles is significantly higher compared to those samples that mainly consist of spherical particles. In Sect. 3.4.1 we described that an increasing content of angular particles corresponds to a decreased filling fraction of a sample. A lower filling fraction results in a lower number of mutual particle contacts and should lead to lower cohesive forces (Blum et al., 2006). However, this effect could be superimposed by the smaller size of silica particles, which are only about half as large as fly ash and ice particles (Fig. 3.2; Table 3.1). Despite the lower filling fraction, there are more silica particles per sample volume and thus more particle-particle bonds. This would increase the tensile stress of a sample (Sánchez and Scheeres, 2014). Additionally, interlocking and higher friction due to increased tensile or shear forces between angular particles (Schellart, 2000) may increase the tensile strength of silica-rich samples. Therefore, both the particle size and shape may be attributed to the higher tensile strength of materials rich in angular silica particles. With our experimental setup we can determine the sum of these effects. However, it is not suitable for the quantitative determination of these individual effects. This is not necessary either because we want to find out which easy to obtain material is better suited to produce comet analog material with the lowest possible tensile strength.

3.4.3 *Surface energy*

In the past, multiple laboratory experiments with different approaches and environmental conditions have been performed to determine the surface energy of silica (Kimura et al., 2015). It has been shown that the surface energy of silica at elevated temperatures (e.g., Fournel et al., 2012; Li, 2013) tends to be about one order of magnitude higher than at room temperature (e.g., Heim et al., 1999; Leroch and Wendland, 2012). Our results show that this trend continues for low temperatures. Below 150 K our silica-rich samples show a surface energy of γ=0.0094 Jm^{-2} that is almost one order of magnitude lower compared to values at room temperature (e.g., Kimura et al., 2015). However, our found surface energy is probably too high as a result of friction between the angular particles that may interlock. The particles can only be separated by the effort of an additional force that could be interpreted as increased geometric cohesion.

The fly ash, on the other hand, which consists of about 60 % SiO_2, has a surface energy of γ=0.00019 Jm^{-2} at 150 K. This value for the surface energy of cooled spherical fly ash is about two orders of magnitude lower than in experiments performed with uncooled samples of pure silica (Gundlach et al., 2018a; Kimura et al., 2015). It is unlikely that same types of intermolecular forces lead to strongly different surface energies of silica and fly ash, since their chemical composition is about 60 % identical (Table 3.1). This would be further indication that the determined surface energy of angular silica is too high.

The surface energy of water ice follows the same decreasing trend. It drops significantly from γ=0.065 Jm^{-2} for samples below freezing point (Ketcham and Hobbs, 1969) to γ=0.0026 Jm^{-2} below 150 K in our experiments. This value was also found by Musiolik and Wurm (2019). With such low surface energy values at low temperatures it is possible to provide water ice-fly ash mixtures as cometary analogues whose tensile strength is well below the tensile strength of uncooled analog materials (Bischoff et al., 2020; Gundlach et al., 2018a; Steinpilz, Teiser, and Wurm, 2019).

3.4.4 *Possible error sources*

It should be noted that Eq. (3.2) is derived from JKR theory (Johnson et al., 1971), which is only valid for spherical particles. Angular silica particles are a more complex material, in which the edges of the particles can be assumed to be particles with very small radii of curvature and their flat sides correspond to very large radii of curvatures. Therefore, the distribution of effective particle sizes derived from the radii of curvature in an angular granular medium varies significantly. This assumed average grain size may result in errors in the derived surface energy.

During the experiments, the samples were cooled down to temperatures <150 K, which prevented sintering of water ice particles (Kuroiwa, 1961). As a result, an increase of the tensile strength of the sample material by sinter necks between water ice particles could be avoided. Therefore, the strength of the samples was determined by the cohesion of directly neighboring particles and the particle shape. However, partial sintering of the sample surface cannot be completely ruled out. Air humidity may penetrate into the cooled polystyrene box, reach under the cooling shield, and may have crystallized on the surface of the samples. This would create a stiff connection between individual particles at the disk surface. However, this process probably had only a negligible influence on the measurement. The measurement of the tensile strength lasted only two to three minutes and to avoid atmospheric moisture the atmosphere in the polystyrene box was made up of evaporated liquid nitrogen. Therefore, the nitrogen atmosphere in the box was colder and heavier than air and did not readily mix with it.

Another factor that could influence the results of the tensile strength measurements is the hydrophilicity of amorphous silica. Air humidity could reach the used silica dust before the sample preparation and probably accumulated on its surface. The bonding of water molecules or silanol groups on the particle surface would be the consequence and could decrease the surface energy of the individual particles (Steinpilz, Teiser, and Wurm, 2019). With an increased availability of moisture, a thin layer of water could form around dust particles. Cooled down, this water would freeze and the

particles would be indistinguishable from water ice particles in terms of surface energy and tensile strength. To avoid this effect the silica used in our experiments was always stored in tightly closed containers, which were only opened briefly for gaining sample components. However, the formation of silanol groups on the particle surfaces cannot be ruled out completely. No measurements however give any hint of this effect, especially since we observed an significantly increased tensile strength of silica-rich samples compared to fly ash-rich samples. Even if the tensile strength would be reduced by the hydrophilicity of silica, it is still much higher than that of samples with fly ash and therefore less suitable to produce samples with low tensile strength.

3.5 CONCLUSION

3.5.1 *Tensile strength and surface energy*

We conducted three series of Brazilian disk test measurements to analyze the tensile strength of samples composed of different cometary analog materials. For this we combined two of the three components: spherical water ice, spherical fly ash particles, or angular silica particles at sizes of few microns. We cooled these materials to temperatures below 150 K. The samples of these series were combinations of a) icy spherical-angular particles, b) icy spherical-spherical particles, and c) dry spherical-angular particles. We conclude that below 150 K the tensile strength and the derived surface energy of silica, fly ash, and water ice mixtures are generally much lower than at room temperature (Gundlach et al., 2018a; Kimura et al., 2015).

At temperatures below 150 K the tensile strength of the sample mixtures was strongly dependent on the amount of ice mixed within the sample and on the particle geometry (Fig. 3.11). We suspect that the friction between angular particles increases, but we cannot quantify this effect with our experiment. This and the mean grain radius of 1.3 µm of pure silica particles lead to the tensile strength of σ=7300 Pa at a filling fraction of Φ=0.43. A direct calculation of the surface energy with JKR based Eq. (3.2) was not feasible in this case, since the particles were not spherical and the friction between particles may distort the tensile strength of the sample. Therefore, the surface energy values for angular silica particles (Figs. 3.9 and 3.10) must be interpreted with caution and could be too high.

The second dust component was fly ash, which consists of about 60 % SiO_2 and is composed of spherical particles with a mean radius of r=2.43 µm (Table 3.1). Our samples of pure cooled fly ash have a filling fraction of Φ=0.84 and a low tensile strength of σ=140 Pa. That corresponds to a surface energy of γ=0.00019 Jm^{-2} and is about two orders of magnitude smaller than pure silica at room temperature (e.g., Kimura et al., 2015). In the samples, which are mainly composed of spherical particles, these particles can easily pass each other by rolling. Hence, the surface energy of the material can be calculated more directly from the tensile strength with Eq. (3.2).

The properties of pure water ice samples were determined to σ=1800 Pa and γ=0.0026 Jm^{-2} at 150 K. These values for tensile strength and surface energy are significantly higher compared to values of fly ash particles. Owing to their spherical shape the ice particles were also not affected by interlocking. Therefore, the tensile strength of the samples was used to calculate the surface energy of water ice.

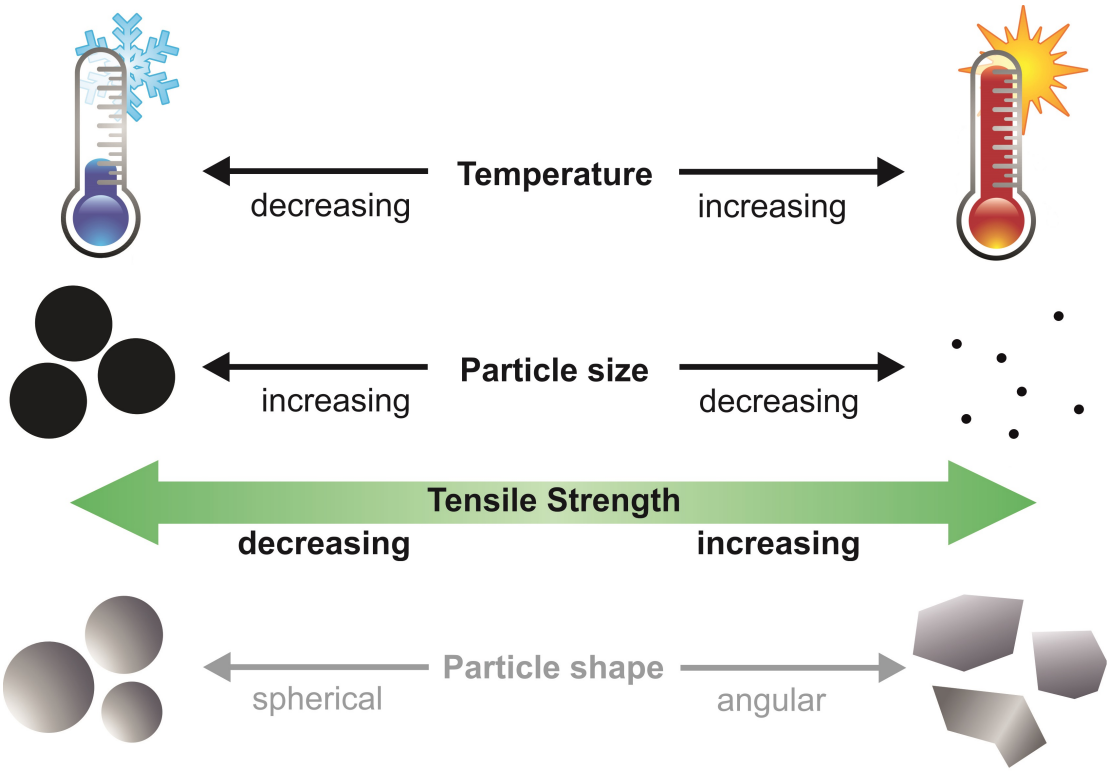

Figure 3.11: Schematic overview of parameters affecting the tensile strength of granular matter in our experiments. Higher temperatures and smaller particle sizes increase the tensile strength of a material. A dependence of the tensile strength on the grain shape can be assumed, but cannot be determined with our measurements.

When two of the three analog materials were mixed, the component with the higher tensile strength dominated the tensile strength of the whole sample. As soon as the abundance of the material with the lower surface energy exceeds 80 vol%, the tensile strength of the mixture decreases quickly toward the value of the component with this lower tensile strength (Fig. 3.7). At that mixing ratio, there are too few direct connections between particles with higher attractive interparticle forces to significantly increase the tensile strength of the whole sample.

3.5.2 *Fly ash as cometary analog material*

Our experiments showed that fly ash can be used as suitable analog material for cometary dust in the laboratory. As a consequence of the very low surface energy of fly ash, samples with a tensile strength of few hundred Pascals and less can be easily produced. This is in the range of the tensile strength of cometary material, as estimated for comet 67P/Churyumov-Gerasimenko (Attree et al., 2018a; Groussin et al., 2015). In contrast to angular silica particles, the spherical shape of the fly ash and water ice particles prevents interlocking. This significantly reduces the friction between the particles so that cohesion remains the dominant force between single particles. Therefore, the spherical shape of fly ash and water ice particles in the laboratory is advantageous to produce samples with very low tensile strength. If more than 20 vol%

water ice is mixed as a volatile material to fly ash, the tensile strength increases rapidly to the value of pure water ice. Assuming that comets can be described as icy dirt balls (Keller, 1989; Pätzold et al., 2016), this effect can be reduced when the ice content in the samples is kept low. The result is a mixture whose tensile strength is still a few hundred Pascals and would be a good analog material for comets in the laboratory.

In the laboratory the small particle diameter of a few microns increases the cohesion of the samples, which exceeds the influence of gravity (Bischoff et al., 2019). We used the ratios of these cohesive and gravitational force in the laboratory and on 67P/Churyumov-Gerasimenko (Bischoff et al., 2019) to estimate the particle size on a comet we are able to simulate with our micron-sized particles in the laboratory. We found that centimeter-sized aggregates (Blum et al., 2014; Güttler et al., 2010, 2019) in the gravitational field of a comet can be scaled down to few micron-sized particles in the laboratory (Durda et al., 2014; Scheeres et al., 2010).

4

SUBLIMATION OF ICE-DUST MIXTURES IN COOLED VACUUM ENVIRONMENTS TO REPRODUCE COMETARY MORPHOLOGIES

David Haack[1] (corresponding author), Anthony Lethuillier[2], Christopher Kreuzig[2], Clément Feller[3], Bastian Gundlach[2], Jürgen Blum[2], Katharina Otto[1]

[1]*Institut für Planetenforschung, Deutsches Zentrum für Luft- und Raumfahrt (DLR), Berlin, Germany*

[2]*Institut für Geophysik und Extraterrestrische Physik, Technische Universität Braunschweig, Braunschweig, Germany*

[3] *Physikalisches Institut, Universität Bern, Bern, Switzerland*

Published in Astronomy&Astrophysics, Volume 649, May 2021, Article Nr. 35
https://doi.org/10.1051/0004-6361/202140435, reproduced with permission ©ESO

ABSTRACT

The morphology of cometary surfaces can provide important information to constrain the composition and evolution of comets. In this work, we investigate the sublimation behavior of comet analog materials and how the sample composition affects the evolution of morphological features in laboratory experiments. In our experiments, we used dust ice mixtures as analog material to form observed cometary morphologies.
We used ice-dust mixtures in different mixing ratios as cometary analog material. In order to obtain realistic results, we scaled the expected cohesive and gravitational forces on comets to laboratory conditions. The samples were placed in a vacuum sublimation chamber and permanently cooled down to temperatures below 150 K to simulate the space environment. In the experiment, the samples were insolated with a light source from two different directions and alterations on the surface were recorded with a camera.
We find that the morphology of sublimation residues of ice-dust mixtures is strongly dependent on the ice-dust ratio as well as the insolation direction. High amounts of ice cause constant surface alteration and lead to exotic morphologies. Low amounts cause fewer and more episodic surface changes during its sublimation. Collapse events resulting in irregular and very rough surfaces occur during horizontal insolation.

4.1 INTRODUCTION

In the past, several space missions have been sent to comets to study their properties at a close range (e.g., ESA's Rosetta mission and NASA's Deep Impact mission). Despite these visits, the activities on the surface of comets are still not well understood. Satellite-based observations have shown that the surfaces of comets become very active as they approach the Sun (Gulkis et al., 2015; Sierks et al., 2015; Snodgrass et al., 2013) by which

we mean the occurrence of sublimation-driven outgassing events. The main process responsible for this activity is the sublimation of volatiles in a shallow subsurface region of a comet. It is caused by the direct radiation of solar energy onto surfaces in an air-less environment. Since comets also consist of nonvolatile minerals, salts, and organic substances, volatile-depleted residues remain after the sublimation of the ices. The pressure drag of sublimating volatiles detaches volatile and nonvolatile particles and gas drag transports them away from the surface (Bischoff et al., 2019; Gundlach et al., 2015; Keller et al., 2017; Kührt and Keller, 1994). In this way, a comet loses material with each orbit around the Sun and diverse morphological features form at its surface. Based on Rosetta data, the tensile strength was estimated from overhangs (Attree et al., 2018a; Groussin et al., 2015), fractures were proposed to be related to desiccation processes (El-Maarry et al., 2015a), and boulder size frequency distributions were used as indicators of evolutionary processes (Pajola et al., 2015, 2016a,b). To enhance our understanding of these sublimation-driven processes, the morphologies of the cometary surfaces as well as the morphologies developing under laboratory conditions need to be further examined. Chemical composition, grain size, porosity, and gravitational and cohesive forces between individual particles decisively determine how the surface of a comet develops. Therefore, the comparison of morphological features in the laboratory with those at a comet's surface may provide information about its composition and could constrain the evolutionary history of comets.

The KOSI laboratory experiments in the 1990s simulated and studied sublimation processes that were expected on the surfaces of comets (e.g., Grün et al., 1989, 1993; Lämmerzahl et al., 1995). In a sublimation chamber, mixtures of water ice and non-volatile analog materials were illuminated by an energy source and the changes in the samples' surfaces were analyzed. After prolonged insolation of the samples, an ice-free cover layer formed, which protected deeper layers from warming up and it prevented further activity.

Cometary science got a recent boost with the Rosetta mission. Since the spacecraft reached comet 67P/Churyumov-Gerasimenko (hereafter 67P), we obtained detailed images of its surface and improved our knowledge of organic materials on a comet (Capaccioni et al., 2015; Goesmann et al., 2015; Raponi et al., 2020). However, in order to properly interpret the morphologies displayed in Rosetta images, an understanding of the nucleus composition, in particular its dust-to-ice ratio, is vital. Therefore, analog studies with vacuum sublimation chambers have been increasingly dedicated to the development of specific morphologic features. The Simulation Chamber for Imaging the Temporal Evolution of Analogue Samples (SCITEAS; Pommerol et al., 2015a) allowed monitoring and photometric analyses of volatile-rich samples during the process of sublimation. The chamber provided temperatures and low pressure comparable to conditions on comets for low heliocentric distances. With this chamber, Poch et al. (2016a,b) investigated the influence of organic materials and mineral components on the sublimation behavior of water ice. The presence of organic material results in significant textural differences on the sample's surface after sublimation of the volatiles. Samples with refractory grains included in the ice matrix (intra-mixtures) produced very porous (foam-like) and highly cohesive structures. On the other hand, when the components were mixed with each other as pure particles (inter-mixtures), more compact and less cohesive residuals at the surface of the samples formed (Poch et al.,

2016a,b). However, the concentrations of nonvolatile components in the initial sample mixtures were very low with up to one mass percent and, therefore, they are not representative of realistic cometary regoliths. Additionally, the arrangement of the samples in molds was not suitable to allow vertical mass transport. This is why the samples could not reproduce the observed morphologies of a cometary surface. Other experiments by Kaufmann and Hagermann (2018) were used to analyze the influence of carbon black on the sublimation of icy surfaces. They verified the hardening of a subsurface layer as described by Kochan et al. (1989) and Kossacki et al. (1997) and the development of an ice-depleted cover with a very low density. Most of these experiments were conducted using a very high and possibly unrealistic volatile content of >90 wt.%. Experiments focusing on the development and evolution of morphologies using a more realistic dust-to-ice ratio are conducted in this work.

Previous experimental work has shown that at temperatures of 150 K and below, the tensile strength of water ice is much lower than previously expected (Gundlach et al., 2018a; Musiolik and Wurm, 2019). Haack et al. (2020) extended these experiments and investigated different mixtures of dust and water ice for their suitability as comet analogs and found that the tensile strength of a mixture is dominated by the component with the highest tensile strength. In this work we use these mixtures to study the morphological evolution of samples in a vacuum sublimation chamber with the aim of reproducing basic morphological structures observed at the surface of 67P. In our experiments, we insolated samples, which were composed of water ice and nonvolatile dust particles in different ratios. We took advantage of the very low tensile strength of spherical water ice and fly ash particles that are mixed together and cooled below 150 K (Haack et al., 2020; Kappel et al., 2020). We also allowed vertical and horizontal mass transport of the sample material by the omission of lateral sample boundaries. The intensity of the insolation was varied and the angle of incidence could be set either vertical or horizontal relative to the surface of the sample. We focused on the conditions under which the sublimation of water ice starts to significantly change the sample texture. Alterations of the sample morphology were analyzed and checked for their relevance with respect to cometary surfaces. We find that the resulting morphological features are dependent on the composition of the samples.

4.2 METHODS

4.2.1 *Selection of materials*

We decided to investigate comet analog materials consisting of binary mixtures of a volatile and a refractory component. This not only keeps the complexity of the experiments within limits but also allowed us to investigate the influence of individual parameters on the morphology after sublimation (e.g., dust-ice ratio, insolation direction).

We used polydisperse water ice spheres with an average radius of 2.4 µm (Table 4.1) as the volatile component of the analog material. This is a first grade approximation since H_2O dominates the amount of volatile materials in 67P (Hässig et al., 2015). Other volatiles such as CO_2 or CO account for only up to 15 mass% abundance relative to H_2O (Biver et al., 2019; Bockelée-Morvan et al., 2016; Läuter et al., 2018). Even

when H_2O dominates, CO_2 and CO ices might play key roles in the activity at large heliocentric distances where water does not sublimate. Our approximation is a first step and other ices will be introduced in future work to see if this makes differences or not.

We used dust as refractory material, whereby a compromise between physical and chemical accuracy had to be found. We decided to use spherical fly ash particles. These have the advantage of not consisting of pure amorphous SiO_2 as in previous experiments, but rather they correspond to the more mineralic composition of plagioclase (Table 4.1). The fly ash particles are polydisperse and of a similar size as the water ice particles used (Fig. 4.1). Additionally, it is possible to produce samples with a very low tensile strength with these spherical particles (Haack et al., 2020) to simulate the low tensile strength of cometary materials (Attree et al., 2018a; Groussin et al., 2015). The filling fraction of the samples describes how much free space is in a volume filled with particles and is with ∼0.4 (Fig. 4.2) higher than observations of 67P suggest (Attree et al., 2018a; Groussin et al., 2015; O'Rourke et al., 2020). In the experiment, the higher filling fraction would lead to more interparticle bonds and thus a higher tensile strength. However, this effect may be reduced by the spherical shape of the particles that reduces interlocking of realistically angular particles and would compensate for their limited freedom of movement (Haack et al., 2020; Kappel et al., 2020). Although olivine and pyroxene may be more suitable cometary refractory analog materials, the difficulties in acquiring these materials in a micrometer-sized spherical shape were disproportionate for this work. Angular particles, however, would greatly increase the tensile strength of the samples (Haack et al., 2020) and could prevent the alteration of the sample morphology during the sublimation experiment.

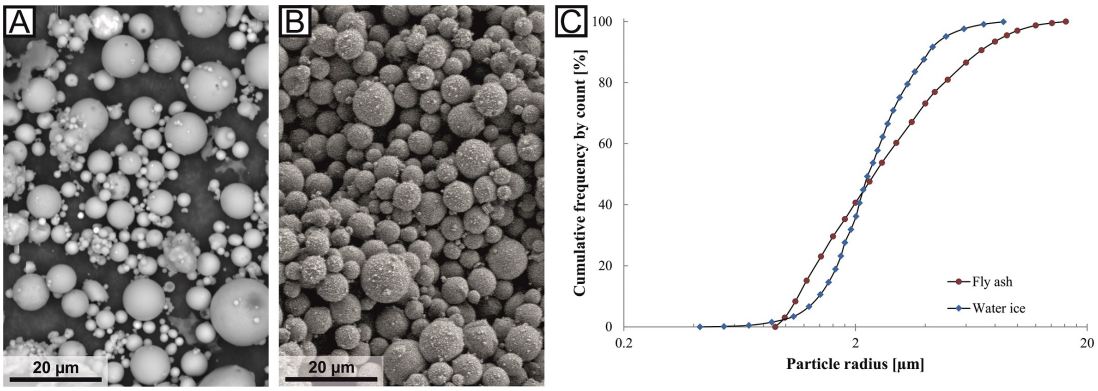

Figure 4.1: Electron-microscopy images and size distribution of the particles used in our experiments. The images of shperical fly ash in *panel A* and water ice particles in *panel B* are at the same scale (modified from Haack et al. (2020)). *Panel C* presents the comparable cumulative size distributions of fly ash (red dots) and water ice (blue diamonds).

Organic materials are also important components of comets (Capaccioni et al., 2015; Goesmann et al., 2015; Raponi et al., 2020; Sandford et al., 2006). However, in this series of experiments, we have omitted organic components in order to cap the complexity of our experiments to be able to attribute a change in morphology to the variation of one individual parameter. The results can be used as a basis for further experiments with more complex sample compositions.

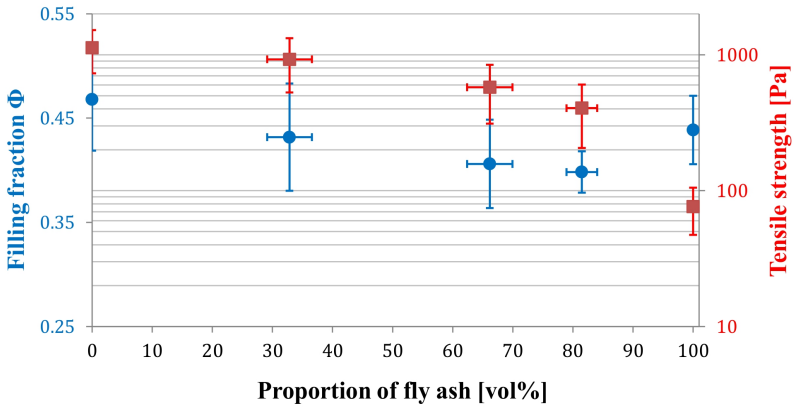

Figure 4.2: Filling fractions and tensile strengths of different water ice-fly ash mixtures. Pure ice corresponds to 0 vol% on the left, and the respective pure fly ash to 100 vol% on the right. The error of the water ice-fly ash mixing ratio originates from the uncertainty as to the ice mass determination.

Table 4.1: Characteristics of water ice and fly ash used to simulate cometary materials. The properties and chemical composition of the particles were measured using an electron microscope before starting the experiments.

	Water ice	Fly ash
Particle shape	spherical	spherical
Particle radius [µm]	2.38±1.11	2.43±1.41
Density [g cm^{-3}]	0.93	2.25
Compd %		
H_2O	100.00	
SiO_2		59.20
Al_2O_3		27.90
Metal oxides		12.90

4.2.2 *Particle scaling*

A major challenge with experiments in the laboratory is Earth's gravitational acceleration, which is higher, by order of magnitudes, than the $\sim 2 \times 10^{-4}\,\mathrm{m\,s^{-2}}$ of comet 67P (Agarwal et al., 2016). Therefore, particles at the surface of the comet are subject to much less gravity and the importance of cohesion between particles is significantly increased (Scheeres et al., 2010; Skorov and Blum, 2012; Sánchez and Scheeres, 2014). Bischoff et al. (2019) present a model according to which decimeter-sized particles on the surface of 67P are subject to approximately equal cohesive and gravitational forces. Between particles smaller than this threshold, the cohesion is dominant; for larger particles, gravity becomes more important. Previous studies have suggested that comets are formed of up to centimeter-sized pebbles (Blum et al., 2014, 2017; Fulle et al., 2016; Kretke and Levison, 2015; Lorek, Lacerda, and Blum, 2018; Zsom et al., 2010). Therefore, cohesive forces should dominate on a comet. To simulate processes in the laboratory that are comparable to processes on cometary surfaces, a way to reduce the influence of gravity compared to cohesive forces on the experiment must be found. According to Bischoff et al. (2019), on Earth, the threshold between gravitational and cohesive dominance is a particle radius of $\sim 35\,\mu\mathrm{m}$. To significantly reduce the relative importance of gravity and to ensure the dominance of cohesive inter-particle forces, the particle radius used in the experiment must be significantly below this size. Water ice and fly ash particles fulfill this criterion, but their cohesion with respect to 67P must be determined.

Images obtained during the Rosetta mission at 67P show complex morphologies, such as cliffs, cracks, or mass movements (El-Maarry et al., 2019; Pajola et al., 2016a; Thomas et al., 2015b), which are morphologically similar to those on Earth. This could indicate that between particles the ratio of cohesive forces and the comet's gravity is comparable to the ratio between these forces on Earth, even if they differ greatly in absolute numbers. If the cohesion forces on a comet were much more dominant than on Earth, exotic structures such as extreme overhangs or cave-like structures could be expected at the comet's surface, which would collapse immediately under Earth's gravity if made of the same material. On the other hand, if gravity was much more dominant, the observed cliffs and boulders would be unstable (Kappel et al., 2020) and the comet's surface would be much smoother in general. Using this appoach, Groussin et al. (2015) have suggested that the ratio of cohesive and gravitational forces at 67P corresponds to that of weak rocks on Earth on a macroscopic scale. We use this suggestion and assume that the ratio between gravity and cohesion on 67P and on Earth is comparable and thus as follows:

$$\frac{F_{G_{67P}}}{F_{C_{67P}}} \approx \frac{F_{G_{\mathrm{Earth}}}}{F_{C_{\mathrm{Earth}}}}\,. \tag{4.1}$$

With given gravitational forces

$$F_G = \frac{4}{3}\pi r^3 \rho g \tag{4.2}$$

of particles on 67P and Earth and the known cohesion

$$F_C = 3\pi r\gamma \tag{4.3}$$

of particles used in the laboratory (Haack et al., 2020), we were able to estimate the corresponding particle size on 67P. In these equations, r is the reduced radius of the particles, ρ is the particle density, g is the gravity acceleration, and γ is the surface energy per unit area. In our experiments, we used mixtures of water ice and fly ash particles with a mean radius of about 2.4 µm (Table 4.1). According to the used approximation, the water ice and fly ash particles in the experiments reflect millimeter-sized particles on 67P. This agrees well with the model of Bischoff et al. (2019) and is in line with the size of hypothesized pebbles of which comets may have been formed initially (Blum et al., 2017; Lorek et al., 2016). Transferred to macroscopic scales, a 2.5 cm high sample in the sublimation chamber would represent a 10 m-high object on 67P.

4.2.3 *Energy scaling*

The scaling of the particle size in the laboratory was intended to increase cohesive inter-particle forces with respect to gravity. As a result, the force that is required to separate the particles from each other and to change the sample morphology was also increased compared to the actual inter-particle cohesive force on the comet. In our experiments, this separating force is the near-surface pressure drag, caused by the vapor pressure of sublimating water ice. To transport single particles or larger aggregates away from their initial positions on the sample's surface, the pressure drag has to exceed the cohesive forces between the particles. Therefore, the applied energy to create the pressure drag in the experiment must be scaled with the particle cohesion to simulate realistic pressure drag-cohesion ratios.

As a first step, we estimated the surface temperature of 67P as a function of its heliocentric distance. The energy balance of insolation and sublimation is given by the Stefan-Boltzmann law plus a term for the sublimation heat flux, derived from Hertz-Knudsen (Kührt and Keller, 1994)

$$\frac{C_s}{R^2}(1-a) = \epsilon\sigma T^4 + \frac{H\,P_v(T)}{\sqrt{2\pi k_B \frac{T}{m}}}\,. \tag{4.4}$$

In this equation, the following notation is used:

C_s	solar constant,	T	temperature,
R	heliocentric distance,	H	latent sublimation heat,
a	albedo,	P_v	vapor pressure,
ϵ	emissivity,	k_B	Boltzmann constant, and
σ	Stefan-Boltzmann constant,	m	molecule mass.

As a second step, we assumed equal ratios of pressure drag F_D and cohesion F_C for 67P and in the laboratory and thus follow:

$$\frac{F_{D_{67P}}}{F_{C_{67P}}} \approx \frac{F_{D_{\text{Earth}}}}{F_{C_{\text{Earth}}}} . \tag{4.5}$$

The pressure drag F_D results from the vapor pressure (Fanale and Salvail, 1984; Gundlach, Skorov, and Blum, 2011) on the particle cross section

$$F_D = \pi r^2 \, 3.56 \times 10^{12} \, \text{Pa} \, \exp\left\{\frac{-6142 \, \text{K}}{T}\right\} . \tag{4.6}$$

With the particle radius r of the analog material, the calculated surface temperature T of 67P from step one, and the cohesion of 67P and the samples, we determined the temperature-dependent gas drag in the laboratory.

The fly ash albedo a was determined to be 0.35 on average in previous measurements. This value was also used as an approximation for the ice-dust mixtures, since the albedo of an ice-bearing sample is mainly determined by the dust component (Chýlek, Ramaswamy, and Srivastava, 1983; Clark and Lucey, 1984; Oehler and Neukum, 1991). Thus the generally low albedo of 67P of 0.06 (Ciarniello et al., 2015) was considered in this scaling and compensated for by a higher energy input. Then we used the temperature derived in Eq. (4.4) to calculate the insolation intensity in the laboratory.

For our spherical water ice particles, which are mixed with dust particles, we estimated an insolation flux of ~ 1 solar constant in the laboratory to simulate a heliocentric distance of 4 AU in our experiments. This was approximately the distance to the Sun, when the Rosetta spacecraft reached 67P and monitored activity at the surface (Tubiana et al., 2015). The maximum of solar radiation to the surface of 67P is reached at its perihelion at 1.24 AU. This would transform into an insolation flux of about 33.6 solar constants in the laboratory to simulate the cohesion-pressure drag ratio. However, this insolation flux was not feasible with our experimental setup.

4.2.4 *Sample preparation*

We conducted a series of sublimation experiments with samples that were composed of water ice and fly ash in different mixing ratios (Haack et al., 2020). These were inter-mixtures, which means that individual particles consisting of a single component were mixed together. Water ice spherules represent the volatile content of a comet and fly ash particles represent the refractory dust components. These mixtures were used to test the dependence of the sublimation of a sample on a) the ice-dust ratio of the mixture and b) the direction of the insolation flux.

The water ice particles were produced with a water droplet dispenser that sprays mist into a Dewar vessel filled with liquid nitrogen (Gundlach et al., 2018b; Haack et al., 2020). The water droplets freeze, forming a suspension of polydisperse spherical water ice particles and liquid nitrogen, and they eventually sink down to the bottom of the Dewar vessel. The amount of water ice in the suspension was determinded by using Archimedes' principle. The weights of a defined volume of pure liquid nitrogen

and of liquid nitrogen with suspended water ice were measured. The densities of liquid nitrogen and water ice are known and allowed the calculation of the mass of water ice in the suspension from the weight difference between both components. Fly ash was directly weighed with a scale.

We produced five different ice-dust mixtures (66, 50, 33, 25, and 20 vol% water ice) by adding predefined amounts of dust into the suspension of liquid nitrogen and a known amount of water ice. This corresponds to dust-ice mass ratios of $\sim$ 1.2, 2.4, 4.8, 7.3, and 9.7, similar to those expected for the nucleus of a comet (Fulle et al., 2018, 2017; Herique et al., 2017; Pätzold et al., 2018; Rotundi et al., 2015). The liquid nitrogen, water ice, and dust particles were mixed manually with a ladle to obtain a homogeneous suspension. Then, the mixtures were filled into a metal cylinder with an inner diameter of 25 mm, which was placed vertically on a permanently nitrogen-cooled sample holder (Fig. 4.3). The viscosity of the mixture in the cylinder was high enough that ice and dust could no longer segregate due to their different densities. The liquid nitrogen as a coolant was necessary to prevent sintering of the ice particles (Gundlach et al., 2018a; Kuroiwa, 1961). Without cooling during the sample preparation, stiff sinter necks could form between ice particles and would lead to higher values for the tensile strength of the sample materials. After the liquid nitrogen of the suspension slowly evaporated from inside the metal cylinder, the cylinder was carefully lifted up. As a result a cylindrical sample of water ice and dust remained on the sample holder. Its diameter was the same as the inner diameter of the cylinder (25 mm) and the height varied between 20 mm and 25 mm. A slow and steady evaporation of the liquid nitrogen was necessary to avoid the formation of cavities within the sample and to reduce their formation at the contact surface with the cylinder. During the preparation, the samples were not mechanically compressed and were held together by their own cohesion. After removing the metal cylinder, the cooled sample holder with the sample on top was quickly placed into the precooled vacuum sublimation chamber and ready for the sublimation experiment.

4.2.5 *Tensile strength*

Before we started the sublimation experiments, we performed a series of measurements to determine the tensile strength of the samples. We prepared 15 samples, each of various ice-dust mixtures in the manner described above, and made sure that all nitrogen had evaporated from the samples. We then determined their weight and volume and were able to calculate the filling fraction Φ of the samples. We started with a water ice content of 100 vol% and reduced it to 0 vol%. The filling fractions of all investigated mixing ratios were between 0.40 and 0.46 (Fig. 4.2). According to Blum et al. (2006), the upper limit of the tensile strength σ of granular matter is

$$\sigma = \frac{9\Phi\gamma}{4r}. \tag{4.7}$$

With the values for the surface energy γ of water ice-fly ash mixtures at liquid nitrogen temperatures (Haack et al., 2020) and the particle radius r, we could determine the tensile strength of the samples. Since pure water ice or fly ash are not suitable as comet analog material, we used mixtures with a water ice content between 66 vol% and

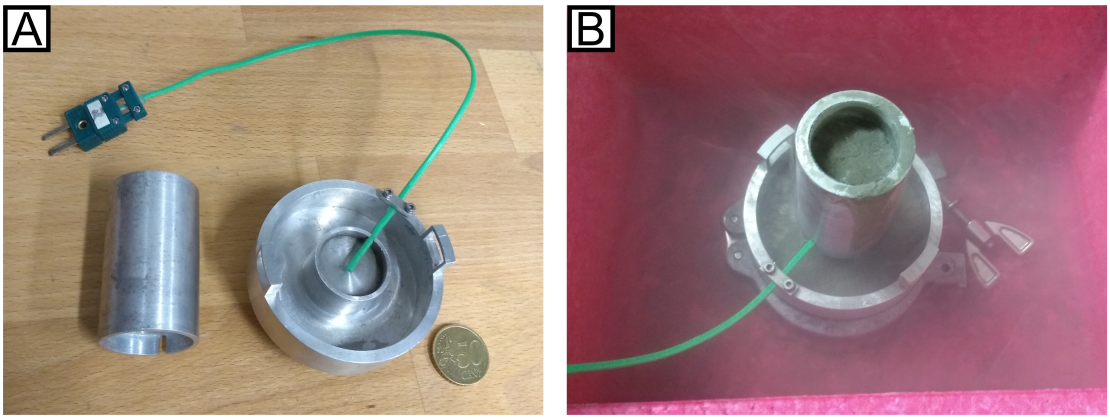

Figure 4.3: Preparation of the samples. *Panel A:* Metal cylinder (left) and sample holder (right) that were used to prepare the samples. The green cable with the connector belongs to one of the thermocouple sensors, which was used to monitor the sample temperature during the experiment. *Panel B:* The metal cylinder was plugged onto the sample holder and filled with a suspension of liquid nitrogen, water ice, and dust particles. To ensure that the setup was constantly cooled while the liquid nitrogen evaporated from the sample mixture, the outer volume of the sample holder was also filled with liquid nitrogen.

20 vol% for the sublimation experiments. This gave tensile strengths of water ice-fly ash mixtures between 930±60 Pa and 400±10 Pa, respectively (Fig. 4.2).

4.2.6 *Sublimation experiments*

For our experiments, we used a cylindrical vacuum sublimation chamber with an inner diameter of 25 cm and a height of 80 cm (Fig. 4.4). Before the start of the experiment, the chamber was closed, cooled down to about 110 K, and flooded with argon. The argon ensured the absence of atmospheric moisture inside the chamber when it was opened to place the sample inside. This prevented altering the sample before the experiment started. To ensure constantly low sample temperatures, which are similar to those of a comet (Kührt, 1984), and to prevent thermal background radiation, an actively cooled shield system was used. This cooling shield is a rectangular metal housing with a side length of 10 cm and with a firm connection to a circuit for continually circulating liquid nitrogen. The cooling shield is coated black on the inside to prevent reflections and has two windows for insolation and observation of the sample inside (Fig. 4.4).

Immediately after preparation, the sample was placed inside the cooling shield. Thereby, the sample holder was firmly screwed to the cooling shield and temperature sensors were connected to the sample holder. Subsequently, the chamber was closed and the atmospheric pressure inside was reduced to $\sim 10^{-7}$ mbar. To ensure that the measurements were performed in a controlled environment, the pressure inside the chamber and the temperature at four positions (sample, cooling shield top and bottom, and nitrogen input) were monitored in parallel (Fig. 4.5). From the beginning of the placement of the sample, a camera with a resolution of 3000 × 2000 pixels was focused at the sample through a window in the sublimation chamber and monitored the sample at a rate of one image per second.

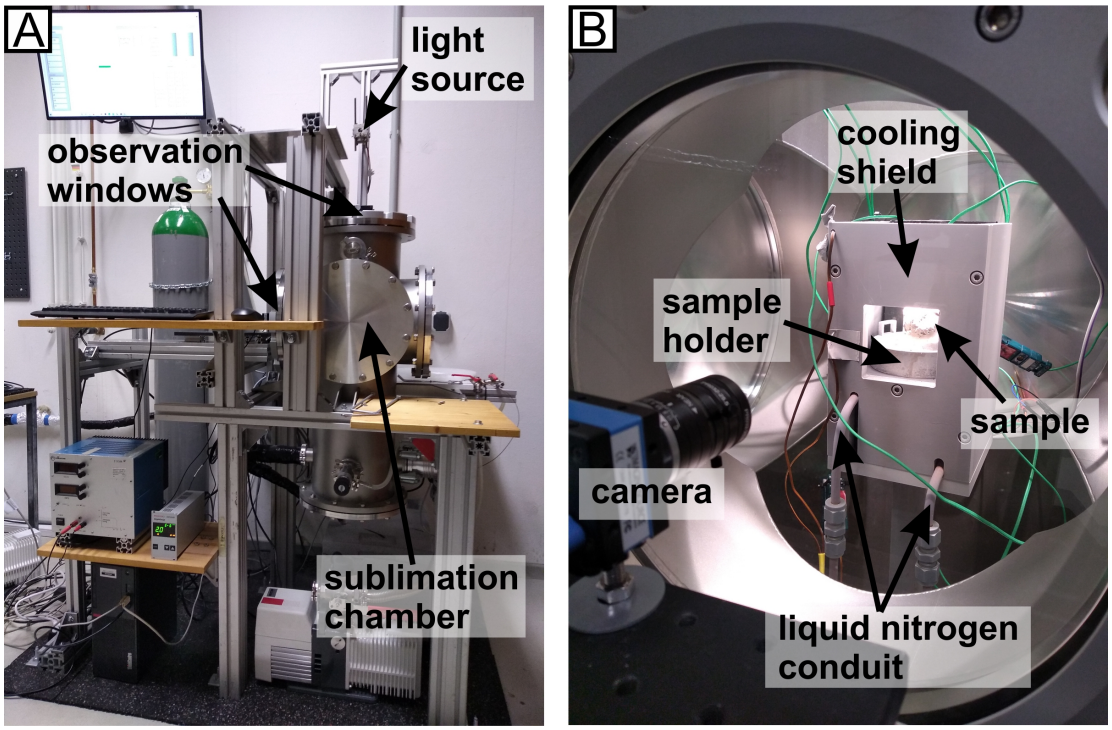

Figure 4.4: Setup of the sublimation experiments. *Panel A:* Cylindrical vacuum sublimation chamber with two observation windows. One is located on the top and one on the lateral side of the chamber. In the configuration shown, the light enters the chamber from above. *Panel B:* View through the lateral observation window into the inside of the vacuum sublimation chamber. The sample holder is firmly attached to the cuboid cooling shield. The object visible inside the cooling shield is the sample insolated from above. The green cables in the chamber belong to the different temperature sensors that monitor the temperature of the sample and the experimental setup. A camera is directed at the sample from outside.

After the pressure inside the chamber had reached its operating value of $\sim 10^{-7}$ mbar, we started to insolate the sample. We used a halogen lamp with variable intensity and a simple mirror and lens system to focus the light on the sample. We also distinguished between insolation vertically to the top of the sample or horizontally to the side. This was implemented to investigate possible differences in material transport. During the experiments, the light source insolated the samples constantly in one direction.

In a first series of experiments, we combined different mixing ratios with horizontal or vertical insolation. For this series of measurements, we chose an insolation flux of ~ 1 solar constant, which corresponds to a heliocentric distance of 4 AU, following the scaling relations. In a second series of experiments, we increased the insolation flux to about 3 solar constants, which represents a heliocentric distance of 3.1 AU. The insolation of a sample lasted up to 20 hours. After that time, the active cooling had to be stopped to replenish the liquid nitrogen supply. At the end of the experiment, the degree of alteration of the samples' surface was analyzed via the camera observations and related to different material compositions and levels and directions of insolation.

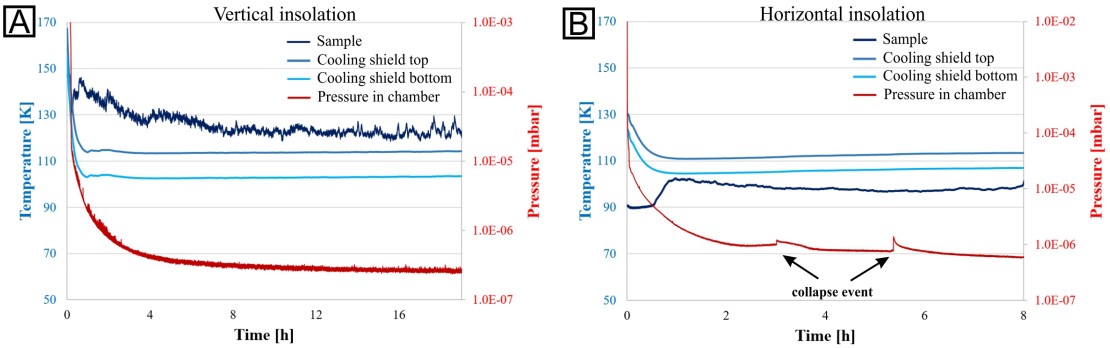

Figure 4.5: Two examples of the monitored pressure and temperatures in the chamber for two samples with 25 vol% water ice, each. The recordings were made every second from the beginning of the experiment to its end. *Panel A:* The insolation with ∼3 solar constants was vertical from above. When the sublimation activity of the sample stopped after about 3 hours, the pressure and temperatures remained stable until the end of the experiment. *Panel B:* The insolation was horizontal from the side. The temperatures of the sample and setup remained approximately stable. The pressure curve shows two short-term increases after 3 and 5.5 hours, which can be attributed to two collapse events on the sample. The sample temperature increased at ∼0.5 h after the remainder of liquid nitrogen vaporized from the sample.

4.3 RESULTS

The experiments of the first series with an insolation flux of about 1 solar constant (corresponding to a heliocentric distance of 4 AU) resulted in no visible alterations of the samples' morphology. Even the samples with the highest fraction of 66 vol% water ice showed no signs of activity under horizontal or vertical insolation, respectively. The samples were removed from the sublimation chamber after about 20 hours. The strength of the samples had increased significantly. They could be gripped with crucible tongs without damaging them. More detailed measurements of the exact tensile strength, porosity, among others, were not feasible because the room temperature and humidity in the laboratory were too high. As a result, frost immediately formed on the surface of the samples and additional sintering of the particles could not be avoided (Kuroiwa, 1961), which would have falsified possible measurement results. After heating up the sample remains to room temperature, it was observed that the subsequently melting ice in the interior of the samples was preserved and did not sublimate.

The second series of experiments with an insolation flux of ∼3 solar constants, which correspond to 3.1 AU, resulted in a broad variety of activities at the samples' surfaces. In addition to different ice-to-dust ratios, vertical and horizontal insolation resulted in different surface activities during the observation periods. The temperature and pressure inside the cooling shield were monitored continuously. In all measurements, the internal sample temperature remained below 150 K and short-term changes in pressure could be attributed to events that changed the sample's surface (Fig. 4.5).

4.3.1 *Vertical insolation*

We analyzed samples with a 66–20 vol% water ice content under vertical insolation flux of ∼3 solar constants. The results could be summarized into three groups, depending on their ice contents.

4.3.1.1 *66 vol% water ice content*

We started the experiments with a high water ice content of 66 vol%. Most noticeable was a fast and intense reshaping of the sample's surface. The sublimating water ice created a permanent and distinctly visible stream of particles that detached from the surface and were ejected away from the sample (Fig. 4.6). No ice-free layer of dust was able to form at any insolated area of the sample. A change in the albedo could not be observed either. As a result, fresh sample material was always present on the surface and was exposed to progressive sublimation. The texture of the sample material appeared granular with a grain size in the submillimeter range. The observed grains were larger than the initially used ice and fly ash particles, which accumulated in these larger aggregates. After about six hours, the constant sublimation process had progressed so far that all water ice had sublimated from the sample and the majority of refractory dust was transported away.

During the evolution of the surface exotic structures, spikes, and extreme overhangs formed, which only collapsed after most of the material had been transported away (Fig. 4.7). These roughly horizontal overhangs reflect the dominance of cohesive forces compared to gravity within the sample material.

4.3.1.2 *50 vol% and 33 vol% water ice content*

As the water ice content of the samples decreased to 50 vol% and 33 vol%, the kinetics of surface alteration decreased significantly. At the beginning of the sublimation experiments, particles were continuously ejected from the sample. But the particle ejection frequency and transport range were significantly reduced, compared to samples with a 66 vol% ice content. Unfortunately, the setup did not allow us to quantify this more precisely. After 15–20 minutes, the phase of active ejection of particles ended for both samples. Material, which was detached from the sample's surface, predominantly fell down because of gravity. The alterations of the samples were mainly limited to their vertical walls. This led to a continuous decrease in the sample's diameter. The loose and ice-depleted material accumulated around the base of the sample and formed a talus of debris (Figs. 4.6 and 4.7). This talus consisted of aggregates up to 0.5 mm in size, consisting of dust particles and small amounts of water ice. The granular structure visible at the talus could also be observed directly in the ice-dust mixture on the sample's surface. Some aggregates reached sizes of up to 1.5 mm, but decayed into smaller fragments as soon as they fell off the sample's surface. In the submillimeter range, the surface appeared very rough. With the particle scaling from Sect. 4.2.2, the observed aggregates would correspond to boulders of some decimeters on the surface of 67P. In contrast to the diameter, the height of the two samples remained stable. At

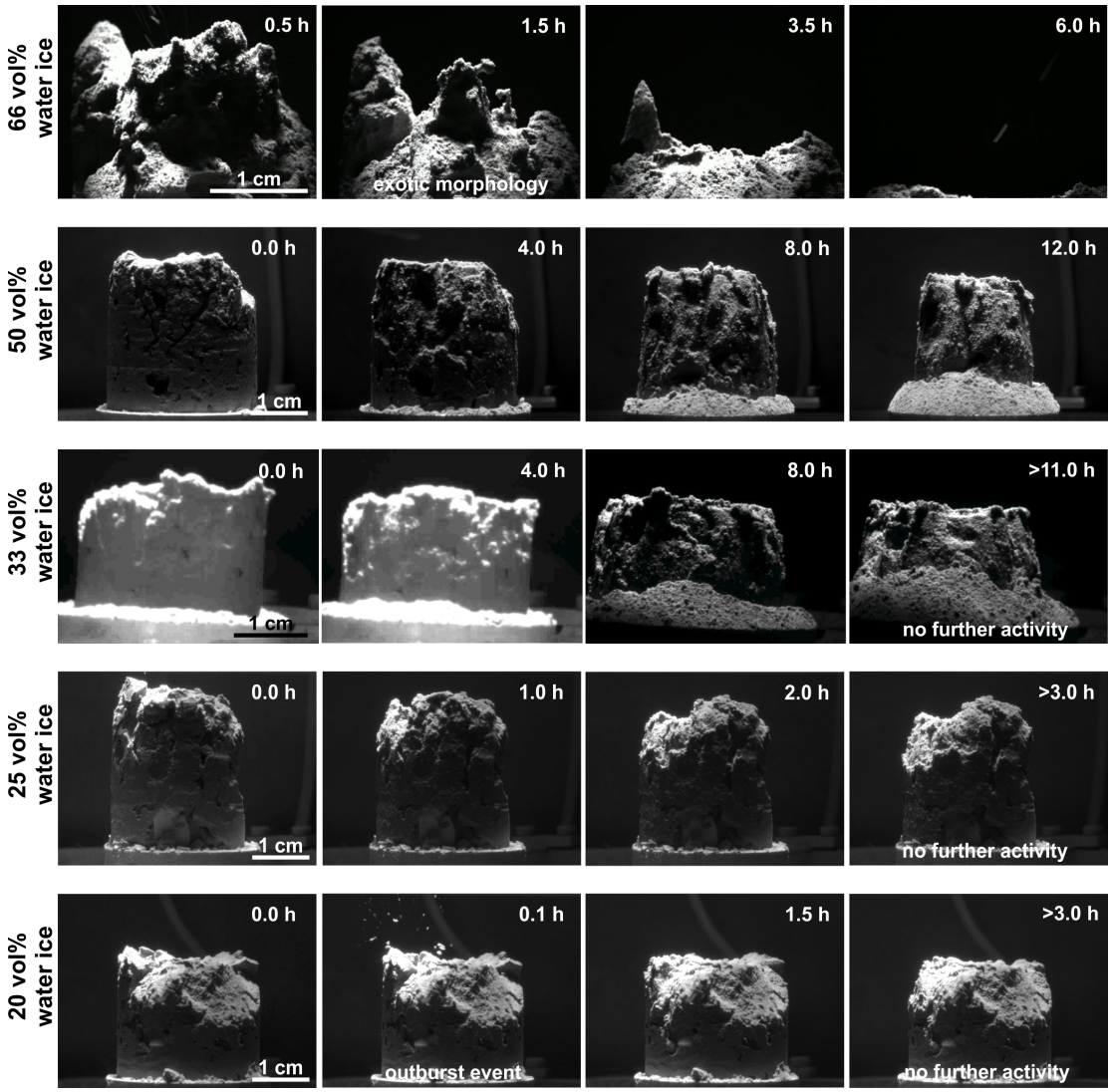

Figure 4.6: Five vertically insolated samples with different dust-to-water ice ratios at an insolation rate of ∼3 solar constants. The image series show how the sublimation activity reduces with a decreasing water ice content (online movies). At a 66 vol% water ice content, several ejected particles are visible as elongated bright dashes (in the panels with a timestamp of 0.5 h and 6.0 h) and the whole sample has disappeared after about 6 h of continuous sublimation. The series of pictures with a 33 vol% and 50 vol% water ice content show the erosion of lateral surfaces, the formation of a talus, and the granular structure of the sample material. The first two images of the series with 33 vol% water ice appear brighter because the filter in front of the camera, which reduces the brightness, was not installed and was added during the experiment. The shape of the samples with a 25 vol% and 20 vol% water ice content changed rather in single events (ejections) and did not experience any further visible changes after about 3 h (see Fig. 4.5A).

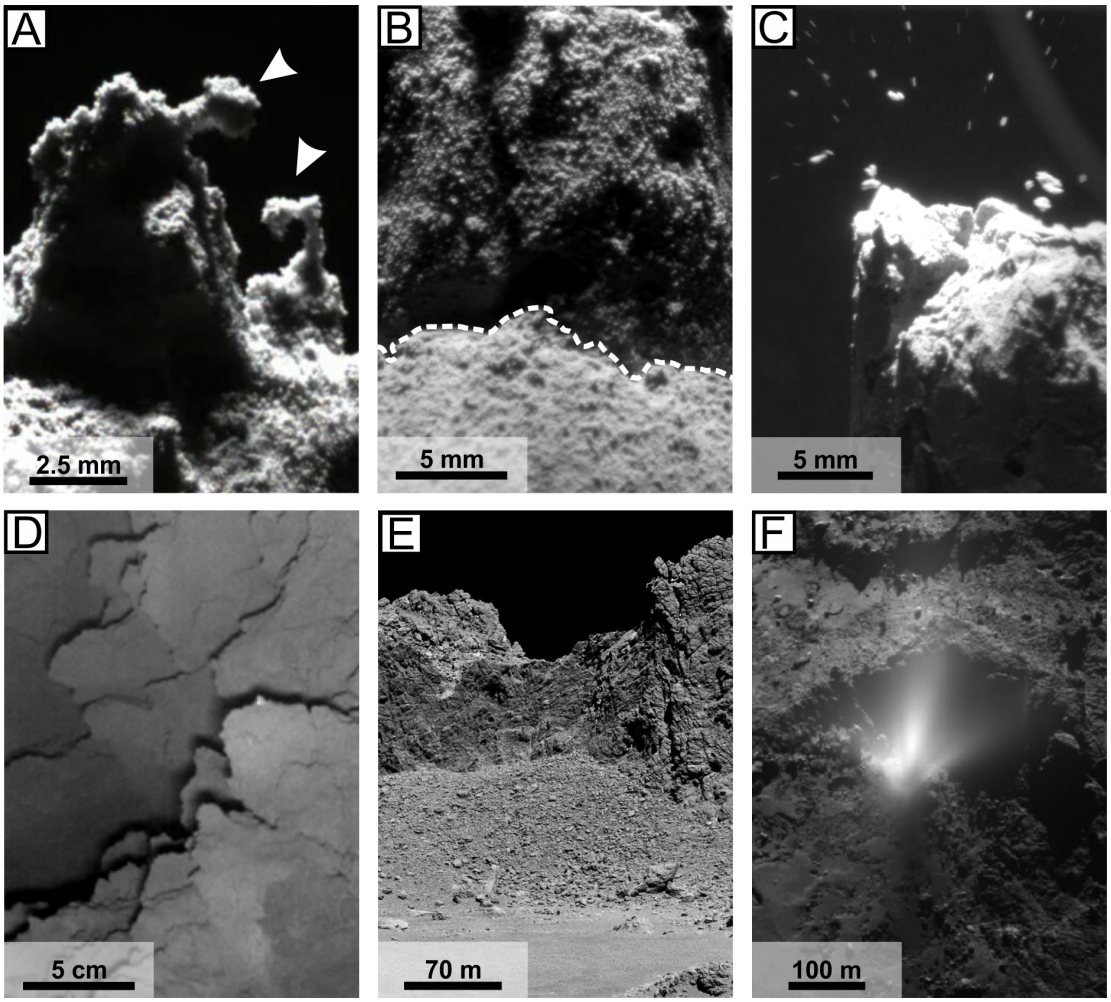

Figure 4.7: Comparison between laboratory results and observations on 67P. Panels A–C show details of different vertically illuminated samples from Fig. 4.6 during the phase of active sublimation in the laboratory. Panels D–F show images of the in situ surface of comet 67P to compare them with the corresponding lab results. *Panel A:* Exotic morphology of the sample with a 66 vol% water ice content. The arrows indicate extreme overhangs, which did not collapse immediately. *Panel B:* Shown is an enlarged section of the sample with a 50 vol% water ice content. The dotted line separates the sample wall (upper area) from the talus of loose debris (lower area). The granular structure of the sample material is clearly visible. The micrometer-sized individual particles (see Fig. 4.1) form aggregates of up to 1.5 mm in size and frequently remain intact when they detach from the sample and accumulate on the talus. This image represents the granular structure of all investigated samples. *Panel C:* The sample with a 20 vol% water ice content in the early phase of the experiment. Several fragments up to a millimeter in size were detached from the sample's surface and ejected in single outburst events. *Panel D:* A detailled image of the surface of 67P taken by the Philae lander. It shows the actual surface of 67P without extreme overhangs as seen in panel A (ROLIS image derived from Schröder et al. (2017)). *Panel E:* A cliff on the comet with a talus of debris material that is reminiscent of laboratory results in panel B. *Panel F:* An outburst plume at the surface of 67P. Agarwal et al. (2016) describe meter-sized boulders that were ejected during these outbursts. Image credits: ESA/Rosetta/MPS for OSIRIS Team MPS/UPD/LAM/IAA/SSO/INTA/UPM/DASP/IDA.

the end of the experiments, a thin layer of dust was observed on the horizontal surface layer of the samples.

The morphological development that both samples underwent seems to be comparable, but it proceeded on different timescales. The surface of the sample with 50 vol% water ice changed continuously until the end of the experiment. In contrast, the evolution of the sample with 33 vol% water ice slowed down noticeably and came to an end after 11 hours. Although the sample was observed for another 7 hours, no further alterations on the surface were observed.

After the remains of the samples were removed from the sublimation chamber, large amounts of water ice were noticed in the center of the remaining samples and some amounts were in the talus material. Additionally, the ice-rich center of the remaining samples was significantly solidified, compared to the start of the experiments, when the samples were extremely fragile. With our setup, it was not possible to determine the amount of ice in the remaining material because it began to thaw after it was removed from the chamber.

4.3.1.3 *25 vol% and 20 vol% water ice content*

The samples with a water ice content of 25 vol% and 20 vol% showed a very similar development. Ejected particles were observed in the first minutes of the experiments and then only sporadically. Samples with both mixing ratios lost limited amounts of material at their directly insolated top surface. A visible loss of material on the lateral surfaces could not be observed. The constant low pressure in the chamber also shows that the sample did not lose any further volatile material after the end of the limited surface erosion (Fig. 4.5A).

A few minutes after the beginning of the experiment with the 20 vol% water ice sample, some major outburst events from the top surface were observed. A large number of up to millimeter-sized fragments detached and were transported away explosively (Fig. 4.7). However, these outburst events were limited to the initial phase of the experiment and did not occur during its further course. Fresh sample material became visible where alterations on the sample's surface occurred. It appeared very similar to the other mixtures and showed a granular structure in the submillimeter range.

Even after prolonged insolation, no further surface changes were observed in either sample type after 3 hours. Comparable to the samples with a higher ice content, the remains of the samples kept their ice content and were strongly solidified when they were removed from the sublimation chamber.

4.3.2 *Horizontal insolation*

Analog to experiments with vertical insolation, we analyzed samples with a 66–20 vol% water ice content under horizontal insolation flux of $\sim$3 solar constants.

4.3.2.1 *66 vol% water ice content*

At the beginning of the insolation, the sample with a 66 vol% water ice content showed intense activity at its surface. Particles and macroscopic aggregates in the submillimeter range detached from the sample and were ejected from its surface. During this process, the vertical and smooth surface of the sample evolved to an irregularly rough surface and a thin layer of dust did accumulate. During this process the activity decreased continuously, and particles and aggregates were ejected less frequently and less far. After about 4 hours, the initially vertical sample wall was tilted and showed only sporadic signs of morphologic alterations. At that time, the sample had lost more than half of its initial material. After an additional 7 hours in the sublimation chamber and with a nearly unchanged morphology, the upper part of the sample collapsed spontaneously. The sample material that remained created a cliff-like structure (Fig. 4.8). The debris accumulated at the base of the sample and decayed into fine dust and aggregates whose grain size did not exceed one millimeter. When trying to examine the remaining sample material at the end of the experiment, we found that the debris appeared almost free of water and the slightest vibration or air-draft would immediately change the position and shape of the remains. Within the "cliff" and at the bottom of the sample, a substantial amount of water ice was still present. However, it could not be determined whether the total ice-to-dust ratio had changed significantly within the remaining sample material.

4.3.2.2 *50 vol% and 33 vol% water ice content*

At the start of the insolation of the sample with 50 vol% ice and dust, respectively, a significant number of particles were ejected from the surface. After a few minutes, the distance covered by the particles decreased significantly and they accumulated at the base of the sample. Over the course of the experiment, a talus of debris grew on the insolated side of the sample (Fig. 4.8). The degree of activity and number of ejected particles remained relatively constant for the first 6 hours, then activity slowed down significantly and came to an end after a total of 12 hours. At that time, the accumulated debris material covered approximately the lower half of the sample. The upper half of the sample appeared to be covered by a thin layer of ice-depleted dust, but underneath this layer the original ice-dust ratio was preserved. The height of the sample and the side facing away from the light remained unchanged throughout the experiment.

The results of the experiment with 33 vol% ice strongly resemble the ones of the experiment with 50 vol% ice. However, the talus of accumulated material at the foot of the sample developed significantly less and the alterations on the sample's surface came to a complete end after 5 hours.

The morphological development of these two samples is very similar to results with vertical insolation. Samples of both series of experiments showed the same granular structure and a talus formed for both types at their base.

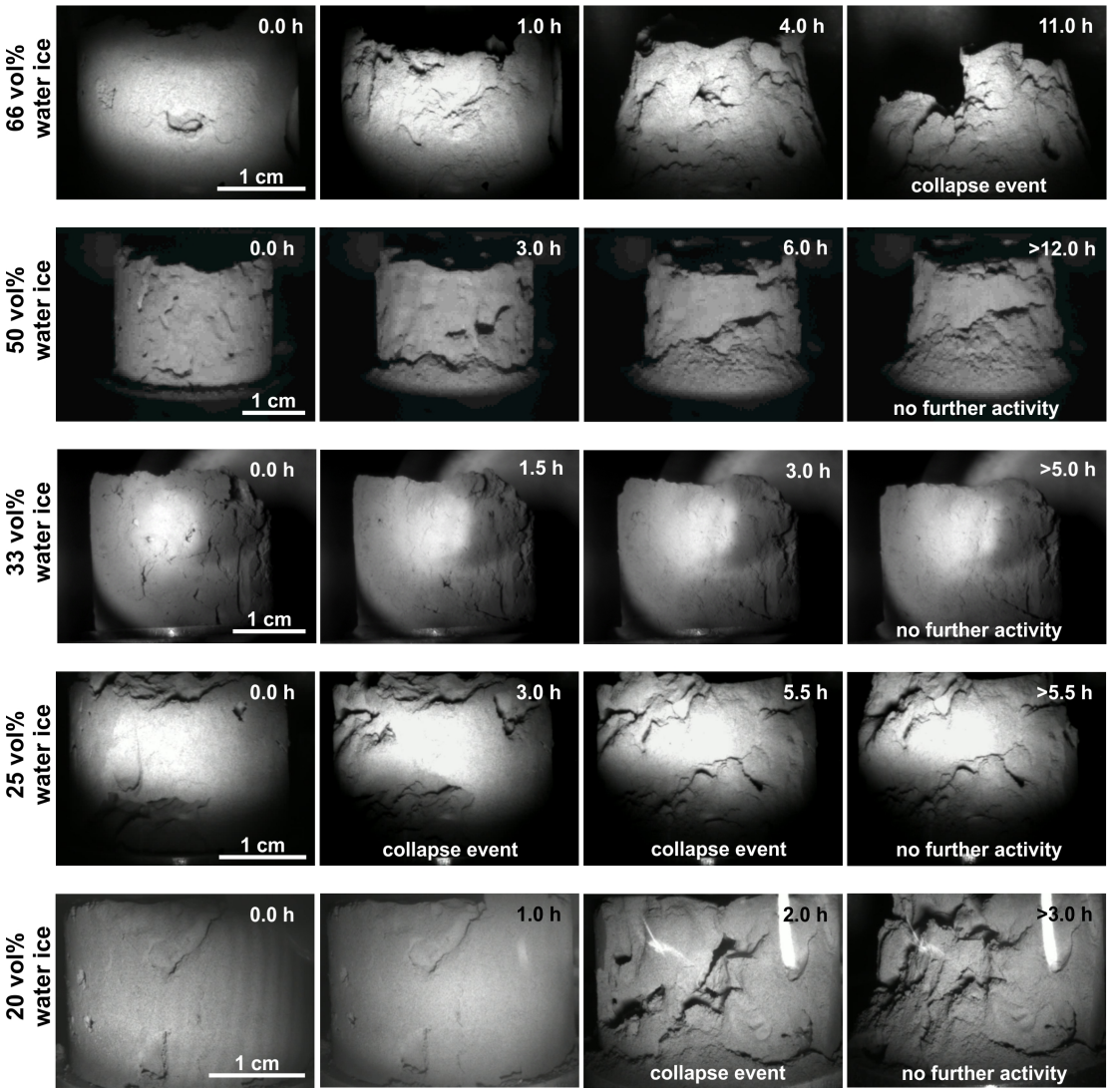

Figure 4.8: Evolution of the five different ice-dust mixtures with horizontal insolation. The occurrence of collapse events with different sample compositions is noticeable (online movies). Samples with a 33 vol% and 50 vol% water ice content show a continuous alteration of their shape until the end of the sublimation activity and formation of talus at their base. At a 25 vol% and 20 vol% water ice content, single events occurred in the form of cliff collapses exposing fresh material on the surface (see Fig. 4.5B). After 5.5 h and 3 h, respectively, no further alterations on the surface were visible. The bright areas in the upper right corner of the images with 20 vol% water ice are reflections of a light source in the laboratory on the observation window of the sublimation chamber.

4.3.2.3 *25 vol% and 20 vol% water ice content*

The sample with a 25 vol% water ice content showed little ejection activity at the beginning, which came to an end after a few minutes. The sample morphology did not change continuously as observed on previous samples, but two collapse events occurred. The first one after 3 hours was limited to a small area, but during the second one after 5.5 hours the whole insolated area collapsed. Both events can be read off well from the changes in the pressure curve (Fig. 4.5, Fig. 4.8), because fresh volatile-containing material was exposed to the surface. This led to an increase in sublimation activity for about 40 min. After the second collapse, the surface of the sample was significantly roughened and became irregular and ejection activity occurred again, and it decreased after about 30 min. From that point on, the morphology of the sample did not alterate until the end of the experiment.

The sample with 20 vol% water ice evolved similarly to that with a 25 vol% water ice content. At the start of the experiment, only a few particles were ejected from the insolated side. After about 2 hours, this side collapsed and left a significantly irregular surface. After some subsequent minor alterations of the sample morphology, no additional changes were observed for the remainder of the experiment.

4.4 DISCUSSION

The following sections discuss the grouped results of experiments with an insolation flux of about 3 solar constants (3.1 AU). Experiments with about 1 solar constant (4 AU) showed no surface alteration and are not discussed.

4.4.1 *Vertical insolation*

4.4.1.1 *66 vol% water ice content*

Samples with a water ice content of 66 vol% are similar in porosity (0.56) and density (0.57 $g\,cm^{-3}$) to 67P (Hornung et al., 2016; Langevin et al., 2017; Pätzold et al., 2018). However, the morphological features and the speed at which these were formed indicate that the high content of volatiles is unlikely to be present at the surface of 67P. The vapor pressure of the sublimating ice entrained all the detached dust particles, so that no ice-depleted cover layer could form. On the entire surface of the sample, fresh and ice-rich material was exposed for the full duration of the observation. This is in contradiction to Deep Impact and Rosetta observations, which showed discrete patches of volatile-rich material on an overall ice-depleted surface (Capaccioni et al., 2015; Sunshine et al., 2006). Furthermore, the high water ice content significantly increases the tensile strength of the sample (Haack et al., 2020). This results in the formation of exotic structures on the sample's surface that do not resemble the 67P morphology (Fig. 4.7). Extreme overhangs and nearly horizontal spikes with material accumulations at their free ends are an expression of very high cohesion between the particles, which was not observed on a comet. This experiment provides further indication that the near-surface composition of comets is dominated by refractory materials and not by

volatile ices (Fulle et al., 2018; Herique et al., 2017; Pätzold et al., 2018).

4.4.1.2 *50 vol% and 33 vol% water ice content*

The increased dust content in samples with a 50 vol% and 33 vol% water ice content reduced the sublimation activity significantly. After 15–20 min, a layer of dust had formed on the horizontal top of the samples and prevented fresh ice from being insolated. Therefore, the height of the samples decreases only slightly during these experiments. This process was already observed in earlier experiments (e.g., Grün et al., 1993; Kührt and Keller, 1994; Lämmerzahl et al., 1995) and could be a source of dust that covers substantial parts of the surface of 67P (Lai et al., 2016; Thomas et al., 2015a). It must be noted that significant amounts of dust are redeposited on 67P and substantial dust blankets do not have to have formed in situ on the comet's surface (Cambianica et al., 2020; El-Maarry et al., 2016; Kramer and Noack, 2015; Lai et al., 2017).

The material loss of the samples occurred mainly on their vertical surfaces and made the granular structure of the samples visible. These grains can easily be removed against cohesion and gravity via pressure drag forces and their size scaling to cometary conditions can be reproduced very well in in situ observations of millimeter- to decimeter-sized particles of 67P (Fulle et al., 2016; Mottola et al., 2015; Ott et al., 2017; Rotundi et al., 2015). In fact, the surface structure also resembles in situ observations from Rolis on Philae. Schröder et al. (2017) and Otto et al. (2020) describe the morphology of the cometary material on an actual millimeter scale. Our experiments are scaled to larger sizes, but the in situ images show cohesive material which we also produced. Despite the vertical walls not being directly insolated in our setup, the small amount of energy that reached the vertical walls was sufficient to sublimate the ice, which has a higher surface energy than fly ash (Haack et al., 2020) and acts as "glue." Diffuse reflections from inside the chamber were unlikely due to the black coating of the inner cooling shield. With the reduced amount of ice, the tensile strength of the sample material decreased and ice-depleted material detached from the surface. Due to the high incidence angle at which the vertical surfaces were insolated, the incoming energy was not sufficient at ejecting the dust particles and aggregates as well as the talus that formed around the sample. Over time, the diameter of the sample decreased while its height remained mostly constant. This process has been suggested to be at work on 67P by Vincent et al. (2016b).

This shows that the durability of an insolated object on a cometary surface depends not only on its material, but also on its shape if some illumination directions are obstructed. At vertical walls, the formation of stable dust layers is limited, so that local morphological features (boulders, cliffs, etc.) on a comet's surface can become the starting point of regressive erosion. With these two experimental setups, we could reproduce retreating scarps and boulder movements at taluses observed on comets 9P or 67P (e.g., El-Maarry et al., 2017; Thomas et al., 2013b). The erosion only comes to rest when irregular surfaces are smoothed and covered by an ice-depleted layer of dust. This could be reproduced in the sample with 33 vol% water ice when after about 11 hours substantial parts of the lateral surface were covered by the talus and enough

dust had accumulated on the meanwhile nonvertical surfaces to prevent progressive erosion.

In 67P, fractures evolved within the cometary material to a length of up to several hundred meters (El-Maarry et al., 2015a; Poulet et al., 2016) and formed networks of polygons. These polygons are predominantly 1–5 meters in width, but they can exceed 13 meters (Auger et al., 2018). They form when a near-surface layer is hardened by the sublimation and condensation of volatile materials (Knapmeyer et al., 2018; Spohn et al., 2015), and tensions can build up in the hardened layer. After the sublimation experiments, we observed the hardening of the samples' interiors, but we did not simulate diurnal cycles. Therefore, the samples were not exposed to a temperature-dependent volume change and subsequent mechanical stress. This may have prevented the formation of crack systems.

It is also possible that the samples in the laboratory were too small to develop a stress field sufficient to create visible fractures in the samples.

4.4.1.3 *25 vol% and 20 vol% water ice content*

The granular structure of the sample material with 25 vol% and 20 vol% water ice appeared to be very similar to that of samples with a higher water ice content. However, the small changes in the morphology of the samples show that the vapor pressure was no longer sufficient to continuously detach and eject particles (Farnham et al., 2007; Finson and Probstein, 1968). The high dust content prevents a simple escape of gaseous water, so that a higher vapor pressure can build up near the sample's surface. This pressure is eventually released in an outburst event, entraining substantial parts of the surface. This could be interpreted as an analogous process of spontaneous jet formation on the rough surface of 67P (Tubiana et al., 2015; Vincent et al., 2015a,b). In the experiment, this process is suppressed after a few minutes by a cover layer of dust, which protected the underlying water ice from sublimation (see Grün et al., 1993; Kührt and Keller, 1994).

This series of experiments showed that the type of sublimation activity and the morphologic appearance of the erosion process are depended on the volatile content. When the volatile content is large, the mass loss is fast but continuous (Fig. 4.6). As the dust content increases, the mass loss per time decreases and single but larger ejection events occur. This shows that sublimation activity is not necessarily a slow and continuous process, just as observed for 67P (Tubiana et al., 2015; Vincent et al., 2016b). It is possible to suggest that the different outburst and activity patterns on 67P could also be attributed to a heterogeneous volatile content in the comet's material with the jet occurring in potentially more dust-rich areas. Vincent et al. (2016b) actually attribute outbursts to areas with steep scarps. We find that the spatial distribution of outburst locations on the nucleus correlates well with morphological region boundaries, especially areas marked by steep scarps or cliffs.

4.4.2 *Horizontal insolation*

Analog to the experiments with vertical insolation, the ice-dust mixtures were insolated horizontally in a series of sublimation experiments. Despite their identical composition,

the morphology of the samples developed differently than under vertical insolation.

4.4.2.1 *66 vol% water ice content*

The sample with 66 vol% water ice showed a similarly high sublimation activity at the beginning of the experiment as under vertical insolation, but this activity decreased after a short time. The vertical wall quickly lost material, became very rough, and eroded more rapidly at the free surface at the top. Therefore, a thin layer of dust could more easily form on less intensively insolated areas. This prevented rapid and complete material loss. After 4 hours, a thin dust layer had formed and only a few particles and aggregates were ejected. Due to the generally low dust content in the sample, the dust layer accumulated slowly, but was sufficient to prevent the complete sublimation of the ice.

After 11 hours in the chamber, the upper part of the sample collapsed (Fig. 4.8). This shows that despite the thin protective dust layer, water sublimated from the sample material below. A comparable process of sublimation of volatiles through the porous mantle of cometary nuclei was reviewed by Belton (2010) and observed on 67P (Oklay et al., 2016). However, the collapse of the sample seems unexpected because remaining water ice in the sample would act as an adhesive. During experiments with vertical insolation, aggregates detached from the sample wall and scaled to a few centimeters to decimeters on a comet. In contrast, the cliff collapse under horizontal insolation in the laboratory would scale to several meters on a comet. In this size range, gravity plays a more important role in the laboratory and on the comet (Bischoff et al., 2019; Sánchez and Scheeres, 2014) and subsequentially the ice-depleted cliff collapsed under its own weight.

A further explanation for the reduced sublimation rate compared to vertical insolation could be found in the sample preparation phase. It cannot be completely excluded that at the moment the sample was placed in the chamber, its surface temperature increased above 150 K and the superficial ice particles started to sinter (Gundlach et al., 2018a; Kuroiwa, 1961). This would have greatly increased the tensile strength of the sample material and made changes in morphology more difficult. In this case, the cliff collapse would have been unlikely.

4.4.2.2 *50 vol% and 33 vol% water ice content*

As under vertical insolation, the samples with a 50 vol% and 33 vol% water ice content altered comparable to continuously receding cliffs and they formed taluses of debris as observed for cometary nuclei (Farnham et al., 2013; Vincent et al., 2015a,b). However, the timescales on which this occurred were different. Due to direct horizontal insolation of the lateral sample's surface, the sublimation phase was more intense but it slowed down much earlier. This resulted in a faster development of the ice-reduced talus and dust layer. They covered substantial areas of the surface much earlier and prevented further sublimation activity such as the ejection of particles. This explains the paradox that despite direct insolation, the sample became inactive more quickly.

The fact that the samples tended to lose material rather continuously than in larger cliff collapses could be due to their water ice content, which increases the tensile strength (Haack et al., 2020). Also the random internal structure of the individual samples may prevent collapses.

4.4.2.3 *25 vol% and 20 vol% water ice content*

The morphological development of the samples with only 25 vol% and 20 vol% water ice was different compared to that with the same volatile content but insolated vertically. The cliff collapses occurred after the insolated area became unstable due to the loss of water by sublimation (Belton, 2010). This could not be observed on horizontal surfaces because vertical mass transport is not possible. Therefore, the mass loss of even volatile-depleted samples was enhanced under horizontal insolation compared to vertical insolation. The reactivated release of volatiles after collapse events corresponds to the observations of 67P where cliff collapses and other mass wasting processes are linked to the local formation of gas jets (Oklay et al., 2016; Steckloff et al., 2016; Vincent et al., 2016b). As the activity of the sample ended, its surface appeared very similar to the rough surface of 67P in close-up images (e.g., Schröder et al., 2017; Vincent et al., 2015a,b).

At the end of the experiments, the final morphologies of the different samples were comparable when insolated horizontally. The stable remains of the samples displayed very rough and irregular surfaces, while the fine-grained debris material formed a talus at the bottom of the sample. However, the formation processes were different: from a longer lasting and uniform sublimation activity of samples with high volatile content to an event-dominated and faster ending activity of samples with low volatile content. Since continuous and thus high sublimation rates would let a comet decay quickly and observations of 67P would suggest episodic activity (Steckloff et al., 2016; Tubiana et al., 2015; Vincent et al., 2016b), a low near-surface ice content up to 20 vol% seems plausible on a comet.

Despite many similarities between morphologies of laboratory experiments and in situ observations, it must be noted that our comet analog material is a rough approximation of the actual cometary material. Thus, in our setup we completely abstained from using organic materials (Capaccioni et al., 2015; Fulle et al., 2017; Goesmann et al., 2015). However, their influence on the development of cometary surfaces cannot be underestimated and must be analyzed in future experiments.

None of the sublimation experiments with an insolation flux of ~ 1 solar constant resulted in visible changes in the sample's surfaces. According to our scaling, this insolation flux corresponds to a heliocentric distance of the comet of $\sim$4 AU and at this distance 67P already showed activity on its surface (Tubiana et al., 2015). For this discrepancy, the following two explanations are possible. 1) The scaling is not sufficiently accurate and the required energy for a simulated heliocentric distance of the comet was underestimated. 2) The sample mixture does not reflect the composition of a comet accurately enough.

Since the physical correlation between sublimation and van der Waals related cohesion have been well described in previous publications as the main suppressor of cometary activity (Chokshi, Tielens, and Hollenbach, 1993; Kührt and Keller, 1994; Scheeres et al., 2010; Skorov and Blum, 2012), it is most likely that the reason for the negative results lies within the sample mixture. The increased albedo and the absence of other volatiles and organic material in the laboratory are major differences to the composition of comets possibly reducing the laboratory cometary activity. Nevertheless, the influence of the albedo on the required energy in the laboratory was taken into account in Eq. (4.4).

A probable explanation for cometary activity at large heliocentric distances is the presence of CO_2, CO, and other super-volatile ices (Bockelée-Morvan and Biver, 2017; Gundlach et al., 2015; Läuter et al., 2018), which start to sublimate at lower temperatures. Since we only used water ice as volatile, this could shift the sublimation activity of the samples to higher insolation fluxes. Additionally, it is conceivable that the presence of organic material in 67P favors the absorption of energy due to their dark color (Ciarniello et al., 2015) and allows ices to sublimate faster on the comet.

4.5 CONCLUSIONS

The insolation flux required to generate sublimation activity on a sample and thus a cometary surface depends on its content of different volatile materials. Using water ice as the only volatile, it was not possible to generate activity at a distance equivalent to about 4 AU in the laboratory. However, at a simulated heliocentric distance of 3.1 AU, pronounced activity could be generated.

All of the prepared sample mixtures presented a similar granular structure. The dust and ice particles, which were used as analog materials, formed submillimeter- to millimeter-sized aggregates. These aggregates would correspond to centimeter-to-decimeter-sized pebbles on 67P and simulate the predicted granular structure of the comet (Blum et al., 2017; Fulle et al., 2016; Pajola et al., 2016b).

The volatile content of the sample has a major influence on the type of sublimation activity (Fig. 4.9). Volatile-rich samples are subject to the generally continuous and rapid loss of ice and dust. Due to the low dust content, no uppermost layer of dust forms, or only slowly, which would prevent extensive sublimation by covering fresher material. Simultaneously, the high water ice content increases the tensile strength (Haack et al., 2020) and allows the formation of exotic morphologies such as spikes or extreme overhangs.

When the amount of dust in the samples increases, the activity comes to an earlier end due to an evolving protective layer of dust. At the same time, the activity gets a more episodic character resulting in outburst events or cliff collapses. The resulting water-depleted deposits are less cohesive, but they form very irregular and more stable surfaces compared to volatile-rich materials.

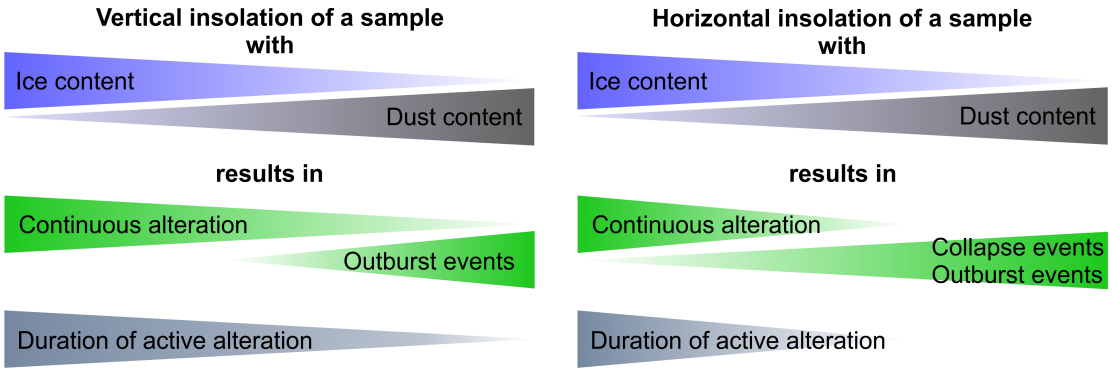

Figure 4.9: Schematic and qualitative overview of parameters affecting the alteration of the sample's surfaces in the experiment. Vertical insolation and high ice content result in a more continuous alteration and increase its duration. Horizontal insolation and high dust content result more often in spontaneous outburst and collapse events and decrease the overall duration of active surface alteration.

The shape of the surface features and the angle at which they are insolated can partly compensate for the effects of different volatile content. Under vertical insolation, layers of dust can form on horizontal surfaces. These layers remain stable due to reduced gravitational transport processes. Thus the underlying, possibly volatile-rich material remains unaffected by sublimation and the height of a sample or an area on a comet remains largely constant.

This changes with the horizontal insolation of features that allow material to fall down (scarps, pits, etc.). If an ice-depleted layer forms on a steep wall, it collapses when its weight exceeds its cohesion and exposes fresh volatile-containing material. This process can repeat episodically and lead to regressive erosion along a scarp. In this geometry, Earth's gravity helps to get rid of desiccated dust mantles. This could perhaps mimic the aerodynamic drag of the escaping gas with the loosened dust bodies on the surface.

The erosion comes to an end when the initial scarp develops an irregular or rough shape that no longer permits vertical mass transport. Additionally, the formation of a talus of debris can cover substantial parts of the original morphological feature and protect it from further erosion. This was typical for mixtures with a moderate water ice content.

Our investigations suggest that a volatile content of more than 50 vol% (<2.4 dust-to-ice mass ratio) in the outer layers of 67P is unlikely since the morphological features generated in the laboratory and high sublimation rates were not found in 67P. Due to the generally low activity of samples with a volatile content of 25 vol% (>7.3 dust-to-ice mass ratio) and less, these values are also unlikely, but they cannot be excluded completely. Our experiments based on the morphologic evolution of surface structures suggest that near the surface, a comet possesses dust-to-ice ratios between these limits. The results obtained in the laboratory are most consistent with observations and predictions for 67P (Fulle et al., 2018; Herique et al., 2017; Pätzold et al., 2018). However, further experiments are necessary to study, in more detail, the influence of organic matter on the morphological development of cometary surfaces.

5

SUBLIMATION OF ORGANIC-RICH COMET ANALOG MATERIALS AND THEIR RELEVANCE IN FRACTURE FORMATION

David Haack[1] (corresponding author), Christopher Kreuzig[2], Bastian Gundlach[2], Jürgen Blum[2], Katharina Otto[1]

[1]*Institut für Planetenforschung, Deutsches Zentrum für Luft- und Raumfahrt (DLR), Berlin, Germany*

[2]*Institut für Geophysik und Extraterrestrische Physik, Technische Universität Braunschweig, Braunschweig, Germany*

Published in Astronomy&Astrophysics, Volume 653, September 2021, Article Nr. 153
https://doi.org/10.1051/0004-6361/202142069, reproduced with permission

ABSTRACT

The morphology of cometary nuclei is the result of an ongoing evolution and can provide valuable information to constrain the composition of comets. In our laboratory experiments we investigated the morphological evolution of comet analog materials, which consist of volatile, dust, and organic components. The laboratory results are aimed to help understand the evolution of cometary surfaces.
We used spherical particles of fly ash and mixtures of ice, glycine, and sodium acetate as analog materials in different mass ratios to reproduce observed cometary morphologies. The cohesive and gravitational properties in the laboratory are scaled to cometary conditions to draw meaningful conclusions from the experimental results. The samples were placed in a vacuum sublimation chamber, cooled down to below 150 K, and were insolated with an external light source. To analyze the morphology of the samples, a camera was used to monitor the alterations of the surface.
Organic components in volatile-rich samples can have a distinct adhesive effect after the volatiles sublimate. During the sublimation process the sample volume decreases and fractures form on the sample surface. Due to the stability of the remaining volatile-depleted material, significant cliff collapses or ejected particles were not observed in the laboratory.

5.1 INTRODUCTION

Comets are primordial objects from the early days of the Solar System. Due to their origin from the outer Solar System beyond the ice lines of volatile materials (Dodson-Robinson et al., 2009), they have been subject to no or only minor alterations since their formation and thus are archives with information about the early Solar System. This makes them interesting targets for space missions that have studied comets at close

range since the mid-1980s (e.g., ESA's Giotto and Rosetta missions and NASA's Stardust and Deep Impact missions). Even with these missions, the processes leading to the formation of comets and their evolution are not yet fully understood (Weissman et al., 2020). Which amounts of volatile and nonvolatile materials are present in a cometary nucleus and which processes alter a comet's surface as it approaches the Sun are still the subject of investigation (Gulkis et al., 2015; Sierks et al., 2015). The sublimation of volatile components, such as CO, CO_2, or H_2O (Biver et al., 2019; Hässig et al., 2015; Läuter et al., 2018), is caused by the insolation of solar energy to the surface and the heat transfer to the shallow subsurface of a comet in an airless environment. During this process, layers of nonvolatile mineralic and organic components (Capaccioni et al., 2015; Goesmann et al., 2015; Raponi et al., 2020) accumulate at the surface and can be redeposited or transported away by the gas drag of continuously sublimating volatiles (Bischoff et al., 2019; Gundlach et al., 2015; Gundlach, Fulle, and Blum, 2020; Keller et al., 2017; Kührt and Keller, 1994). With each orbit around the Sun, a comet loses more material via progressive erosion (Thomas et al., 2015a) and a variety of morphologies are formed on its surface, such as cliffs, fractures, and rocky or flat areas (El-Maarry et al., 2019; Pajola et al., 2016a; Thomas et al., 2015b). The appearance of morphological features are determined by the chemical composition, grain size, porosity, and cohesive and gravitational forces of the comet's nucleus. Therefore, the reproduction and analysis of cometary morphologies in the laboratory may provide information about the composition and evolutionary history of comets in space.

Laboratory experiments, such as the KOSI (KOmetenSImulation) project in the 1990s, have studied sublimation processes that are expected to take place on comets (Grün et al., 1989, 1993; Lämmerzahl et al., 1995). As part of the KOSI project, a sample container was filled with mixtures of nonvolatile analog materials and ices and was placed in a sublimation chamber. After the samples were insolated with an energy source, an ice-free layer formed on their surfaces, preventing energy transport to underlying layers and further sublimation processes after a few hours. With the Rosetta mission and its landing module Philae, cometary science and laboratory analog experiments increasingly came into focus. The measurements and detailed images of comet 67P/Churyumov-Gerasimenko (hereafter 67P) provided by the spacecraft significantly increased our knowledge of comets. Nevertheless, the influence of detected volatiles, organic compounds, and their abundances (e.g., Capaccioni et al., 2015; Hässig et al., 2015; Läuter et al., 2018; Raponi et al., 2020) on the evolution of the comet remains a research objective vital to the interpretation of cometary surfaces.

In order to more precisely determine the properties of materials that could be considered for analog experiments, several series of measurements have been performed. It was found that the tensile strength of water ice at temperatures below 150 K is much lower than expected (Gundlach et al., 2018b; Musiolik and Wurm, 2019). This temperature limit should not be exceeded in the experiment; if so, water ice particles start to sinter and stiff connections form between the particles (Gundlach et al., 2018a; Kuroiwa, 1961). Furthermore, it was shown that spherical particles could produce samples whose low tensile strengths and filling factors are closer to those of comets than of samples made of angular particles (Haack et al., 2020). The filling factor describes the ratio of a volume filled with particles. Besides applications in the laboratory, these

findings were also used to calibrate numerical models of comet simulations (Kappel et al., 2020).

Analog experiments with the Simulation Chamber for Imaging the Temporal Evolution of Analogue Samples (SCITEAS; Pommerol et al., 2015a) allowed photometric studies and visual observation of sublimating sample surfaces at temperatures and pressures similar to those expected on the surface of comets at low heliocentric distances. Poch et al. (2016a,b) used SCITEAS to investigate the influence of organic and mineralic components on the sublimation behavior of water ice. They found that the texture of the residuals after sublimation of the ice differed significantly depending on whether the nonvolatile components were included in the ice matrix (intra-mixtures) or were added as pure substances to pure ice particles (inter-mixture). The residuals of intra-mixtures were extremely porous and foam-like, and cohesive large flakes sometimes ejected from the surface. Inter-mixtures formed more compact and less cohesive residuals on the sample surface during the sublimation process. However, the aim of these experiments was not to realistically reproduce cometary morphologies. Therefore, the amount of nonvolatile materials accounted for less than one percent by mass in the mixtures and was not representative of cometary regolith. Kaufmann and Hagermann (2018) conducted sublimation experiments with water ice and carbon black and, like Poch et al. (2016b), observed a solidified subsurface layer under an ice-depleted and low-density cover layer. This suggests the subsurface hardening of volatile-rich and porous materials due to sublimation and recondensation (Kochan et al., 1989; Kossacki et al., 1997).

Most of these experiments were not aimed at reproducing cometary morphologies and were performed with volatile contents of >90 vol%, which are atypical for comets. To produce more realistic morphologies in the laboratory, Haack et al. (2021) performed sublimation experiments with more representative dust-ice ratios. They used fly ash (a by-product of industrial coal combustion) as the mineralic dust component and water ice particles as the volatile. The amount of ice in the sample material ranged between 66 vol% and 25 vol%, as presumed for comets (Fulle et al., 2018; Herique et al., 2017; Pätzold et al., 2018). In addition, they allowed horizontal and vertical mass transport of the sample material and found that the resulting sublimation activities and morphologies depend on the insolation angle in addition to the volatile content.

We decided to expand on previous experiments with refractory fly ash and volatile water ice (Haack et al., 2020, 2021) and added organic components as analog materials to the mixtures. The organic components consisted of sodium acetate and glycine in equal parts per mass, which are confirmed on 67P and are nonvolatile materials under our experimental conditions. Based on the findings of the Rosetta satellite mission and laboratory measurements, we prepared sample mixtures of volatile and nonvolatile materials in different ratios as plausible on a comet (Choukroun et al., 2020; Haack et al., 2021). For this, we took advantage of the low tensile strength of granular matter composed of spherical particles at temperatures below 150 K (Gundlach et al., 2018b; Haack et al., 2020). The aim of the experiments is to investigate the influence of organic components on the sublimation activity and the evolution of the sample morphology and to analyze the results for their relevance with respect to cometary surfaces.

5.2 METHODS

5.2.1 *Selection of materials*

As in previous sublimation experiments (Haack et al., 2021), polydisperse fly ash spheres, with an average radius of about 2.4 µm and a density of 2.25 g cm^{-3}, were used as a refractory dust analog. This material is a compromise between physical and chemical accuracy of dust on a comet. Fly ash corresponds to the mineralic composition of plagioclase (Haack et al., 2021) and is therefore more representative of a mineralic component of a comet compared to particles of pure SiO_2. Due to their spherical shape, mutual particle interlocking is prevented. Furthermore, it is possible to produce samples with a very low tensile strength in the laboratory (Haack et al., 2020; Kappel et al., 2020) to simulate the physical properties of cometary materials (Attree et al., 2018a; Groussin et al., 2015). The minerals olivine and pyroxene would be more accurate chemical analogs, but micrometer-sized particles of these minerals are only available with an angular shape. This would result in a drastic increase in the tensile strength of the sample material (Haack et al., 2020) and could reduce or prevent the alteration of the sample surface during the experiments.

As volatile analog material, we used polydisperse water ice spheres with an average radius of about 2.4 µm. Water ice dominates the volatile materials on 67P (Hässig et al., 2015) and was used as a first grade approximation of the volatile component of a comet. Other volatiles, such as CO or CO_2, contribute 15 mass% to the amount of volatile materials on 67P (Biver et al., 2019; Bockelée-Morvan et al., 2016; Läuter et al., 2018) and may play an important role in the evolution of a comet but were omitted to limit the complexity of the experiments. This is a reasonable limitation because in our experiments we simulated cometary conditions in which the sublimation of water may predominate since CO or CO_2 are more volatile and would already be sublimated in the simulated scenario. However, the influence of other ices on the activity of a simulated comet should be studied in future experiments.

The additional third component should be a combination of organic materials that is nonvolatile both on a cometary surface and under experimental conditions. Since the composition of the organic components of a comet is very complex (Altwegg et al., 2017; Capaccioni et al., 2015; Goesmann et al., 2015), we had to limit the number of organic components in our experiments to a few materials that may represent the chemical properties of a large variety of organic materials on a comet. We used a combination of sodium acetate ($NaCH_3COO$) and glycine ($C_2H_5NO_2$) in equal amounts, which are confirmed as components of 67P (e.g., Altwegg et al., 2016; Elsila, Glavin, and Dworkin, 2009; Rubin et al., 2019; Schuhmann et al., 2019). Sodium acetate represents organic ions and salts, and glycine is a simple amino acid and stands for a group of organic components that can potentially form larger and complex molecules. This selection of organic analog materials is very limited and cannot reflect the complexity of organic materials on a comet; however, this was inevitable since the actual composition of organic components on a comet is not fully understood and we had to limit the complexity of the experiments. Other combinations of organic materials could be conceivable, but a limited selection would generally not be able to simulate the complete variety of organic material on a comet. An additional reason for the

chemical limitation was the feasibility of the experiments in terms of the components' toxicity. The nonvolatile character of the organic components was confirmed in previous measurements with the same experimental setup.

We omitted the usage of additional materials to reduce the sample's albedo. This is not realistic because comets have a very low albedo (Ciarniello et al., 2015; Keller et al., 1986) and absorb insolated radiation much better than the analog material. However, this effect was taken into account in the energy scaling (see Haack et al., 2021) and led to increased insolation rates in the laboratory. This allowed the direct comparison of the obtained results with previous sublimation experiments without organic components (Haack et al., 2021), where all samples had an albedo of ∼0.35. This decision also kept the complexity of the experiment within limits and reduced the number of possibly interfering effects at the sample's surfaces.

5.2.2 *Sample preparation*

To keep the results comparable to those of previous experiments, the sample preparation method was adapted from Gundlach et al. (2018b) and Haack et al. (2020). Water mist was generated with a droplet dispenser and sprayed into a Dewar vessel containing liquid nitrogen. The droplets froze in the liquid nitrogen to form polydisperse spherical ice particles and sank to the bottom of the container.

We modified this method: The droplet dispenser was filled with an aqueous solution of the organic molecules instead of pure water. For this, sodium acetate and glycine were mixed in equal mass ratios (hereafter referred to as organics) and completely dissolved in water. In order to study the influence of different ratios of organic materials and water, two solutions were prepared, with the organic-to-water mass ratios of 10:100 and 5:100.

The resulting particles in the Dewar vessel consisted of organic components enclosed in an ice matrix. The advantage of this method was that the pure organic analog materials did not have to be shaped into micrometer-sized spheres to be comparable to fly ash and water ice particles. In addition, Hadraoui et al. (2019) suggested that glycine embedded in a sublimating ice matrix reproduces the emitted glycine detected in the coma of 67P most realistically.

Archimedes' principle was used to determine the amount of organic-bearing ice particles in the Dewar vessel. The weights of the same volumes of pure liquid nitrogen and of the liquid nitrogen-ice suspension were measured. Using the weight difference of the two measurements and the known densities of liquid nitrogen and ice (Table 5.1), the mass of ice in the Dewar vessel was calculated. After the amount of ice particles in the vessel was determined, a scale was used to add predefined amounts of fly ash to the suspension. The relative amounts of ice to fly ash were selected between 20 and 40 mass%; they correspond to the ratios estimated for the nucleus of 67P (Fulle et al., 2018; Herique et al., 2017; Pätzold et al., 2018) and are comparable to those of the sublimation experiments carried out by Haack et al. (2021).

A cylindrical metal mold was filled with the suspensions of organic-bearing ice, fly ash, and liquid nitrogen in the Dewar vessel, which were thoroughly mixed. The mold had an inner diameter of 25 mm and was placed vertically on a metal sample holder (see Haack et al., 2021). The mold and sample holder were cooled with liquid nitrogen

Table 5.1: Molar mass and density of components used to simulate cometary materials.

	Molar mass [g mol^{-1}]	Density [g cm^{-3}]
Fly ash		2.25
H_2O (ice)	18.02	0.93
$NaCH_3COO$	82.03	1.52
$C_2H_5NO_2$	75.07	1.60
N_2 (liquid)	28.01	0.807

before the sample mixture was added in. As the nitrogen of the suspension slowly evaporated, only the ice-organic and fly ash particles remained in the cylinder. When the nitrogen had completely evaporated, the cylindrical mold was removed from the sample holder, uncovering solid but extremely porous samples (Haack et al., 2021) with the diameter of the mold. The samples were immediately placed in the vacuum sublimation chamber prepared for the measurement. This procedure ensured that the sample temperature did not exceed 150 K and prevented sintering of the ice particles.

To determine the cohesive force between the organic-bearing ice particles, their tensile strength and surface energy were determined with other samples of the same mixture before the sublimation experiments. For this purpose, the Brazilian disk test method was used, as described in previous experiments (Bischoff et al., 2020; Gundlach et al., 2018b; Haack et al., 2020). With a particle radius, r, of 2.4 µm and a filling factor, Φ, of 0.46, the tensile strength of ice with 10 mass% organics at 150 K amounts to 1300 ± 250 Pa, compared to 1100 ± 210 Pa for pure water ice (Haack et al., 2020). Following Blum et al. (2006), the upper limit for the surface energy, γ, is

$$\gamma = \frac{4r\sigma}{9\Phi}. \tag{5.1}$$

With the values of the tensile strength, σ, the surface energy of the used organic-rich ice is 0.0029 ± 0.0006 Jm^{-2}, compared to 0.0026 ± 0.0005 Jm^{-2} for pure water ice (Haack et al., 2020). These values are the same within measurement error, and therefore we can use the previous values of tensile strength and surface energy from Haack et al. (2020) for further calculations of different organic-bearing ice-dust mixtures.

In previous measurements, the albedo of fly ash was determined to be 0.35. This value was also assumed for our sample mixtures since the albedo of ice-bearing mixtures is mainly determined by the dust component (Chýlek, Ramaswamy, and Srivastava, 1983; Clark and Lucey, 1984; Oehler and Neukum, 1991).

5.2.3 *Scaling to cometary conditions*

To obtain meaningful results from the experiments, the conditions in the laboratory must be scaled to the conditions on a comet. The most important difference between the two environments is the gravity that is by orders of magnitudes higher in the laboratory compared to the $\sim 2 \times 10^{-4}$ m s^{-2} on comet 67P (Agarwal et al., 2016). To solve this problem, we used the same scaling for particle size as for the experiments described in

Haack et al. (2021). The scaling relates the ratios of gravity and particle-size-dependent cohesion in the laboratory and on 67P. With known gravity $F_G = \frac{4}{3}\pi r^3 \rho g$ and cohesion $F_C = 3\pi r\gamma$ in the laboratory (Haack et al., 2020) and the known gravity on 67P, the corresponding cohesion and thus particle size on the comet can be estimated with

$$\frac{F_{G_{67P}}}{F_{C_{67P}}} \approx \frac{F_{G_{\text{Earth}}}}{F_{C_{\text{Earth}}}}\,. \tag{5.2}$$

In these equations, r is the particle radius, ρ is the particle density, g is the gravitational acceleration, and γ is the surface energy. According to the determined values of the surface energy and the scaling of Haack et al. (2021), the fly ash and organic-rich ice particles with a radius of $\sim$2.4 µm represent millimeter-sized particles on 67P. This is in line with the size of hypothesized pebbles, which may have initially formed comets (Blum et al., 2014, 2017; Fulle et al., 2016; Lorek et al., 2016; Lorek, Lacerda, and Blum, 2018). On a macroscopic scale, a 2.5 cm object in the laboratory would correspond to an object of about 10 m in size on 67P. This could be a cliff, a large boulder, or other morphological features on the comet (El-Maarry et al., 2019; Pajola et al., 2016a; Thomas et al., 2015b) that would be subject to progressive alteration by the sublimation of volatile materials.

After increasing the cohesive forces by reducing the particle size, the insolated energy in the experiment had to be adapted to reflect realistic cometary conditions. The insolated energy heats the ice at the surface, which sublimates and creates a near-surface vapor pressure according to the Clapeyron-Clausius equation $P_v = Ae^{-B/T}$, where T is the temperature of the ice and A and B are constants with values $A = 3.56 \times 10^{12}$ Pa and $B = 6142$ K for water ice (Fanale and Salvail, 1984). The vapor pressure acts on the particle cross section and creates a pressure drag, $F_D = \pi r^2 P_v$, on the particles of the sample, where r is the particle radius. When the F_D on the particles exceeds their cohesion, F_C, individual particles or particle aggregates detach from the sample's surface and can be transported away. To compare this process in the laboratory with 67P, this scaling relates the ratios of insolation-dependent pressure drag and particle cohesion of the sample and on 67P as described in Haack et al. (2021) and follows

$$\frac{F_{D_{67P}}}{F_{C_{67P}}} \approx \frac{F_{D_{\text{Earth}}}}{F_{C_{\text{Earth}}}}\,. \tag{5.3}$$

This second scaling ensures that the insolated energy on the sample surface is sufficient to sublimate the water ice and can be related to the corresponding insolation rate on 67P.

When Rosetta reached 67P and monitored activity on its surface, the comet had a heliocentric distance of about 4 AU (Tubiana et al., 2015). According to the energy scaling, this distance can be simulated with $\sim$1 solar constant in the laboratory. When 67P reaches its perihelion at 1.24 AU, the solar insolation reaches its maximum. This insolation flux would transform to about 33.6 solar constants in the laboratory (Haack et al., 2021). However, the experimental setup was not built to provide this amount of energy. With the solar simulator used in our experiments, a maximum insolation rate of 1.9 solar constants was reachable. This corresponds to a heliocentric distance of 3.6 AU for 67P. Activity has already been observed on the surface of 67P at this distance (Snodgrass et al., 2013; Tubiana et al., 2015).

5.2.4 *Sublimation experiments*

The experiments were performed in the vacuum sublimation chamber, which was also used in Haack et al. (2021). Before the sample was placed, the chamber was cooled to about 110 K and flooded with argon to prevent atmospheric moisture from entering the chamber when it was opened for sample insertion. The sample holder, with the sample on top, was firmly mounted inside a cooling shield within the chamber and connected to temperature sensors. The cooling shield was a rectangular metal housing, with a side length of 10 cm, which was actively cooled with liquid nitrogen throughout the duration of the experiments. It has two openings, one on its top to allow insolation of the sample from above and one on its side surface for visual observation of the sample (see Fig. 4 in Haack et al. 2021). This mitigated the alteration of the samples by background thermal radiation during the experiments.

After the mounting of the sample holder, the chamber was closed immediately and the pressure and temperature inside were reduced to $\sim 10^{-7}$ mbar and below 150 K, respectively, to simulate conditions similar to those of a comet (Kührt, 1984). When pressure and temperature reached operating values, a solar simulator was used to insolate the sample vertically from above with an insolation flux of 1.9 solar constants. According to the energy scaling, this corresponds to a heliocentric distance of about 3.6 AU. To verify the temperature stability during the experiments, temperature sensors were used to monitor the sample and the cooling shield. A camera with a 3000 by 2000 pixel sensor was focused at the sample through a side window of the sublimation chamber and captured images (25 µm per pixel) at a frame rate of one image per second.

Two series of experiments with three measurements each were performed with two different fixed organic-ice mass ratios, 5:100 and 10:100. The subsequently added amount of dust led to 300:100, 500:100, and 700:100 mass ratios with respect to ice for both series (Table 5.2). This represents ice-dust ratios as suggested by observations on 67P (Fulle et al., 2018, 2017; Herique et al., 2017) and by laboratory experiments (Haack et al., 2021). A reference measurement was performed without organics to directly infer the influence of organics on the evolution of the sample morphology. The insolation stopped after a maximum of 20 hours of measurements, when the supply of liquid nitrogen to cool the sublimation chamber had to be replenished. At the end of the experiment, the images taken with the camera were analyzed in terms of the degree of alterations on the sample surface with respect to the sample compositions.

5.3 RESULTS

To obtain a reference measurement of organic-free material, a sample with an ice-dust mass ratio of 100:500 was placed in the chamber. With vertical insolation, particles were only sporadically ejected from the top in the first minutes of the experiment. Significant surface alteration was limited to the vertical surface. Material detached from the vertical side wall and fell down due to gravity. In this process, larger areas of the wall collapsed repeatedly. This altered the shape of the sample from cylindrical to more conical, with decreasing diameter toward the top (Fig. 5.1). A difference between the albedo of ice-depleted and fresh material could not be detected.

Table 5.2: Relative mass ratios of organics, ice, and dust used for various sample mixtures in the sublimation experiments. The ice fraction was normalized to 100 for ease of reference. The dust volume with respect to the bulk material is given in parentheses.

	Organics	Ice	Dust (vol%)
Organic free reference	0	100	500 (67)
	5	100	300 (59)
Low organic content	5	100	500 (70)
	5	100	700 (77)
	10	100	300 (62)
High organic content	10	100	500 (73)
	10	100	700 (79)

Areas where fresh material was exposed to the sample surface appeared very rough, with a granular texture in the submillimeter range. The detached material accumulated directly at the base of the sample as ice-depleted granular dust. The surface alteration rate decreased throughout the experiment, and after about 12 hours the activity came to an end. Unfortunately, the experimental setup was not designed to monitor mass loss during the experiments, so the results were limited to visual observations.

By the end of the experiment, an ice-depleted non-cohesive dust layer had formed on the remaining sample material, and large amounts of ice were observed in the center of the remains. The remaining ice-rich material had solidified significantly compared to the sample material at the start of the experiment. However, with the setup used, it was not possible to determine the exact amount of remaining ice and the sample's tensile strength because frost formed on the sample immediately after it was removed from the sublimation chamber and the ice began to thaw.

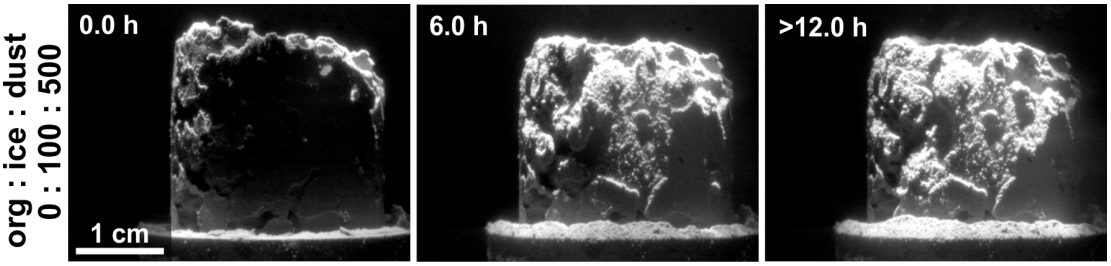

Figure 5.1: Sublimation experiment without organic components as reference. It was performed to obtain a reference to samples with organic components. The series shows how the surface of a sample with an ice-dust mass ratio of 100:500 evolves under a vertical insolation of 1.9 solar constants. The shape of the sample altered as material detached and fell off the lateral surfaces as individual grains or local cliff collapses. No further surface alterations were observed after 12 hours. A time lapse of the evolution is available as an online movie.

5.3.1 *Low organic content*

We started the first series of measurements with an organic-ice-dust mass ratio of 5:100:300 and increased the dust content in two steps, to 5:100:500 and 5:100:700, respectively. In all measurements the reduction of the samples' volume was most noticeable as the ice sublimated (Fig. 5.2). No solid material detached in the form of ejected particles or cliff collapses, and we did not observe any transport away from the surface via other mass movement processes. As a result, none of the three samples produced visible areas where fresh material was exposed to the surface. In contrast to organic-free ice-dust mixtures, material loss from all organic-bearing samples appeared to be caused by sublimating ice only. On the lateral surface of the sample with the lowest dust content (5:100:300), the sample volume decreased and short fractures of 2–3 mm formed during the sublimation phase. This process slowed down during the experiment, and no further change was observed after 12 hours. With increasing dust content and a correspondingly lower amount of organic-rich ice, the formation of fractures became less evident. On the sample surface with the lowest content of the organic-rich ice (5:100:700), no distinct fractures could be observed. On this sample, the surface alteration was generally less significant and stopped after 8 hours.

At the end of the experiment, the sample residues were removed from the sublimation chamber and a mantle of ice-depleted material a few millimeters thick was observed. The mantle material was extremely porous and fragile but preserved its shape after the ice had sublimated. In contrast to the organic-free reference experiment, the ice-depleted material did not decay into granular dust under the influence of gravity. The ice-depleted mantle covered the sample center, where ice remained preserved. As observed in the organic-free reference sample and in previous sublimation experiments (e.g., Haack et al., 2021; Kaufmann and Hagermann, 2018; Poch et al., 2016b), the ice-containing sample center was significantly solidified compared to the start of the experiment. No change in albedo before and after the experiment was detected on the side wall of any of the three samples.

5.3.2 *High organic content*

In the second series of measurements, the mass of organic material was doubled with respect to the amount of water ice. The mass ratios of dust were increased in three steps and were comparable to those of the first series of measurements (Table 5.2). The vertical insolation of 1.9 solar constants remained unchanged.

The samples of this measurement series presented a volume loss, which appeared qualitatively increased compared to samples with lower organic content (Fig. 5.3). No mass transport of solid material away from the surface was observed in any of the three samples. In the course of the experiments, distinct fractures developed on the lateral side of the samples. These fractures were more pronounced than in experiments with lower organic content, frequently exceeded 5 mm in length, and formed poorly developed networks. The angles at which they intersected were variable. The fractures evolved most distinctly, and the apparently highest volume loss was observed on the sample with the lowest dust content (10:100:300). The phase of observable surface alteration for this sample with the lowest dust content ended after about 12 hours.

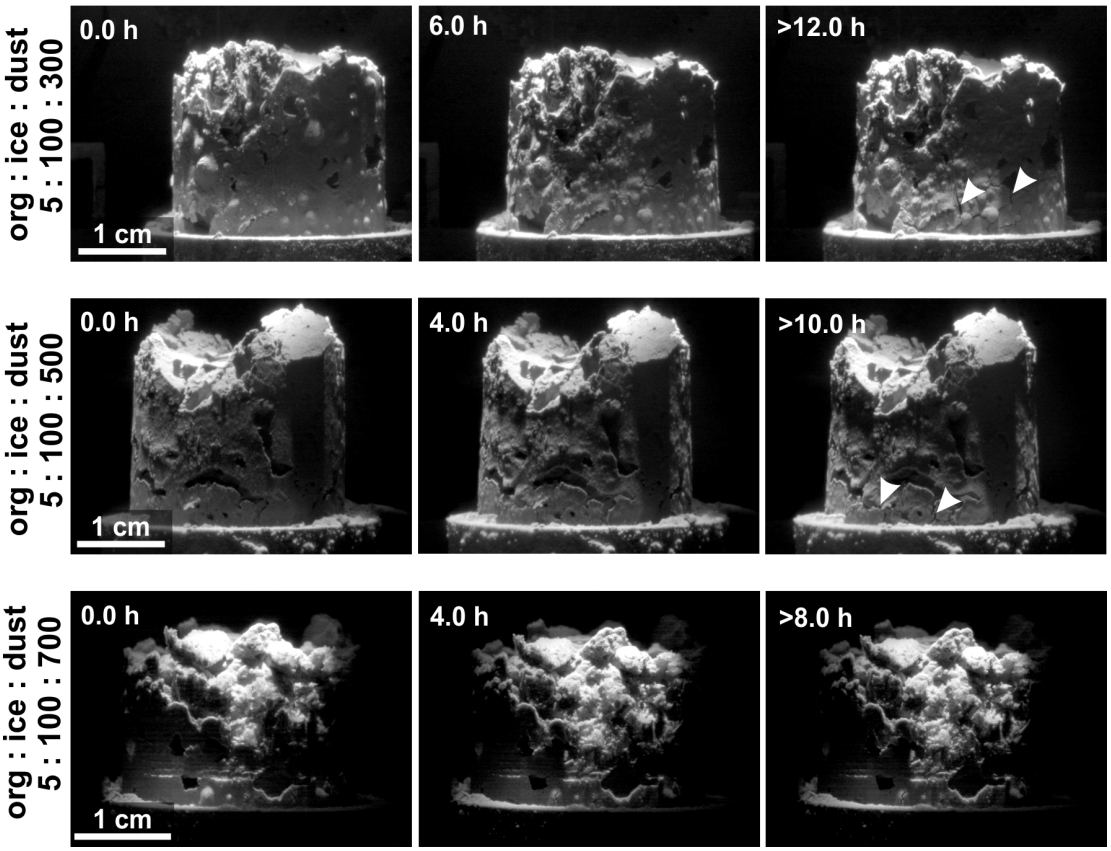

Figure 5.2: Three vertically insolated samples with different organic-to-ice-to-dust mass ratios at an insolation rate of 1.9 solar constants. The image series show the alterations of the sample surfaces as a function of increasing dust content (online movies). The decreasing sample volume and formation of fractures (some marked with arrows) is most evident at a component mass ratio of 5:100:300 and reduces significantly with increasing dust content. The surface-altering activity of the first sample comes to an end after 12 hours. The following series show the dust-dependent reduction of the surface alterations and the timescales on which they occur. At a maximum relative dust amount of 5:100:700 per mass, the duration of visible sample alteration is reduced to 8 hours.

In contrast to the first series, the sample with the highest dust content (10:100:700) also showed significant fracturing. However, the volume decrease was reduced and less rapid compared to samples with lower dust content. The phase of visible surface alteration of the sample with the highest dust content came to an end after about 6 hours. The comparison between the two series of measurements showed that the duration of the observable surface alteration depends predominantly on the dust content and not on the amount of the organic component. An increased dust content generally leads to reduced phases of surface alteration.

After the remains of the samples were removed from the sublimation chamber at the end of the experiments, an ice-depleted mantle on the surface, which enveloped an ice-rich core, was observed. This is in analogy to the results of the experiments with low organic content. The thickness of the mantle at the side surfaces reduced from more than 3 millimeters to about 1 millimeter as the dust content of the samples increased. Despite its high porosity, the mantle material was cohesive enough that

fragments could be manually removed without disintegrating into granular dust. No change in the albedo of the sample materials before and after the experiments was observed.

The results of organic-rich sublimation experiments differ significantly from those without organics. The observed activities and morphologies at the sample surfaces are less diverse (no cliff collapses, outbursts etc.) and less dependent on the volatile content compared to the alterations of samples without organics (Fig. 5.1; see also Haack et al., 2021). In all observed samples, the surface alterations were dominated by volume loss and fracture formation that proceeded continuously with no distinct individual events.

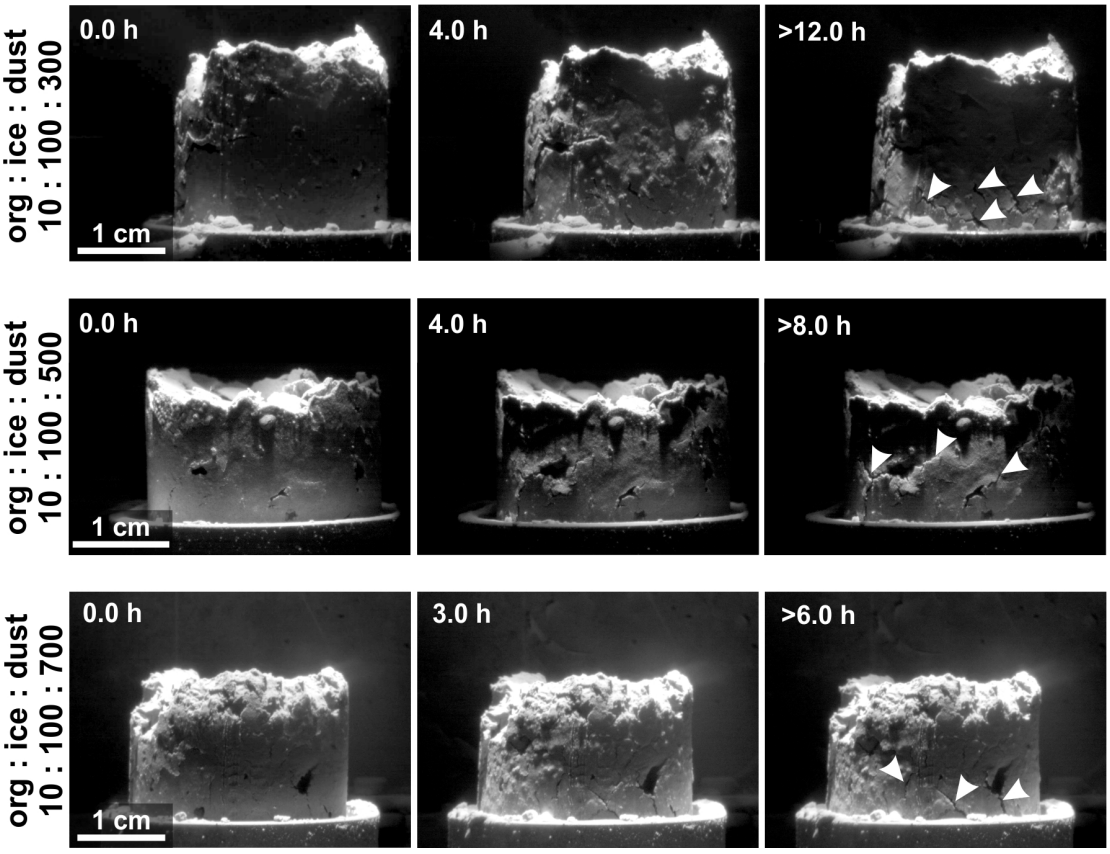

Figure 5.3: Evolution of three sample surfaces with high organic content under vertical insolation. The reduction in the sample volume and the formation of fractures (some marked with arrows) can be observed in all three image series (online movies). This surface evolution is most distinctly observable in the top series, with an organic-to-ice-to-dust mass ratio of 10:100:300, whose phase of activity ended after 12 hours. The degree of surface alteration and its duration decreased with increasing amounts of the dust component and ended after 8 and 6 hours, respectively.

5.4 DISCUSSION

The observations obtained with the organic-free reference measurement are in line with those presented by Haack et al. (2021), even though the insolation flux is somewhat reduced compared to the previous experiments. The test shows that, with our

experimental setup, a sample without organic components loses substantial amounts of nonvolatile material and is subject to a significantly different morphological evolution than samples with organics.

At 150 K, the addition of glycine and sodium acetate to water ice in a mass ratio of 10:100 only increases the surface energy of the ice particles within the measurement inaccuracy of the surface energy of pure water ice. We assume that this difference between organic-to-ice mixtures of 5:100 and pure ice is even smaller and cannot be determined with sufficient accuracy because of the limitations of the Brazilian disk test method. Therefore, we extrapolated the average surface energies of mixtures of dust, ice, and organics by using the values of previous Brazilian disk tests with ice-dust mixtures without organics (Haack et al., 2020) to estimate the tensile strength of each sample material.

The volume fractions of dust in the samples with different mixing ratios range from about 60 vol% for the lowest dust content (X:100:300) to almost 80 vol% for the highest dust content (X:100:700; Table 5.2). The different amounts of organics have only a minor influence on the various volume fractions of the sample mixtures because of their small share in the total mass of the samples. With the sample's filling factor of 0.41 (Haack et al., 2021), the tensile strength values of the samples were calculated and range between 540 Pa for the lowest and 360 Pa for the highest dust content. This is somewhat above the high end predicted for materials on 67P by Groussin et al. (2015). Other estimates give an even lower strength of only a few pascals for cometary material (Attree et al., 2018a; O'Rourke et al., 2020). Since the size scaling is based on the comparison of cohesion on 67P and in the laboratory, it should be considered with caution. However, it is not unrealistic since hypothetical samples with a filling factor between 0.15 and 0.37, as assumed for 67P (Fulle et al., 2016; Herique et al., 2019; Pätzold et al., 2016), would have a calculated tensile strength equivalent to that given by Groussin et al. (2015). With the method of sample preparation used, such low filling factors are not achievable. Therefore, the tensile strength in the laboratory is higher compared to on 67P.

5.4.1 *Low organic content*

In contrast to samples of previous sublimation experiments that investigated pure dust-ice mixtures, the samples with added organic components showed no broad diversity in their morphological evolution with respect to their variable volatile content. The two observed types of alterations were the reduction in the sample volume and the formation of fractures on the surface.

The volume reduction can be explained by the sublimation of the water ice. The organic components in the ice matrix (intra-mixture) remained in the sample after the sublimation of the ice and adhesively kept the dust particles in contact with one another. It is unlikely that significant amounts of organic material was transported away with the sublimating ice. Otherwise, analogous to the sample without organic components, the dust particles would have detached from the sample surface and fallen down (Fig. 5.1).

However, the effect of the organic material as a "glue" (Bischoff et al., 2020) holding the dust particles together remained sufficient to compensate for the loss of volatiles.

Ice, with its higher surface energy compared to dust (Gundlach et al., 2018b; Haack et al., 2020; Kimura et al., 2015), prevents disintegration of the sample before its sublimation. After sublimation, a mixture of dust and organics remains, the tensile strength of which is higher than that of pure dust. Therefore, after the sublimation of the ice, the organic-rich samples do not disintegrate into individual dust particles, in contrast to what was observed in the reference measurement without organics and as described in Haack et al. (2021). The resulting free space was partially refilled by the remaining dust particles, which caused the samples to shrink. The observation that the ice-depleted material did not form a foam-like texture (Poch et al., 2016b) is probably due to the fact that the fraction of nonvolatile materials was much higher in our experiments. The reduced volume loss of samples with increased dust content can be explained by the lower ice content, which creates less free space after sublimation.

The reduced duration of sublimation activity results from the faster development of ice-depleted mantle material as the dust content of individual samples increases. The mantle protects underlying ice-containing layers from insolation and thus from further sublimation. A comparable process was already observed in previous experiments (e.g., Grün et al., 1993; Haack et al., 2021; Lämmerzahl et al., 1995), where an ice-depleted layer was formed of loose dust but not of cohesive material, unlike in our experiments.

The decrease in volume during sublimation created tensile stresses in the ice-depleted mantle and led to the formation of contraction cracks. This process is comparable to drying shrinkage due to the loss of volatiles and the formation of desiccation cracks on Earth (Peron et al., 2009; Sima, Jiang, and Zhou, 2014). Desiccation is also one of the proposed processes responsible for the formation of fractures on comets (El-Maarry et al., 2015a; Poulet et al., 2016). However, in the samples with a low content of organics, the fractures were only a few millimeters long, mostly isolated, and did not form networks. This could indicate that the amount of organic adhesive between the dust particles was sufficient to keep them attached to the original sample but allowed limited movement of the dust particles into the evolving free space. Accordingly, the ice-depleted material had a degree of plasticity that reduced the formation of fractures and prevented fractures altogether in the case of high dust contents. Another explanation for the absence of distinct fracture networks could be the limited surface area of the samples, which prevented the formation of extended fracture patterns.

Another process that can create fractures on the surface of a comet is repeated thermal contraction and expansion (Attree et al., 2018b; Auger et al., 2018; El-Maarry et al., 2015a; Spohn et al., 2015). This is a slow process, requires periodical cycles of insolation, and produces polygonal patterns typical in periglacial landscapes on Earth (French, 2017). In the laboratory, however, we did not perform insolation cycles and thus did not trigger any periodic thermal contraction or expansion. This explanation for the origin of fractures is therefore not applicable for our experiments. The formation of fractures by tectonics and compressive stress is conceivable on comets (Franceschi et al., 2020; Thomas et al., 2015b) but can be excluded in our laboratory experiments.

The formation of an ice-rich layer below the ice-depleted mantle can be explained by the recondensation and/or sintering of ice (Kossacki et al., 2015; Seiferlin, Spohn, and Benkhoff, 1995; Spohn and Benkhoff, 1990; Thomas, Ratke, and Kochan, 1994). This process has been observed many times in previous sublimation experiments (e.g., Grün et al., 1993; Kaufmann and Hagermann, 2018; Poch et al., 2016b) and is

likely on 67P (Gundlach, Fulle, and Blum, 2020; Knapmeyer et al., 2018; Lethuillier et al., 2016; Spohn et al., 2015). In this process, water vapor migrates from near-surface layers deeper into the sample and recondenses there into a solid material (Gundlach, Fulle, and Blum, 2020; Kührt and Keller, 1994). Additionally, a temperature increase in near-surface layers due to insolated energy can trigger the sintering of ice particles (Gundlach et al., 2018a). In these cases, stiff connections of ice form between the particles and significantly increase the tensile strength of the material (Gundlach et al., 2018a; Kuroiwa, 1961). Nevertheless, due to the reduced formation of fractures in this series of measurements, comparison with fracture-related morphologies of 67P is of limited significance.

5.4.2 *High organic content*

The doubled amount of organics in the second series of measurements enhanced the decrease in the sample volume and enhanced the formation of irregularly shaped fractures as the ice sublimated. The duration of the active phase of sample alteration was comparable to that of the first series with respect to the same ice-dust ratios. Due to the limitations of the experimental setup, the physical properties of the remaining material could not be measured after the experiment, so the analysis could only be done using the images taken by the camera (Fig. 5.3). Therefore, direct comparison of volume changes of different samples should be treated with caution since the whole sample was not observed and misperceptions could occur due to the camera's perspective. However, it is clear that the visually increased volume loss and intensified formation of fractures on the surface differ significantly compared to the first series. A possible explanation is increased inter-particle forces due to the higher organic content acting as an adhesive. The higher inter-particle forces would reduce the mobility of the particles and tend to make the mantle material less plastic compared with the low organics scenario (Gröger, Tüzün, and Heyes, 2003; Valverde et al., 1998). The consequence would be an increased formation of tensile fractures due to the volume loss. This process is comparable to the formation of desiccation cracks on Earth (Peron et al., 2009; Rayhani, Yanful, and Fakher, 2008; Sima, Jiang, and Zhou, 2014), which occur in a cohesive material due to the loss of volatiles.

As in the first series with low organic content, the possibility that the fractures result from thermal stress can be excluded. Such a possibility is contradicted by the fact that no periodically changing insolation was realized and that a large number of fractures occurred on the side surfaces of the samples, which were insolated only at very high angles of incidence.

Evolved networks of intersecting fractures are known to have been caused by terrestrial desiccation processes and on 67P may have been caused by thermal stresses (Attree et al., 2018b; Auger et al., 2018; El-Maarry et al., 2019, 2015a; Spohn et al., 2015), although none formed here. Occasionally, fractures intersected, but not at a preferred angle typical of polygonal fracture networks (Auger et al., 2018; French, 2017; Peron et al., 2009). However, it cannot be excluded that the observed fractures represent an early stage of a slowly forming network or that polygonal networks could form in the analog material if the sample's surface area or the insolation rate were increased. These considerations suggest that polygonal networks do not necessarily have to be

restricted to the near-surface hardened layer of a comet (Kochan et al., 1989; Kossacki et al., 2015; Spohn et al., 2015). Taking the size scaling of the laboratory experiments into account, irregular meter-sized desiccation cracks may form on a comet due to volatile loss (Poulet et al., 2016), while large polygonal networks could be generated by thermal stresses due to diurnal heating periods (e.g., Attree et al., 2018b; Auger et al., 2018; Spohn et al., 2015, see our Fig. 5.4).

As described in Sect. 5.3.2, larger and more numerous fractures were formed in volatile-rich samples. In parallel, the period of visible surface alteration and the thickness of the ice-depleted mantle are increased. This could indicate that fractures in volatile-rich samples propagate deeper into the material, where exposed volatiles also start to sublimate. This could cause existing fractures to propagate farther or new fractures to form. On a comet, these propagating fractures could locally increase the sublimation activity and lead to outgassing events (Höfner et al., 2017; Skorov et al., 2016; Vincent et al., 2016a).

In all our experiments, water ice was the only volatile used. As mentioned in Sect. 5.2.1, water dominates the amount of all volatiles on 67P (e.g., Biver et al., 2019; Hässig et al., 2015; Läuter et al., 2018), and the potential sublimation and recondensation of CO_2 does not result in a substantial solidification of a subsurface crust, since individual CO_2 crystals do not form bridges to H_2O crystals (Kochan et al., 1989). Therefore, water ice is expected to be the dominant volatile in the upper centimeters of the comet surface (Filacchione et al., 2016; Gundlach, Fulle, and Blum, 2020). Nevertheless, the influence of other volatiles on the evolution of a comet cannot be underestimated and remains a subject of investigation for future experiments.

The absence of collapse events or ejected fragments (Tubiana et al., 2015; Vincent et al., 2016a; Vincent et al., 2015a,b) from the sample surface could indicate that the sample mixtures do not simulate the actual composition of a comet accurately enough. It is also conceivable that an increased and periodically changing insolation in combination with the low albedo of a comet (Ciarniello et al., 2015; Keller et al., 1986) could have a significant effect on the evolution of the patterns and depths of fracture systems in future experiments.

5.5 CONCLUSIONS

A number of sublimation experiments were performed with samples containing variable amounts of organic, volatile, and dust components. The focus of the experiments was to study samples that contain the organic molecules glycine and sodium acetate (Altwegg et al., 2016; Elsila, Glavin, and Dworkin, 2009; Rubin et al., 2019; Schuhmann et al., 2019). Comparison with organic-free sample material showed that an insolation flux of 1.9 solar constants, equivalent to a simulated heliocentric distance of 3.6 AU, was sufficient to sublimate the near-surface volatile water component and to alter the sample surface. The addition of a few mass percent of organic material to a volatile-rich sample fundamentally changes the evolution of the sample morphology. The evolution of sample surfaces with organics was characterized by a loss of volume and the formation of fractures at the surface. These fractures were compared with those on 67P (Auger et al., 2018; El-Maarry et al., 2015a; Poulet et al., 2016; Spohn et al., 2015) and discussed with respect to their relevance to fracture formation on 67P.

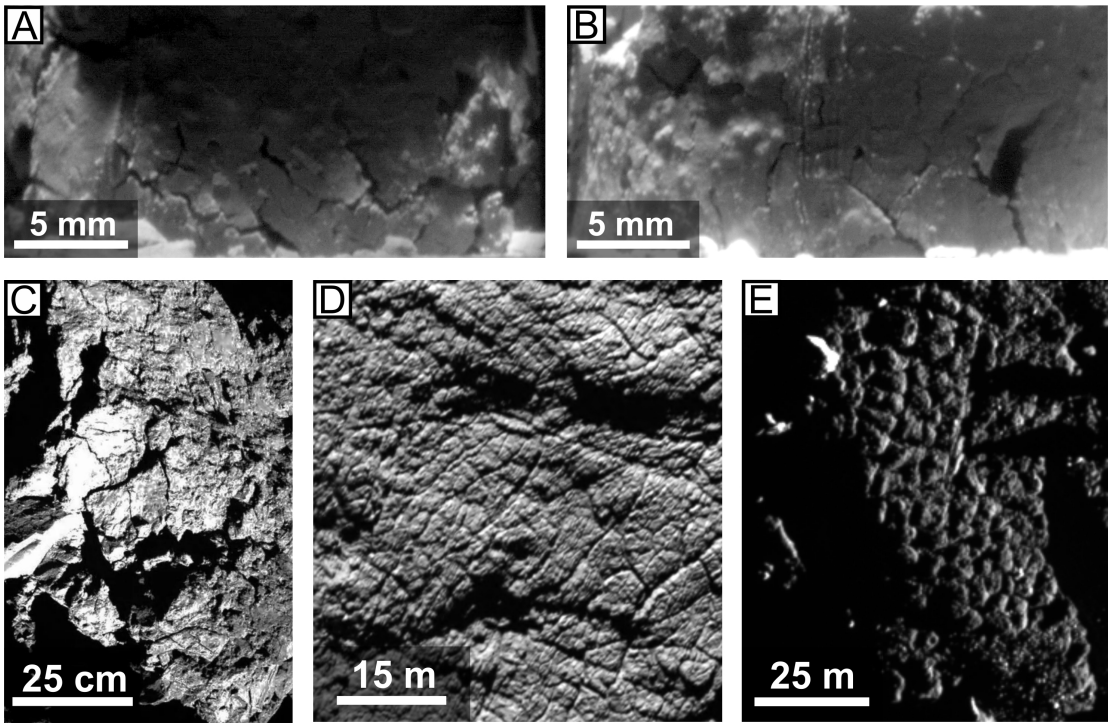

Figure 5.4: Comparison of fractures generated in the laboratory (*Panels A and B*) and observed on 67P (*Panels C–E*). *Panel A:* Close-up of the sample with the lowest dust fraction (10:100:300) from Fig. 5.3. Distinct and irregularly shaped fractures form a poorly developed network on the side wall of the sample. *Panel B:* Enlarged section of the sample with the highest dust content (10:100:700) from Fig. 5.3. The length and pattern of evolving fractures are comparable to those on samples with lower dust content, but they are significantly narrower. *Panel C:* Detailed image of fractures on the surface of 67P, taken by the Philae lander. Several irregular cracks are visible on a rough and dust-free surface. The fracture patterns correspond most closely to those on *Panel B.* Image credit: ESA/Rosetta/Philae/CIVA. *Panel D:* Fracture network on the surface of 67P. The fractures form a pattern of polygons with widths of up to 5 m. *Panel E:* Evolved polygonal structures, caused by fractures on the surface of 67P. Image credits: ESA/Rosetta/MPS for OSIRIS Team MPS/UPD/LAM/IAA/SSO/INTA/UPM/DASP/IDA.

The volatile content of the samples had a distinct influence on the duration of the surface alteration and on the degree of volume loss. The alteration of ice-rich samples lasted longer than that of samples with initially lower amounts of ice, and the former qualitatively lost more of their volume. These processes became less distinct with an increasing dust content of the samples. At the end of the experiments the thickness of ice-depleted material on the top and side surfaces was significantly higher for samples with initially high ice content compared to samples with lower ice content. This mantle prevented sublimation of ice from the sample center, and with increasing mantle thickness the surface alteration came to an end. The mantle material was extremely porous but was stable enough not to disintegrate into individual dust particles when mechanically stressed after the experiment. The nonvolatile organic components remained in the sample and acted as an adhesive between the individual dust particles, consolidating the ice-depleted material. The more organic material initially added to the sample, the more stable the ice-reduced mantle appeared.

In ice-depleted mantles with initially high organic content, the dust particles were less mobile compared to samples with low organic content. As a result, the mantle material became less plastic. The loss of sublimating ice caused the mantle material to contract, resulting in near-surface tensile stresses and the formation of fractures. These fractures propagated farther into the sample's subsurface as sublimation of the ice continued. This allowed further sublimation of ice from subsurface layers, which presumably would be protected from sublimation by a fracture-free mantle. The fractures in the experiment remained mostly separated from one another and did not form polygonal structures as observed on 67P (Auger et al., 2018; El-Maarry et al., 2015a, 2016). However, this could be a result of the limited dimensions of the experimental setup. With a larger sample surface and a more intense insolation, the formation of polygonal structures due to volatile loss cannot be excluded. We conclude that the formation of fractures and, possibly, networks on a comet is not necessarily limited to a hardened subsurface layer and its diurnal thermal contraction (Attree et al., 2018b; Auger et al., 2018; Spohn et al., 2015). On meter scales, fractures on a comet could also result from the loss of sublimating volatiles, comparable to desiccation processes on Earth.

In our experiments we used nonvolatile-to-volatile ratios from 3 to 7 per mass, as inferred on 67P (Fulle et al., 2018, 2017; Herique et al., 2017; Pätzold et al., 2018) and confirmed in previous sublimation experiments (Haack et al., 2021). In future experiments, our restriction to glycine and acetate as organic analogs could be extended to other organic materials detected on 67P. Also, further experiments are necessary to investigate the influence of other volatiles, such as CO_2, the influence of increased insolation flux, and the influence of a drastically reduced albedo on the morphological evolution of cometary surfaces.

6

SUMMARY AND CONCLUSION

6.1 SUMMARY

To draw conclusions about the near-surface properties of cometary nuclei, three series of consecutive laboratory experiments were performed. The aim was to compare the morphological evolution of samples in a vacuum sublimation chamber with morphological features on 67P to draw conclusions about the cometary material. For this purpose, samples without lateral boundaries were used for the first time, which could also simulate material transport from cliffs or scarps. The three series of laboratory experiments were designed as a sequence. The first step analyzed the suitability of different analog materials, the second investigated the sublimation behavior of simple dust-ice mixtures, and the third extended the sublimation experiments to include organic components to the samples. The design of the experiments was not intended to simulate a perfect comet. Because of the great complexity of the processes on a comet, special attention was paid to the parameters dust-ice ratio, tensile strength, insolation, and their comparability with conditions on 67P. For this purpose, compromises were made between chemical composition and physical parameters such as particle shape and size. In this chapter, the results of these experiments are summarized and related to each other.

In Chapter 3, three different granular materials were tested for their suitability as comet analogs. For this purpose, the tensile strength was determined for angular silica, spherical fly ash, spherical water ice particles, and various combinations of two of each of these materials. The size of the different particles varied between $\sim$2.5–5 µm. To determine the tensile strength, the Brazilian disk test method was used, in which pressure was applied to cylindrical samples until they broke. From the pressure applied at the moment of cracking, the tensile strength and surface energy of the material could be determined. To prevent sintering of the water ice particles (Gundlach et al., 2018a; Kuroiwa, 1961) and to simulate as realistic as possible the temperature on a comet (Blum et al., 2014; Kührt, 1984), the samples were cooled to below 150 K.

The tensile strength of granular sample mixtures is strongly dependent on the particle geometry. Irregularly shaped silica particles interlock easily and provide samples with an increased tensile strength of 7300 Pa, compared to spherical fly ash particles with 140 Pa, respectively. The tensile strength of spherical ice particles lies between the two dust components at 1800 Pa. Due to their spherical shape, fly ash and ice particles are not affected by interlocking, and their surface energy can be determined directly. Derived from the tensile strength at below150 K, the surface energy is 0.19 mJ m^{-2} for fly ash and 2.6 mJ m^{-2} for water ice. This is about two orders of magnitude less than at room temperature (Ketcham and Hobbs, 1969; Kimura et al., 2015). This allows the preparation of dust-rich analog materials with a tensile strength of a few hundred Pascals. This value is comparable to that assumed for 67P (Attree et al., 2018a; Groussin et al., 2015). Therefore, despite being more realistic, irregularly

shaped particles are less suitable as analog materials. In addition, spherical particles are much easier to model numerically, and model-based simulations can be compared and calibrated with the experimental results (Kappel et al., 2020). Using the ratios between gravity and size-dependent cohesive forces in the laboratory and on 67P, the particle size in the laboratory can be scaled to the corresponding particle sizes on 67P. It was found that ∼5 µm sized particles in the laboratory reflect millimeter to centimeter sized aggregates on 67P. In this way, objects on the surface of 67P that are up to several tens of meters in size can be simulated in the laboratory with samples only a few centimeters in size.

The study in Chapter 4 describes the morphological evolution of different dust-ice mixtures in a vacuum sublimation chamber. At a simulated heliocentric distance of 3.1 AU, the sublimation activity and the evolving morphologies are strongly dependent on the volatile content and the insolation angle. Due to sublimation and ejected particles, volatile-rich samples are subject of continuous and rapid loss of ice and dust. Due to the higher surface energy of ice compared to dust, the tensile strength of ice-rich samples is increased, leading to the formation of exotic morphologies such as spikes or extreme overhangs. With increased amount of dust in the samples, the sublimation activity gets an increasingly episodic character that is expressed in cliff collapses and outburst events. In addition, a protective layer of dust on the irregular surface causes the sublimation activity to end earlier.

The shape of morphological features and the angle of incidence of the insolation can compensate for the effects of different dust-ice ratios. Vertical insolation of a horizontal surface can result in the formation of a stable dust layer that reduces or prevents further activity. During horizontal insolation of vertical surfaces, such as at pits or scarps, ice-depleted material falls down as a result of collapse events and does not form a protective layer. This repeatedly exposes fresh ice-rich material to the surface, which sublimates again and leads to regressive erosion. This process comes to an end when the initially vertical feature develops a sloping and rough surface that does not allow further vertical mass transport, or when a talus of debris covers substantial parts of the feature.

A comparison of the morphological features in the laboratory and on 67P suggests that a volatile content above 50 vol% (<2.4 dust-to-ice mass ratio) is very unlikely on the comet, since none of the exotic morphologies from the laboratory were found on 67P. Because of the generally very low sublimation activity of samples with 25 vol% volatile content (>7.3 dust-to-ice mass ratio), it is unlikely that less volatile material is present on the comet. These results are consistent with other observations and predictions for 67P (Fulle et al., 2018; Herique et al., 2017; Pätzold et al., 2018).

In Chapter 5, the experimental setup with sublimating dust-ice mixtures is extended to include organic components. The dust-to-ice mass ratio between 3 and 7 of the various sample mixtures is slightly modified by the addition of a few mass percent of a combination of glycine and sodium acetate. Both organic molecules have been detected in the coma of comets (Elsila, Glavin, and Dworkin, 2009; Rubin et al., 2019; Schuhmann et al., 2019) and their combination is an approximation to simulate diverse organic materials of a comet. At a simulated heliocentric distance of 3.6 AU, the samples show significant volume loss and irregular fractures evolve on their surface. Comparable with organic-free dust-ice mixtures, the intensity and duration of the

sublimation activity increases or decreases as the initial ice content of the samples increases or decreases. Significant differences to organic-free samples are observable in the properties of the ice-depleted residues. The organic components remain in the samples and act adhesively between the dust particles, preventing their detachment from the surface. The ice-depleted residues form a very porous, but stable surface layer, which thickens overtime and prevents further sublimation activity.

When the ice sublimates, more free space is created between the dust particles. This free space is partially refilled by dust particles, resulting in a loss of volume of the ice-depleted material. Since the dust particles adhesively stick to each other by the organics, the ice-depleted residues do not disintegrate into individual particles, but form a porous layer that can adapt to morphological changes to a limited extent. If the surface-near tensile stress exceeds the adhesion, the layer cracks and fractures develop that are comparable to desiccation cracks. With increasing organic content, the dust particles stick together more firmly, become less mobile, and macroscopic fractures evolve more easily and in greater numbers.

Polygonal fracture patterns, as known from diurnal thermal contraction processes on 67P, could not be reproduced. This suggests that fractures on cometary surfaces are not necessarily limited to a solidified sub-surface layer (Attree et al., 2018b; Auger et al., 2018; Spohn et al., 2015). Desiccation processes are an additional plausible explanation for fractures on cometary surfaces.

6.2 CONCLUSION

The experiments show that despite simplification of the material composition and under the influence of Earth's gravity, it is possible to reproduce basic evolutionary processes of cometary surfaces in the laboratory. To understand the influence of changing a single parameter in the experiment on the evolution of the morphology, the composition of the samples, insolation flux, and insolation angle were varied separately. To limit the complexity and number of experiments, the albedo was not changed and no additional volatiles were used. This allows for the first time a systematic analysis of the morphological evolution of comet analogs with gradually modified properties and facilitates the comparability of the different results among each other. The main findings of the experiments are:

- Comparison of the morphologies, cliff collapses, and outbursts produced in the sublimation experiments with observations on 67P confirms the modeled mass ratio of non-volatile to volatile components on 67P to be between 3 and 7 (Fulle et al., 2018; Herique et al., 2017; Pätzold et al., 2018).

- The surfaces of organics-bearing samples contract during ice sublimation, forming fractures resembling desiccation cracks. Thus, fracture formation on cometary surfaces is not limited to diurnal thermal contraction of a hardened sub-surface layer (Attree et al., 2018b; Auger et al., 2018; Spohn et al., 2015).

- During sublimation of the ice of organics-bearing samples, the organics remain and act as adhesive between the dust particles. Without organics ice-depleted residues decay to low-cohesive fragments or single particles.

- It is possible to prepare granular comet analogs from spherical particles. The tensile strength (400–900 Pa) and filling fraction (0.40–0.43) of the analogs reflect the corresponding values of 67P more realistically (Attree et al., 2018a; Groussin et al., 2015) than analogs from angular particles.

- The surface energy of dust and ice at temperatures below 150 K is reduced by about two orders of magnitude compared to room temperature (Kimura et al., 2015).

- The addition of a few mass percent of organic material to an ice matrix only slightly increases the surface energy of the ice particles.

- Comparability of observations on 67P and laboratory experiments can be achieved, if the particle size in the laboratory is reduced to a few micrometers. This reduces the influence of terrestrial gravity on the experiment and, with comparable ratios of cohesion and gravity on Earth and on 67P, enables the simulation of millimeter- to centimeter-sized particles on 67P.

Due to a lack of data on comets, a systematic analysis of morphological evolution in previous experiments was associated with large uncertainties. The results presented in this thesis confirm for the first time a number of assumptions that have been made about comet nuclei. This work paves the way for further studies combining physical and geoscientific methods to gain new insights into comets. The Starting point for further experiments could be the determination of quantitative material loss or a changed material strength during, respectively after, the sublimation process. Further important questions that can still be investigated are the quantitative effects of a more intense or cyclic insolation and the influence of a reduced sample albedo. Also, the influence of other volatile and organic components such as CO_2, NH_3, or CH_4 should not be underestimated and could be research objects of future studies.

These experiments lead to a better understanding of how our solar system was formed and how it evolved. The results would explain more precisely the role of comets as a source of volatiles such as water and carbon dioxide, as well as a wide range of organic substances on other celestial bodies and on Earth in particular.

BIBLIOGRAPHY

Agarwal, Jessica et al. (2016). "Acceleration of individual, decimetre-sized aggregates in the lower coma of comet 67P/Churyumov–Gerasimenko." In: *Monthly Notices of the Royal Astronomical Society* 462.Suppl1, S78–S88. ISSN: 0035-8711. DOI: 10.1093/mnras/stw2179.

Altwegg, Kathrin et al. (2016). "Prebiotic chemicals - amino acid and phosphorus - in the coma of comet 67P/Churyumov-Gerasimenko." In: *Science Advances* 2.5. DOI: 10.1126/sciadv.1600285.

Altwegg, Kathrin et al. (June 2017). "Organics in comet 67P - a first comparative analysis of mass spectra from ROSINA-DFMS, COSAC and Ptolemy." In: *Monthly Notices of the Royal Astronomical Society* 469.Suppl 2, S130–S141. ISSN: 0035-8711. DOI: 10.1093/mnras/stx1415.

Attree, N. et al. (2018a). "Tensile strength of 67P/Churyumov-Gerasimenko nucleus material from overhangs." In: *Astronomy & Astrophysics* 611, A33. ISSN: 0004-6361, 1432-0746. DOI: 10.1051/0004-6361/201732155.

Attree, Nicholas, Olivier Groussin, Laurent Jorda, Sergey Rodionov, A-T Auger, Nicolas Thomas, Yann Brouet, Olivier Poch, Ekkehard Kührt, Martin Knapmeyer, et al. (2018b). "Thermal fracturing on comets-Applications to 67P/Churyumov-Gerasimenko." In: *Astronomy & Astrophysics* 610, A76.

Auger, A.-T. et al. (2018). "Meter-scale thermal contraction crack polygons on the nucleus of comet 67P/Churyumov-Gerasimenko." In: *Icarus* 301, pp. 173 –188. ISSN: 0019-1035. DOI: https://doi.org/10.1016/j.icarus.2017.09.037.

Barucci, M. A. et al. (2016). "Detection of exposed H2O ice on the nucleus of comet 67P/Churyumov-Gerasimenko - as observed by Rosetta OSIRIS and VIRTIS instruments." In: *A&A* 595, A102. DOI: 10.1051/0004-6361/201628764.

Belton, Michael J.S. (2010). "Cometary activity, active areas, and a mechanism for collimated outflows on 1P, 9P, 19P, and 81P." In: *Icarus* 210.2, pp. 881 –897. ISSN: 0019-1035. DOI: https://doi.org/10.1016/j.icarus.2010.07.007.

Bischoff, D., B. Gundlach, M. Neuhaus, and J. Blum (2019). "Experiments on cometary activity: ejection of dust aggregates from a sublimating water-ice surface." In: *Monthly Notices of the Royal Astronomical Society* 483.1, pp. 1202–1210. ISSN: 0035-8711. DOI: 10.1093/mnras/sty3182.

Bischoff, D., C. Kreuzig, D. Haack, B Gundlach, and J Blum (2020). "Sticky or not sticky? Measurements of the tensile strength of microgranular organic materials." In: *Monthly Notices of the Royal Astronomical Society* 497.3, pp. 2517–2528. ISSN: 0035-8711. DOI: 10.1093/mnras/staa2126.

Biver et al. (2019). "Long-term monitoring of the outgassing and composition of comet 67P/Churyumov-Gerasimenko with the Rosetta/MIRO instrument." In: *A&A* 630, A19. DOI: 10.1051/0004-6361/201834960.

Blum, J., B. Gundlach, S. Mühle, and J. M. Trigo-Rodriguez (2014). "Comets formed in solar-nebula instabilities! - An experimental and modeling attempt to relate the

activity of comets to their formation process." In: *Icarus* 235, pp. 156–169. ISSN: 0019-1035. DOI: 10.1016/j.icarus.2014.03.016.

Blum, J., R. Schrapler, Bjorn J. R. Davidsson, and Josep M. Trigo-Rodriguez (2006). "The Physics of Protoplanetesimal Dust Agglomerates. I. Mechanical Properties and Relations to Primitive Bodies in the Solar System." In: *The Astrophysical Journal* 652.2, pp. 1768–1781. ISSN: 0004-637X. DOI: 10.1086/508017.

Blum, J. et al. (2017). "Evidence for the formation of comet 67P/Churyumov-Gerasimenko through gravitational collapse of a bound clump of pebbles." In: *Monthly Notices of the Royal Astronomical Society* 469.Suppl2, S755–S773. ISSN: 0035-8711. DOI: 10.1093/mnras/stx2741.

Bockelée-Morvan, D. and N. Biver (2017). "The composition of cometary ices." In: *Philosophical Transactions of the Royal Society A: Mathematical, Physical and Engineering Sciences* 375.2097, p. 20160252. DOI: 10.1098/rsta.2016.0252.

Bockelée-Morvan, D. et al. (2016). "Evolution of CO2, CH4, and OCS abundances relative to H2O in the coma of comet 67P around perihelion from Rosetta/VIRTIS-H observations." In: *Monthly Notices of the Royal Astronomical Society* 462.1, S170–S183. ISSN: 0035-8711. DOI: 10.1093/mnras/stw2428.

Britt, DT, DC Boice, BJ Buratti, H Campins, RM Nelson, J Oberst, BR Sandel, SA Stern, LA Soderblom, and N Thomas (2004). "The morphology and surface processes of Comet 19/P Borrelly." In: *Icarus* 167.1, pp. 45–53.

Brown, Michael E (2000). "Near-infrared spectroscopy of Centaurs and irregular satellites." In: *The Astronomical Journal* 119.2, p. 977.

Brownlee, Donald E. et al. (2004). "Surface of Young Jupiter Family Comet 81P/Wild 2: View from the Stardust Spacecraft." In: *Science* 304.5678, pp. 1764–1769. ISSN: 0036-8075. DOI: 10.1126/science.1097899.

Cambianica, P. et al. (2020). "Time evolution of dust deposits in the Hapi region of comet 67P/Churyumov-Gerasimenko." In: *A&A* 636, A91. DOI: 10.1051/0004-6361/202037485. URL: https://doi.org/10.1051/0004-6361/202037485.

Capaccioni, F. et al. (2015). "The organic-rich surface of comet 67P/Churyumov-Gerasimenko as seen by VIRTIS/Rosetta." In: *Science* 347.6220. ISSN: 0036-8075. DOI: 10.1126/science.aaa0628.

Chýlek, Petr, V. Ramaswamy, and Vandana Srivastava (1983). "Albedo of soot-contaminated snow." In: *Journal of Geophysical Research: Oceans* 88.C15, pp. 10837–10843. DOI: 10.1029/JC088iC15p10837.

Chokshi, Arati, A. G. G. M. Tielens, and D. Hollenbach (1993). "Dust Coagulation." In: *apj* 407, p. 806. DOI: 10.1086/172562.

Choukroun, Mathieu et al. (2020). "Dust-to-Gas and Refractory-to-Ice Mass Ratios of Comet 67P/Churyumov-Gerasimenko from Rosetta Observations." In: *Space Science Reviews* 216. DOI: 10.1007/s11214-020-00662-1.

Ciarniello, M. et al. (2015). "Photometric properties of comet 67P/Churyumov-Gerasimenko from VIRTIS-M onboard Rosetta." In: *A&A* 583, A31. DOI: 10.1051/0004-6361/201526307.

Clark, Roger N. and Paul G. Lucey (1984). "Spectral properties of ice-particulate mixtures and implications for remote sensing: 1. Intimate mixtures." In: *Journal of Geophysical Research: Solid Earth* 89.B7, pp. 6341–6348. DOI: 10.1029/JB089iB07p06341.

Dodson-Robinson, Sarah E., Karen Willacy, Peter Bodenheimer, Neal J. Turner, and Charles A. Beichman (2009). "Ice lines, planetesimal composition and solid surface density in the solar nebula." In: *Icarus* 200.2, pp. 672–693. ISSN: 0019-1035. DOI: https://doi.org/10.1016/j.icarus.2008.11.023.

Duncan, Martin, Thomas Quinn, and Scott Tremaine (1988). "The origin of short-period comets." In: *The Astrophysical Journal* 328, pp. L69–L73.

Durda, D. D., P. Sanchez, A. Fischer, G. Devaud, D. J. Scheeres, S. E. Roark, P. F. Kaptchen, and R. Dissly (2014). "The Size Distribution of "Boulders" Formed During Slope Failure in Piles of Self-Cohesive Powders: Application to the Morphology of Regoliths on Small Asteroids." In: *Lunar and Planetary Science Conference*. Vol. 45. event: Lunar and Planetary Science Conference. LPI, p. 2015. URL: http://adsabs.harvard.edu/abs/2014LPI....45.2015D.

El-Maarry, M.R., O. Groussin, H. U. Keller, N. Thomas, J.-B. Vincent, S. Mottola, M. Pajola, K. Otto, C. Herny, and S. Krasilnikov (2019). "Surface Morphology of Comets and Associated Evolutionary Processes: A Review of Rosetta's Observations of 67P/Churyumov-Gerasimenko." In: *Space Science Reviews* 215.4, p. 36. ISSN: 1572-9672. DOI: 10.1007/s11214-019-0602-1.

El-Maarry, M.R. et al. (2015a). "Fractures on comet 67P/Churyumov-Gerasimenko observed by Rosetta/OSIRIS." In: *Geophysical Research Letters* 42.13, pp. 5170–5178. DOI: https://doi.org/10.1002/2015GL064500.

El-Maarry, M.R. et al. (2015b). "Regional surface morphology of comet 67P/Churyumov-Gerasimenko from Rosetta/OSIRIS images." In: *A&A* 583, A26. DOI: 10.1051/0004-6361/201525723.

El-Maarry, M.R. et al. (2016). "Regional surface morphology of comet 67P/Churyumov-Gerasimenko from Rosetta/OSIRIS images: The southern hemisphere." In: *A&A* 593, A110. DOI: 10.1051/0004-6361/201628634.

El-Maarry, M.R. et al. (2017). "Surface changes on comet 67P/Churyumov-Gerasimenko suggest a more active past." In: *Science* 355.6332, pp. 1392–1395. ISSN: 0036-8075. DOI: 10.1126/science.aak9384.

Elsila, Jamie E, Daniel P Glavin, and Jason P Dworkin (2009). "Cometary glycine detected in samples returned by Stardust." In: *Meteoritics & planetary science* 44.9, pp. 1323–1330.

Emerich, C, JM Lamarre, VI Moroz, M Combes, NF Sanko, Yu V Nikolsky, F Rocard, R Gispert, N Coron, JP Bibring, et al. (1988). "Temperature and size of the nucleus of comet P/Halley deduced from IKS infrared Vega 1 measurements." In: *Exploration of Halley's comet*. Springer, pp. 839–842.

Fanale, Fraser P. and James R. Salvail (1984). "An idealized short-period comet model: Surface insolation, H2O flux, dust flux, and mantle evolution." In: *Icarus* 60.3, pp. 476 –511. ISSN: 0019-1035. DOI: https://doi.org/10.1016/0019-1035(84)90157-X.

Farnham, T.L., D. Bodewits, J.-Y. Li, J. Veverka, P. Thomas, and M.J.S. Belton (2013). "Connections between the jet activity and surface features on Comet 9P/Tempel 1." In: *Icarus* 222.2. Stardust/EPOXI, pp. 540 –549. ISSN: 0019-1035. DOI: https://doi.org/10.1016/j.icarus.2012.06.019.

Farnham, T.L. et al. (2007). "Dust coma morphology in the Deep Impact images of Comet 9P/Tempel 1." In: *Icarus* 187.1. Deep Impact Mission to Comet 9P/Tempel 1,

Part 1, pp. 26 –40. ISSN: 0019-1035. DOI: https://doi.org/10.1016/j.icarus.2006.10.036.

Fernández, Julio A (1980). "On the existence of a comet belt beyond Neptune." In: *Monthly Notices of the Royal Astronomical Society* 192.3, pp. 481–491.

Filacchione, Gianrico, Maria Cristina De Sanctis, Fabrizio Capaccioni, Andrea Raponi, Federico Tosi, Mauro Ciarniello, P Cerroni, Giuseppe Piccioni, MT Capria, Ernesto Palomba, et al. (2016). "Exposed water ice on the nucleus of comet 67P/Churyumov–Gerasimenko." In: *Nature* 529.7586, pp. 368–372.

Finson, M. J. and R. F. Probstein (1968). "A theory of dust comets. I. Model and equations." In: *apj* 154, pp. 327–352. DOI: 10.1086/149761.

Fournel, F., L. Continni, C. Morales, J. Da Fonseca, H. Moriceau, F. Rieutord, A. Barthelemy, and I. Radu (2012). "Measurement of bonding energy in an anhydrous nitrogen atmosphere and its application to silicon direct bonding technology." In: *Journal of Applied Physics* 111.10, p. 104907. DOI: 10.1063/1.4716030.

Franceschi, Marco et al. (2020). "Global-scale brittle plastic rheology at the cometesimals merging of comet 67P/Churyumov-Gerasimenko." In: *Proceedings of the National Academy of Sciences* 117.19, pp. 10181–10187. ISSN: 0027-8424. DOI: 10.1073/pnas.1914552117.

French, Hugh M (2017). *The periglacial environment*. John Wiley & Sons.

Fulle, M., J Blum, S F Green, B Gundlach, A Herique, F Moreno, S Mottola, A Rotundi, and C Snodgrass (2018). "The refractory-to-ice mass ratio in comets." In: *Monthly Notices of the Royal Astronomical Society* 482.3, pp. 3326–3340. ISSN: 0035-8711. DOI: 10.1093/mnras/sty2926.

Fulle, M., J. Blum, and A. Rotundi (2019). "How Comets Work." In: *The Astrophysical Journal* 879.1, p. L8. DOI: 10.3847/2041-8213/ab2898.

Fulle, M., V. Della Corte, A. Rotundi, S. F. Green, M. Accolla, L. Colangeli, M. Ferrari, S. Ivanovski, R. Sordini, and V. Zakharov (2017). "The dust-to-ices ratio in comets and Kuiper belt objects." In: *Monthly Notices of the Royal Astronomical Society* 469.Suppl 2, S45–S49. ISSN: 0035-8711. DOI: 10.1093/mnras/stx983.

Fulle, M. et al. (2016). "Comet 67P/Churyumov–Gerasimenko preserved the pebbles that formed planetesimals." In: *Monthly Notices of the Royal Astronomical Society* 462.Suppl1, S132–S137. ISSN: 0035-8711. DOI: 10.1093/mnras/stw2299.

Glassmeier, Karl-Heinz, Hermann Boehnhardt, Detlef Koschny, Ekkehard Kührt, and Ingo Richter (2007). "The Rosetta Mission: Flying Towards the Origin of the Solar System." In: *Space Science Reviews* 128.1, pp. 1–21. ISSN: 1572-9672. DOI: 10.1007/s11214-006-9140-8.

Goesmann, Fred et al. (2015). "Organic compounds on comet 67P/Churyumov-Gerasimenko revealed by COSAC mass spectrometry." In: *Science* 349.6247. ISSN: 0036-8075. DOI: 10.1126/science.aab0689.

Gröger, Torsten, Ugur Tüzün, and David M Heyes (2003). "Modelling and measuring of cohesion in wet granular materials." In: *Powder Technology* 133.1, pp. 203–215. ISSN: 0032-5910. DOI: https://doi.org/10.1016/S0032-5910(03)00093-7.

Grün, E. et al. (1989). "Laboratory Simulation of Cometary Processes: Results from First Kosi Experiments." In: *International Astronomical Union Colloquium* 116.1, pp. 277–297. DOI: 10.1017/S0252921100109728.

Grün, E. et al. (1993). "Development of a dust mantle on the surface of an insolated ice-dust mixture: results from the KOSI-9 experiment." In: *Journal of Geophysical Research: Planets* 98.E8, pp. 15091–15104. ISSN: 2156-2202. DOI: 10.1029/93JE01134.

Groussin, O. et al. (2015). "Gravitational slopes, geomorphology, and material strengths of the nucleus of comet 67P/Churyumov-Gerasimenko from OSIRIS observations." In: *Astronomy& Astrophysics* 583, A32. ISSN: 0004-6361, 1432-0746. DOI: 10.1051/0004-6361/201526379.

Güttler, C., J. Blum, A. Zsom, C. W. Ormel, and C. P. Dullemond (2010). "The outcome of protoplanetary dust growth: pebbles, boulders, or planetesimals? - I. Mapping the zoo of laboratory collision experiments." In: *Astronomy& Astrophysics* 513, A56. ISSN: 0004-6361, 1432-0746. DOI: 10.1051/0004-6361/200912852.

Güttler, C. et al. (2019). "Synthesis of the morphological description of cometary dust at comet 67P/Churyumov-Gerasimenko." In: *Astronomy& Astrophysics* 630, A24. ISSN: 0004-6361, 1432-0746. DOI: 10.1051/0004-6361/201834751.

Gulkis, Samuel et al. (2015). "Subsurface properties and early activity of comet 67P/Churyumov-Gerasimenko." In: *Science* 347.6220. ISSN: 0036-8075. DOI: 10.1126/science.aaa0709.

Gundlach, B., J. Blum, H. U. Keller, and Y. V. Skorov (2015). "What drives the dust activity of comet 67P/Churyumov-Gerasimenko?" In: *Astronomy& Astrophysics* 583, A12. ISSN: 0004-6361, 1432-0746. DOI: 10.1051/0004-6361/201525828.

Gundlach, B., M. Fulle, and J. Blum (Feb. 2020). "On the activity of comets: understanding the gas and dust emission from comet 67/Churyumov–Gerasimenko's south-pole region during perihelion." In: *Monthly Notices of the Royal Astronomical Society* 493.3, pp. 3690–3715. ISSN: 0035-8711. DOI: 10.1093/mnras/staa449.

Gundlach, B., J. Ratte, J. Blum, J. Oesert, and S. N. Gorb (2018a). "Sintering and sublimation of micrometre-sized water-ice particles: the formation of surface crusts on icy Solar System bodies." In: *Monthly Notices of the Royal Astronomical Society* 479.4, pp. 5272–5287. ISSN: 0035-8711. DOI: 10.1093/mnras/sty1839.

Gundlach, B., K. P. Schmidt, C. Kreuzig, D. Bischoff, F. Rezaei, S. Kothe, J. Blum, B. Grzesik, and E. Stoll (2018b). "The tensile strength of ice and dust aggregates and its dependence on particle properties." In: *Monthly Notices of the Royal Astronomical Society* 479.1, pp. 1273–1277. ISSN: 0035-8711. DOI: 10.1093/mnras/sty1550.

Gundlach, B., Yu.V. Skorov, and J. Blum (2011). "Outgassing of icy bodies in the Solar System - I. The sublimation of hexagonal water ice through dust layers." In: *Icarus* 213.2, pp. 710 –719. ISSN: 0019-1035. DOI: https://doi.org/10.1016/j.icarus.2011.03.022.

Haack, D., O. Katharina, B. Gundlach, C. Kreuzig, D. Bischoff, E. Kührt, and J. Blum (2020). "Tensile strength of dust-ice mixtures and their relevance as cometary analog material." In: *A&A* 642, A218. DOI: 10.1051/0004-6361/202037763.

Haack, D., A. Lethuillier, C. Kreuzig, C. Feller, B. Gundlach, A. Pommerol, J. Blum, and K. A. Otto (2021). "Sublimation of ice-dust mixtures in cooled vacuum environments to reproduce cometary morphologies." In: *A&A* 649, A35. DOI: 10.1051/0004-6361/202140435.

Hadraoui, K. et al. (2019). "Distributed glycine in comet 67P/Churyumov-Gerasimenko." In: *A&A* 630, A32. DOI: 10.1051/0004-6361/201935018.

Harker, David E., Charles E. Woodward, and Diane H. Wooden (2005). "The Dust Grains from 9P/Tempel 1 Before and After the Encounter with Deep Impact." In: *Science* 310.5746, pp. 278–280. ISSN: 0036-8075. DOI: 10.1126/science.1119143.

Hässig, M. et al. (2015). "Time variability and heterogeneity in the coma of 67P/Churyumov-Gerasimenko." In: *Science* 347.6220. ISSN: 0036-8075. DOI: 10.1126/science.aaa0276.

Heim, Lars-Oliver, Jürgen Blum, Markus Preuss, and Hans-Jürgen Butt (1999). "Adhesion and friction forces between spherical micrometer-sized particles." In: *Physical Review Letters* 83.16, p. 3328.

Herique, A., W. Kofman, P. Beck, L. Bonal, I. Buttarazzi, E. Heggy, J. Lasue, A. C. Levasseur-Regourd, E. Quirico, and S. Zine (2017). "Cosmochemical implications of CONSERT permittivity characterization of 67P/CG." In: *Monthly Notices of the Royal Astronomical Society* 462.Suppl 1, S516–S532. ISSN: 0035-8711. DOI: 10.1093/mnras/stx040.

Herique, A., W. Kofman, S. Zine, J. Blum, J.-B. Vincent, and V. Ciarletti (2019). "Homogeneity of 67P/Churyumov-Gerasimenko as seen by CONSERT: implication on composition and formation." In: *A&A* 630, A6. DOI: 10.1051/0004-6361/201834865. URL: https://doi.org/10.1051/0004-6361/201834865.

Hills, JG (1981). "Comet showers and the steady-state infall of comets from the Oort cloud." In: *The Astronomical Journal* 86, pp. 1730–1740.

Höfner, Sebastien, J-B Vincent, Jürgen Blum, Björn JR Davidsson, Holger Sierks, Mohamed Ramy El-Maarry, Jakob Deller, Marc Hofmann, Xuan Hu, Maurizio Pajola, et al. (2017). "Thermophysics of fractures on comet 67P/Churyumov-Gerasimenko." In: *Astronomy & Astrophysics* 608, A121.

Hornung, Klaus et al. (2016). "A first assessment of the strength of cometary particles collected in-situ by the COSIMA instrument onboard ROSETTA." In: *Planetary and Space Science* 133. Cosmic Dust VIII, pp. 63 –75. ISSN: 0032-0633. DOI: https://doi.org/10.1016/j.pss.2016.07.003.

Hsieh, Henry H., David Jewitt, and Yanga R. Fernández (2009). "Albedos of main-belt comets 133P/Elst-Pizarro and 176P/Linear." In: *The Astrophysical Journal* 694.2, pp. L111–L114. DOI: 10.1088/0004-637x/694/2/l111.

Jewitt, David (1999). "KUIPER BELT OBJECTS." In: *Annual Review of Earth and Planetary Sciences* 27.1, pp. 287–312. DOI: 10.1146/annurev.earth.27.1.287.

Johnson, Kenneth Langstreth, Kevin Kendall, A. D. Roberts, and David Tabor (1971). "Surface energy and the contact of elastic solids." In: *Proceedings of the Royal Society of London. A. Mathematical and Physical Sciences* 324.1558, pp. 301–313. DOI: 10.1098/rspa.1971.0141.

Kappel, D., M. Sachse, D. Haack, and K. A. Otto (2020). "Discrete element modeling of boulder and cliff morphologies on comet 67P/Churyumov-Gerasimenko." In: *Astronomy& Astrophysics* 641, A19. ISSN: 0004-6361, 1432-0746. DOI: 10.1051/0004-6361/201937152.

Kaufmann, Erika and Axel Hagermann (2018). "Constraining the parameter space of comet simulation experiments." In: *Icarus* 311, pp. 105–112. ISSN: 00191035. DOI: 10.1016/j.icarus.2018.03.025.

Keller, H. U. (1989). "Comets - dirty snowballs or icy dirtballs?" In: *Physics and Mechanics of Cometary Materials*. Ed. by James J. Hunt and T. Duc Guyenne. Vol. 302. ESA Special Publication, pp. 39–45.

Keller, H. U. et al. (1986). "First Halley Multicolour Camera imaging results from Giotto." In: *Nature* 321.6067, pp. 320–326. ISSN: 1476-4687. DOI: https://doi.org/10.1038/321320a0.

Keller, H. U. et al. (2017). "Seasonal mass transfer on the nucleus of comet 67P/Churyumov-Gerasimenko." In: *Monthly Notices of the Royal Astronomical Society* 469.Suppl 2, S357–S371. ISSN: 0035-8711. DOI: 10.1093/mnras/stx1726.

Kelley, Michael S, Don J Lindler, Dennis Bodewits, Michael F A'Hearn, Carey M Lisse, Ludmilla Kolokolova, Jochen Kissel, and Brendan Hermalyn (2013). "A distribution of large particles in the coma of Comet 103P/Hartley 2." In: *Icarus* 222.2, pp. 634–652.

Ketcham, W. M. and P. V. Hobbs (1969). "An experimental determination of the surface energies of ice." In: *The Philosophical Magazine: A Journal of Theoretical Experimental and Applied Physics* 19.162, pp. 1161–1173. DOI: 10.1080/14786436908228641.

Kührt, E. (1984). "Temperature profiles and thermal stresses in cometary nuclei." In: *Icarus* 60.3, pp. 512–521. ISSN: 0019-1035. DOI: 10.1016/0019-1035(84)90158-1.

Kührt, E. and H. U. Keller (1994). "The Formation of Cometary Surface Crusts." In: *Icarus* 109.1, pp. 121–132. ISSN: 0019-1035. DOI: 10.1006/icar.1994.1080.

Kimura, Hiroshi, Koji Wada, Hiroki Senshu, and Hiroshi Kobayashi (2015). "Cohesion of amorphous silica spheres: Toward a better understanding of the coagulation growth of silicate dust aggregates." In: *The Astrophysical Journal* 812.1, p. 67. ISSN: 0004-637X. DOI: 10.1088/0004-637X/812/1/67.

Kissel, Jochen, DE Brownlee, K Büchler, BC Clark, H Fechtig, E Grün, K Hornung, EB Igenbergs, EK Jessberger, FR Krueger, et al. (1986). "Composition of comet Halley dust particles from Giotto observations." In: *Nature* 321.6067, pp. 336–337.

Knapmeyer, M., H.-H. Fischer, J. Knollenberg, K.J. Seidensticker, K. Thiel, W. Arnold, C. Faber, and D. Möhlmann (2018). "Structure and elastic parameters of the near surface of Abydos site on comet 67P/Churyumov–Gerasimenko, as obtained by SESAME/CASSE listening to the MUPUS insertion phase." In: *Icarus* 310, pp. 165 –193. ISSN: 0019-1035. DOI: https://doi.org/10.1016/j.icarus.2017.12.002.

Kochan, H., K. Roessler, L. Ratke, M. Heyl, H. Hellmann, and G. Schwehm (1989). "Crustal strength of different model comet materials." In: *Physics and Mechanics of Cometary Materials*. Ed. by James J. Hunt and T. Duc Guyenne. Vol. 302. ESA Special Publication, pp. 115–119.

Kossacki, K.J., N.I. Kömle, J. Leliwa-Kopystyński, and G. Kargl (1997). "Laboratory Investigation of the Evolution of Cometary Analogs: Results and Interpretation." In: *Icarus* 128.1, pp. 127 –144. ISSN: 0019-1035. DOI: https://doi.org/10.1006/icar.1997.5701.

Kossacki, Konrad J, Tilman Spohn, Axel Hagermann, Erika Kaufmann, and Ekkehard Kührt (2015). "Comet 67P/Churyumov–Gerasimenko: Hardening of the sub-surface layer." In: *Icarus* 260, pp. 464–474.

Kothe, Stefan, Jürgen Blum, René Weidling, and Carsten Güttler (2013). "Free collisions in a microgravity many-particle experiment. III. The collision behavior of sub-millimeter-sized dust aggregates." In: *Icarus* 225.1, pp. 75 –85. ISSN: 0019-1035. DOI: https://doi.org/10.1016/j.icarus.2013.02.034.

Kramer, Tobias and Matthias Noack (2015). "Prevailing dust-transport directions on comet 67P/Churyumov-Gerasimenko." In: *The Astrophysical Journal* 813.2, p. L33. DOI: 10.1088/2041-8205/813/2/l33.

Kretke, K.A. and H.F. Levison (2015). "Evidence for pebbles in comets." In: *Icarus* 262, pp. 9 –13. ISSN: 0019-1035. DOI: https://doi.org/10.1016/j.icarus.2015.08.017.

Kuroiwa, Daisuke (1961). "A Study of Ice Sintering." In: *Tellus* 13.2, pp. 252–259. DOI: 10.3402/tellusa.v13i2.9450.

Lai, I. L. et al. (2016). "Mapping of the source regions of the dust jets on comet 67P/Churyumov-Gerasimenko." In: *AGU Fall Meeting Abstracts*, P43A–2087.

Lai, Ian-Lin et al. (Feb. 2017). "Gas outflow and dust transport of comet 67P/Churyumov–Gerasimenko." In: *Monthly Notices of the Royal Astronomical Society* 462.Suppl 1, S533–S546. ISSN: 0035-8711. DOI: 10.1093/mnras/stx332.

Langevin, Y. et al. (2017). "Optical properties of cometary particles collected by the COSIMA mass spectrometer on-board Rosetta during the rendezvous phase around comet 67P/Churyumov–Gerasimenko." In: *Monthly Notices of the Royal Astronomical Society* 469.Suppl 2, S535–S549. ISSN: 0035-8711. DOI: 10.1093/mnras/stx2070.

Leroch, Sabine and Martin Wendland (2012). "Simulation of Forces between Humid Amorphous Silica Surfaces: A Comparison of Empirical Atomistic Force Fields." In: *The Journal of Physical Chemistry C* 116.50. PMID: 23378869, pp. 26247–26261. DOI: 10.1021/jp302428b.

Lethuillier, Anthony, Alice Le Gall, Michel Hamelin, Walter Schmidt, Klaus J. Seidensticker, Réjean Grard, Valérie Ciarletti, Sylvain Caujolle-Bert, Hans-Herbert Fischer, and Roland Trautner (2016). "Electrical properties and porosity of the first meter of the nucleus of 67P/Churyumov-Gerasimenko - As constrained by the Permittivity Probe SESAME-PP/Philae/Rosetta." In: *A&A* 591, A32. DOI: 10.1051/0004-6361/201628304.

Levison, Harold F. and Martin J. Duncan (1997). "From the Kuiper Belt to Jupiter-Family Comets: The Spatial Distribution of Ecliptic Comets." In: *Icarus* 127.1, pp. 13–32. ISSN: 0019-1035. DOI: https://doi.org/10.1006/icar.1996.5637.

Li, Diyuan and Louis Ngai Yuen Wong (2013). "The Brazilian Disc Test for Rock Mechanics Applications: Review and New Insights." In: *Rock Mechanics and Rock Engineering* 46.2, pp. 269–287. ISSN: 1434-453X. DOI: 10.1007/s00603-012-0257-7.

Li, Dong-ling (2013). "Low temperature Si/Si wafer direct bonding using a plasma activated method." In: *Journal of Zhejiang University SCIENCE C* 14.4, pp. 244–251. DOI: 10.1631/jzus.C12MNT02.

Lämmerzahl, P., J. Gebhard, E. Grün, and G. Klees (1995). "Gas release from ice/dust mixtures: results from eleven KOSI experiments." In: *Planetary and Space Science*. Small Bodies in the Solar System - Origin, Evolution, and Significance for the Formation of Planets 43.3, pp. 363–373. ISSN: 0032-0633. DOI: 10.1016/0032-0633(94)00121-7.

Lorek, S., B. Gundlach, P. Lacerda, and J. Blum (2016). "Comet formation in collapsing pebble clouds - What cometary bulk density implies for the cloud mass and dust-to-ice ratio." In: *A&A* 587, A128. DOI: 10.1051/0004-6361/201526565.

Lorek, S., P. Lacerda, and J. Blum (2018). "Local growth of dust- and ice-mixed aggregates as cometary building blocks in the solar nebula." In: *A&A* 611, A18. DOI: 10.1051/0004-6361/201630175.

Läuter, Matthias, Tobias Kramer, Martin Rubin, and Kathrin Altwegg (Nov. 2018). "Surface localization of gas sources on comet 67P/Churyumov-Gerasimenko based on DFMS/COPS data." In: *Monthly Notices of the Royal Astronomical Society* 483.1, pp. 852–861. ISSN: 0035-8711. DOI: 10.1093/mnras/sty3103.

Meisner, T., G. Wurm, and J. Teiser (2012). "Experiments on centimeter-sized dust aggregates and their implications for planetesimal formation." In: *Astronomy& Astrophysics* 544, A138. ISSN: 0004-6361, 1432-0746. DOI: 10.1051/0004-6361/201219099.

Mottola, S. et al. (2015). "The structure of the regolith on 67P/Churyumov-Gerasimenko from ROLIS descent imaging." In: *Science* 349.6247. ISSN: 0036-8075. DOI: 10.1126/science.aab0232.

Murphy, W. F. (1982). "Effects of Microstructure and Pore Fluids on the Acoustic Properties of Granular Sedimentary Materials." PhD thesis. Stanford University.

Musiolik, Grzegorz and Gerhard Wurm (2019). "Contacts of Water Ice in Protoplanetary Disks-Laboratory Experiments." In: *The Astrophysical Journal* 873.1, p. 58. DOI: 10.3847/1538-4357/ab0428.

O'Rourke, Laurence et al. (2020). "The Philae lander reveals low-strength primitive ice inside cometary boulders." In: *Nature* 586. DOI: 10.1038/s41586-020-2834-3.

Oehler, A. and G. Neukum (1991). "Visible and near IR albedo measurements of ice/dust mixtures." In: *Geophysical Research Letters* 18.2, pp. 253–256. DOI: 10.1029/91GL00174.

Oklay, N. et al. (2016). "Variegation of comet 67P/Churyumov-Gerasimenko in regions showing activity." In: *A&A* 586, A80. DOI: 10.1051/0004-6361/201527369.

Omura, Tomomi and Akiko M. Nakamura (2017). "Experimental study on compression property of regolith analogues." In: *Planetary and Space Science*. Special Issue: Cosmic Dust IX 149, pp. 14–22. ISSN: 0032-0633. DOI: 10.1016/j.pss.2017.08.003.

Ott, T et al. (2017). "Dust mass distribution around comet 67P/Churyumov-Gerasimenko determined via parallax measurements using Rosetta's OSIRIS cameras." In: *Monthly Notices of the Royal Astronomical Society* 469.Suppl 2, S276–S284. ISSN: 0035-8711. DOI: 10.1093/mnras/stx1419.

Otto, K A et al. (2020). "Surface roughness of asteroid (162173) Ryugu and comet 67P/Churyumov–Gerasimenko inferred from in situ observations." In: *Monthly Notices of the Royal Astronomical Society* 500.3, pp. 3178–3193. ISSN: 0035-8711. DOI: 10.1093/mnras/staa3314.

Pajola, M. et al. (2015). "Size-frequency distribution of boulders >=7 m on comet 67P/Churyumov-Gerasimenko." In: *A&A* 583, A37. DOI: 10.1051/0004-6361/201525975.

Pajola, M. et al. (2016a). "Aswan site on comet 67P/Churyumov-Gerasimenko: Morphology, boulder evolution, and spectrophotometry." In: *Astronomy& Astrophysics* 592, A69. ISSN: 0004-6361, 1432-0746. DOI: 10.1051/0004-6361/201527865.

Pajola, M. et al. (2016b). "The pebbles/boulders size distributions on Sais: Rosetta's final landing site on comet 67P/Churyumov–Gerasimenko." In: *Monthly Notices of the Royal Astronomical Society* 469.Suppl 2, S636–S645. ISSN: 0035-8711. DOI: 10.1093/mnras/stx1620.

Peron, Hervé, Lyesse Laloui, Tomasz Hueckel, and Liang Bo Hu (2009). "Desiccation cracking of soils." In: *European Journal of Environmental and Civil Engineering* 13.7-8, pp. 869–888. DOI: 10.1080/19648189.2009.9693159.

Poch, Olivier, Antoine Pommerol, Bernhard Jost, Nathalie Carrasco, Cyril Szopa, and Nicolas Thomas (2016a). "Sublimation of ice-tholins mixtures: A morphological and spectro-photometric study." In: *Icarus* 266, pp. 288–305. ISSN: 0019-1035. DOI: 10.1016/j.icarus.2015.11.006.

Poch, Olivier, Antoine Pommerol, Bernhard Jost, Nathalie Carrasco, Cyril Szopa, and Nicolas Thomas (2016b). "Sublimation of water ice mixed with silicates and tholins: Evolution of surface texture and reflectance spectra, with implications for comets." In: *Icarus* 267, pp. 154–173. ISSN: 0019-1035. DOI: 10.1016/j.icarus.2015.12.017.

Pommerol, A., B. Jost, O. Poch, M.R. El-Maarry, B. Vuitel, and N. Thomas (2015a). "The SCITEAS experiment: Optical characterizations of sublimating icy planetary analogues." In: *Planetary and Space Science* 109-110, pp. 106 –122. ISSN: 0032-0633. DOI: https://doi.org/10.1016/j.pss.2015.02.004.

Pommerol, A. et al. (2015b). "OSIRIS observations of meter-sized exposures of H2O ice at the surface of 67P/Churyumov-Gerasimenko and interpretation using laboratory experiments." In: *A&A* 583, A25. DOI: 10.1051/0004-6361/201525977.

Poulet, F., A. Lucchetti, J.-P. Bibring, J. Carter, B. Gondet, L. Jorda, Y. Langevin, C. Pilorget, C. Capanna, and G. Cremonese (2016). "Origin of the local structures at the Philae landing site and possible implications on the formation and evolution of 67P/Churyumov–Gerasimenko." In: *Monthly Notices of the Royal Astronomical Society* 462.Suppl 1, S23–S32. ISSN: 0035-8711. DOI: 10.1093/mnras/stw1959.

Powell, M. J. (1979). "Site percolation in randomly packed spheres." In: *Physical Review B* 20.10, pp. 4194–4198. DOI: 10.1103/PhysRevB.20.4194.

Preusker, F. et al. (2017). "The global meter-level shape model of comet 67P/Churyumov-Gerasimenko." In: *A&A* 607, p. L1. DOI: 10.1051/0004-6361/201731798.

Pätzold, M. et al. (2016). "A homogeneous nucleus for comet 67P/Churyumov-Gerasimenko from its gravity field." In: *Nature* 530.75887588, pp. 63–65. ISSN: 1476-4687. DOI: 10.1038/nature16535.

Pätzold, Martin, Thomas P Andert, Matthias Hahn, Jean-Pierre Barriot, Sami W Asmar, Bernd Häusler, Michael K Bird, Silvia Tellmann, Janusz Oschlisniok, and Kerstin Peter (2018). "The Nucleus of comet 67P/Churyumov–Gerasimenko – Part I: The global view – nucleus mass, mass-loss, porosity, and implications." In: *Monthly Notices of the Royal Astronomical Society* 483.2, pp. 2337–2346. ISSN: 0035-8711. DOI: 10.1093/mnras/sty3171.

Quirico, E. et al. (2015). "Composition of comet 67P/Churyumov-Gerasimenko refractory crust as inferred from VIRTIS-M/Rosetta Spectro-Imager." In: *46th Lunar and Planetary Science Conference (2015)*, pp. 2092–2092. URL: https://elib.dlr.de/101332/.

Raponi, A. et al. (2020). "Infrared detection of aliphatic organics on a cometary nucleus." In: *Nature Astronomy* 5, pp. 500–505. ISSN: 2397-3366. DOI: 10.1038/s41550-019-0992-8.

Rayhani, M.H.T., E.K. Yanful, and A. Fakher (2008). "Physical modeling of desiccation cracking in plastic soils." In: *Engineering Geology* 97.1, pp. 25–31. ISSN: 0013-7952. DOI: https://doi.org/10.1016/j.enggeo.2007.11.003.

Rogers, John J. W. and William B. Head (1961). "Relationships between porosity, median size, and sorting coefficients of synthetic sands." In: *Journal of Sedimentary*

Research 31.3, pp. 467–470. ISSN: 1527-1404. DOI: 10.1306/74D70BA5-2B21-11D7-8648000102C1865D.

Rotundi, Alessandra et al. (2015). "Dust measurements in the coma of comet 67P/Churyumov-Gerasimenko inbound to the Sun." In: *Science* 347.6220. ISSN: 0036-8075. DOI: 10.1126/science.aaa3905.

Rubin, Martin et al. (July 2019). "Elemental and molecular abundances in comet 67P/Churyumov-Gerasimenko." In: *Monthly Notices of the Royal Astronomical Society* 489.1, pp. 594–607. ISSN: 0035-8711. DOI: 10.1093/mnras/stz2086.

Sandford, Scott A. et al. (2006). "Organics Captured from Comet 81P/Wild 2 by the Stardust Spacecraft." In: *Science* 314.5806, pp. 1720–1724. ISSN: 0036-8075. DOI: 10.1126/science.1135841.

Scheeres, D.J., C.M. Hartzell, P. Sánchez, and M. Swift (2010). "Scaling forces to asteroid surfaces: The role of cohesion." In: *Icarus* 210.2, pp. 968–984. ISSN: 0019-1035. DOI: 10.1016/j.icarus.2010.07.009.

Schellart, W. P. (2000). "Shear test results for cohesion and friction coefficients for different granular materials: scaling implications for their usage in analogue modelling." In: *Tectonophysics* 324.1, pp. 1–16. ISSN: 0040-1951. DOI: 10.1016/S0040-1951(00)00111-6.

Schröder, S.E. et al. (2017). "Close-up images of the final Philae landing site on comet 67P/Churyumov-Gerasimenko acquired by the ROLIS camera." In: *Icarus* 285, pp. 263 –274. ISSN: 0019-1035. DOI: https://doi.org/10.1016/j.icarus.2016.12.009.

Schuhmann, Markus et al. (2019). "CHO-Bearing Molecules in Comet 67P/Churyumov-Gerasimenko." In: *ACS Earth and Space Chemistry* 3.9, pp. 1854–1861. DOI: 10.1021/acsearthspacechem.9b00094.

Schulz, Rita et al. (2015). "Comet 67P/Churyumov-Gerasimenko sheds dust coat accumulated over the past four years." In: *Nature* 518, pp. 216 –218. ISSN: 1476-4687. DOI: https://doi.org/10.1038/nature14159.

Seiferlin, K, T Spohn, and J Benkhoff (1995). "Cometary ice texture and the thermal evolution of comets." In: *Advances in Space Research* 15.10, pp. 35–38.

Sierks, Holger et al. (2015). "On the nucleus structure and activity of comet 67P/Churyumov-Gerasimenko." In: *Science* 347.6220. ISSN: 0036-8075. DOI: 10.1126/science.aaa1044.

Sima, Jun, Mingjing Jiang, and Chuangbing Zhou (2014). "Numerical simulation of desiccation cracking in a thin clay layer using 3D discrete element modeling." In: *Computers and Geotechnics* 56, pp. 168–180. ISSN: 0266-352X. DOI: https://doi.org/10.1016/j.compgeo.2013.12.003.

Skorov, Yuri and Jürgen Blum (2012). "Dust release and tensile strength of the non-volatile layer of cometary nuclei." In: *Icarus* 221.1, pp. 1–11. ISSN: 0019-1035. DOI: 10.1016/j.icarus.2012.01.012.

Skorov, Yuri, L Rezac, P Hartogh, AT Bazilevsky, and HU Keller (2016). "A model of short-lived outbursts on the 67P from fractured terrains." In: *Astronomy & Astrophysics* 593, A76.

Sánchez, P. and D. J. Scheeres (2014). "The strength of regolith and rubble pile asteroids." In: *Meteoritics& Planetary Science* 49.5, pp. 788–811. ISSN: 1945-5100. DOI: 10.1111/maps.12293.

Snodgrass, C., Tubiana, C., Bramich, D. M., Meech, K., Boehnhardt, H., and Barrera, L. (2013). "Beginning of activity in 67P/Churyumov-Gerasimenko and predictions for 2014-2015." In: *A&A* 557, A33. DOI: 10.1051/0004-6361/201322020.

Soderblom, L. A. et al. (2002). "Observations of Comet 19P/Borrelly by the Miniature Integrated Camera and Spectrometer Aboard Deep Space 1." In: *Science* 296.5570, pp. 1087–1091. ISSN: 0036-8075. DOI: 10.1126/science.1069527.

Spohn, T and J Benkhoff (1990). "Thermal history models for KOSI sublimation experiments." In: *Icarus* 87.2, pp. 358–371.

Spohn, T. et al. (2015). "Thermal and mechanical properties of the near-surface layers of comet 67P/Churyumov-Gerasimenko." In: *Science* 349.6247. ISSN: 0036-8075. DOI: 10.1126/science.aab0464.

Steckloff, Jordan K., Kevin Graves, Masatoshi Hirabayashi, H. Jay Melosh, and James E. Richardson (2016). "Rotationally induced surface slope-instabilities and the activation of CO2 activity on comet 103P/Hartley 2." In: *Icarus* 272, pp. 60 –69. ISSN: 0019-1035. DOI: https://doi.org/10.1016/j.icarus.2016.02.026.

Steinpilz, Tobias, Jens Teiser, and Gerhard Wurm (2019). "Sticking Properties of Silicates in Planetesimal Formation Revisited." In: *The Astrophysical Journal* 874.1, p. 60. ISSN: 0004-637X. DOI: 10.3847/1538-4357/ab07bb.

Stern, S Alan (2003). "The evolution of comets in the Oort cloud and Kuiper belt." In: *Nature* 424.6949, pp. 639–642.

Sunshine, J. M. et al. (2006). "Exposed Water Ice Deposits on the Surface of Comet 9P/Tempel 1." In: *Science* 311.5766, pp. 1453–1455. ISSN: 0036-8075. DOI: 10.1126/science.1123632.

Sunshine, Jessica M, Olivier Groussin, Peter H Schultz, Michael F A Hearn, Lori M Feaga, Tony L Farnham, and Kenneth P Klaasen (2007). "The distribution of water ice in the interior of Comet Tempel 1." In: *Icarus* 191.2, pp. 73–83.

Thomas, H., L. Ratke, and H. Kochan (1994). "Crushing strength of porous ice-mineral bodies-relevance for comets." In: *Advances in Space Research* 14.12, pp. 207 –216. ISSN: 0273-1177. DOI: https://doi.org/10.1016/0273-1177(94)90271-2.

Thomas, Nicolas et al. (2015a). "Redistribution of particles across the nucleus of comet 67P/Churyumov-Gerasimenko." In: *A&A* 583, A17. DOI: 10.1051/0004-6361/201526049.

Thomas, Nicolas et al. (2015b). "The morphological diversity of comet 67P/Churyumov-Gerasimenko." In: *Science* 347.6220, aaa0440–1–6. ISSN: 0036-8075, 1095-9203. DOI: 10.1126/science.aaa0440.

Thomas, P.C. et al. (2013a). "Shape, density, and geology of the nucleus of Comet 103P/Hartley 2." In: *Icarus* 222.2. Stardust/EPOXI, pp. 550–558. ISSN: 0019-1035. DOI: https://doi.org/10.1016/j.icarus.2012.05.034.

Thomas, P.C. et al. (2013b). "The nucleus of Comet 9P/Tempel 1: Shape and geology from two flybys." In: *Icarus* 222.2. Stardust/EPOXI, pp. 453 –466. ISSN: 0019-1035. DOI: https://doi.org/10.1016/j.icarus.2012.02.037.

Tubiana, C, Colin Snodgrass, I Bertini, S Mottola, J-B Vincent, L Lara, S Fornasier, J Knollenberg, Nicolas Thomas, Marco Fulle, et al. (2015). "67P/Churyumov-Gerasimenko: Activity between March and June 2014 as observed from Rosetta/OSIRIS." In: *A&A* 573, A62. DOI: 10.1051/0004-6361/201424735.

Ulamec, Stephan et al. (2016). "Rosetta Lander – Landing and operations on comet 67P/Churyumov–Gerasimenko." In: *Acta Astronautica* 125. Rosetta and Philae at comet 67P/Churyumov-Gerasimenko, pp. 80–91. ISSN: 0094-5765. DOI: https://doi.org/10.1016/j.actaastro.2015.11.029. URL: https://www.sciencedirect.com/science/article/pii/S0094576515004336.

Valverde, José Manuel, Antonio Ramos, Antonio Castellanos, and P. Keith Watson (1998). "The tensile strength of cohesive powders and its relationship to consolidation, free volume and cohesivity." In: *Powder Technology* 97.3, pp. 237–245. ISSN: 0032-5910. DOI: https://doi.org/10.1016/S0032-5910(98)00025-4.

Vincent, J.-B. et al. (2016a). "Are fractured cliffs the source of cometary dust jets? Insights from OSIRIS/Rosetta at 67P/Churyumov-Gerasimenko." In: *Astronomy& Astrophysics* 587, A14. ISSN: 0004-6361, 1432-0746. DOI: 10.1051/0004-6361/201527159.

Vincent, J.-B. et al. (2016b). "Summer fireworks on comet 67P." In: *Monthly Notices of the Royal Astronomical Society* 462.Suppl 1, S184–S194. ISSN: 0035-8711. DOI: 10.1093/mnras/stw2409.

Vincent, Jean-Baptiste, Nilda Oklay, Simone Marchi, Sebastian Höfner, and Holger Sierks (2015a). "Craters on comets." In: *Planetary and Space Science* 107. VIII Workshop on Catastrophic Disruption in the Solar System, pp. 53 –63. ISSN: 0032-0633. DOI: https://doi.org/10.1016/j.pss.2014.06.008.

Vincent, Jean-Baptiste et al. (2015b). "Large heterogeneities in comet 67P as revealed by active pits from sinkhole collapse." In: *Nature* 523, pp. 63–66. DOI: https://doi.org/10.1038/nature14564.

Weissman, Paul, Alessandro Morbidelli, Björn Davidsson, and Jürgen Blum (2020). "Origin and evolution of cometary nuclei." In: *Space Science Reviews* 216.1, pp. 1–40.

Yang, R. Y., R. P. Zou, and A. B. Yu (2000). "Computer simulation of the packing of fine particles." In: *Phys. Rev. E* 62 (3), pp. 3900–3908. DOI: 10.1103/PhysRevE.62.3900.

Zsom, Ormel, C. W., Güttler, C., Blum, J., and Dullemond, C. P. (2010). "The outcome of protoplanetary dust growth: pebbles, boulders, or planetesimals? *** - II. Introducing the bouncing barrier." In: *A&A* 513, A57. DOI: 10.1051/0004-6361/200912976.

COLOPHON

This document was typeset using the typographical look-and-feel `classicthesis` developed by André Miede and Ivo Pletikosić. The style was inspired by Robert Bringhurst's seminal book on typography "*The Elements of Typographic Style*".